UNIVERSITÀ DEGLI STUDI DI NAPOLI
FEDERICO II

Doctoral Dissertation
Doctoral Program in Industrial Engineering (35th Cycle)

**Giovanni Francesco Giuzio**

# Implementation of sustainable systems towards Net Zero Energy Infrastructures

## methodology and design criteria

**Supervisors:**

Prof. Annamaria Buonomano

Prof. Adolfo Palombo

**Co-Supervisors:**

Ing. Antonio Bonati

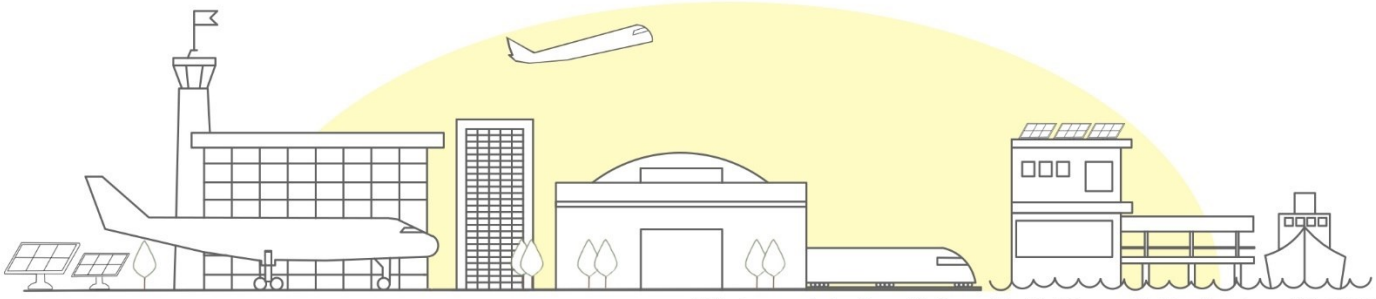

Università degli Studi di Napoli Federico II 2022

UNIVERSITÀ DEGLI STUDI DI NAPOLI
FEDERICO II

Doctoral Dissertation
Doctoral Program in Industrial Engineering (35th Cycle)

# Implementation of sustainable systems towards Net Zero Energy Infrastructures

## methodology and design criteria


**GIOVANNI FRANCESCO GIUZIO**

******

**Supervisors:**
Prof. Annamaria Buonomano
Prof. Adolfo Palombo

**Co-Supervisors:**
Ing. Antonio Bonati


**Doctoral Examination Committee:**

| | |
|---|---|
| Prof. Umberto Berardi, | Reyerson University and Politecnico di Bari |
| Prof. Davide Astiaso Garcia, | Università degli Studi di Roma La Sapienza |
| Prof. Ilaria Ballarini, | Politecnico di Torino |
| Prof. Gianpiero Evola, | Università degli Studi di Catania |
| Dr. Claudia Masselli, | Università degli Studi di Napoli Federico II |


Università degli Studi di Napoli Federico II
2022

# Declaration

I hereby declare that the contents and organization of this dissertation constitute my own original work and does not compromise in any way the rights of third parties, including those relating to the security of personal data.

Giovanni Francesco Giuzio

2022

# Abstract

The higher global temperatures associated with global warming are causing catastrophic climatic events and disrupting local ecosystems. A deep transformation of all human systems is imperative in order to limit global warming. An unprecedented reduction in the use of primary energy is necessary to achieve a climate-neutral society. Among others, there is the urgent need to renovate the building heritage and rethink the way we design new constructions. Infrastructures and public buildings can serve as virtuous examples in the common challenge of achieving the goal of net-zero energy, or the more ambitious net-zero emissions.

This thesis, which is one of the main outcomes of a three-year Ph.D. program in Industrial Engineering at the University of Naples Federico II, presents and discusses the results of the research activity conducted on energy efficiency solutions for buildings. In particular, the study focuses on **infrastructure buildings** such as railway stations, airports, ports, etc. which are experiencing important changes as the demand for mobility is growing fast.

The goal of this dissertation is threefold. First, the research aims at exploring the current practices and technologies suitable for the construction and operation of transportation buildings. Second, the analysis targets to identify innovative solution and methodologies to improve the sustainability and carbon footprint of these infrastructures. Third, the study intends providing guidelines to design low-consuming buildings as well as renovate existing ones in order to substitute traditional systems that no longer suit to the new decarbonisation needs.

In order to achieve these goals, this work makes extensive use of numerical simulation; specifically, a novel workflow based on Building Information Modeling to Building Energy Modeling (**BIM2BEM**) was developed, identifying it as a valuable tool for architects and engineers. With the aim of exploring a wide range of energy efficiency measures, four case studies developed during my doctoral studies are analysed as they represent relevant examples of four infrastructure building categories: **maritime stations**, **railway stations**, **airports**, and **railway technical buildings**.

From all the carried-out analyses, I demonstrated the potentials of the proposed methodology to investigate the implementation of sustainable systems and measures in high energy performance infrastructure buildings; promising results are, in fact, achieved by energy, economic and environmental points of view. Finally, useful **design criteria** are extrapolated from this study to increase the current knowledge about energy-saving techniques in transportation infrastructures.

# Table of contents

# List of Figures

# List of Tables

# Background

Climate change is one of the most serious challenges facing our world today. Our planet is experiencing significant and accelerated global warming that began over a century ago. Reductions in energy consumption and carbon emissions have become the most important strategic objective of the future development.

In December 2015, 195 countries of the world agreed the first legally binding international treaty on climate change, the Paris Agreement which commits all countries to achieve a climate neutral world by mid-century. However, the implementation of Paris Agreement requires synergies and long-term strategies as well as economic and social transformation [1]. This ambitious target needs to face the population and urbanization growth and the improvements in living standards. A wealthy population consumes more resources and demands more mobility services.

Tackling climate change issues calls for the implementation of energy efficiency measures and policy for the sustainable transition of our economy. Urgent actions are necessary to reduce global energy demands. European Commission (EC) responded with the European Green Deal, launched in 2020, a set of policy initiatives and fund packages aimed at making European Union (EU) the first net-zero greenhouse gases emitter by 2050, with the important intermediate target of achieving the at least 55% emissions reduction for 2030. To promote the clean energy transition, it is crucial to cut the energy consumptions of buildings and transportation sectors, which have together a huge impact on the air quality of urban areas and accounts for two third of the global energy consumption and of worldwide GHG emissions [2].

In October 2020, the EC presented its **Renovation wave** strategy, as part of the European Green Deal. It contains an action plan with concrete

regulatory, financing and enabling measures to boost building renovation. Its objective is to at least double the annual energy renovation rate of buildings by 2030 and to foster deep renovation. Furthermore, to accomplish the 2030 target proposed by the European Commission, the EU must reduce buildings' greenhouse gas emissions by 60%, their energy consumption by 14%, and the energy consumption of heating and cooling by 18% [3]. A revision of the Energy Performance of Buildings Directive (the last version dates back to 2018) is one of its key initiatives in order to meet the targets set for 2050. The Renovation Wave identifies 3 focus areas:

- Refurbishing worst-performing buildings and reducing energy poverty;
- Improve public buildings and social infrastructures in terms of energy efficiency;
- Decarbonising heating and cooling needs.

# Introduction

A shift toward green buildings is particularly important as buildings consume **a third of global energy** in both developed and developing societies.

Compared with other large buildings, railway / metro and maritime stations, as well as airports, have a huge impact in terms of energy consumption due to their characteristics. Generally, their energy consumption level is higher than those of common public buildings due to the number of services provided [4]. Such buildings are often the fundamental nodes for the management of the entire transport network, housing important high-consuming devices for communication and signaling.

Passenger stations and other transports facilities, mostly the newly built ones, are massive structures with high window-to-wall ratios and large floor spaces. They are also characterized by high occupancy rates and continuous operation (24h – 7d). According to a recent report about energy consumption in large railway stations funded by the Asian Development Bank [5], newly built stations (after 2003) consume around 60% less energy than older stations, revealing significant opportunities for energy use reduction from retrofitting existing facilities.

Due to the rapid economic development and increases in the living standards, passengers are demanding increased comfort and greater services, which has led to increasing efforts in the design process. Well-designed stations have stringent requirements on indoor air temperature, volume of fresh air, and lighting levels, with comfortable indoor environment in waiting halls as top priority. Fresh air, which is an important consideration for cooling load calculation, is also a key indicator of the health and hygiene condition in the station. After COVID-19 outbreak, adequate air exchange

rates have become a priority which inevitably lead to higher energy expenditures if proper measures are not taken into consideration [6].

Indoor lighting design should provide sufficient illumination throughout the building and be environment friendly, whilst elevators should be designed to balance passenger waiting times with energy use. Conveyor systems used for freights and passenger luggage are intensive energy-consumer equipment. Therefore, passenger comfort and energy-saving strategies are often conflicting priorities that need to be carefully balanced during the design phase.

The newly built stations have been becoming more and more sophisticated and, the use of complex mechanical and electrical systems has been increasing. The high complexity of station design makes it impossible to use a single strategy to reduce energy consumption. Therefore, it is available to use a combination of interrelated strategies and integrated automatic control system. It is essential to build a low-carbon facility through intelligent building controls designed in response to environmental and equipment performance requirements.

However, the design of the building, lighting, HVAC systems, security, water systems, and control systems are often not integrated with each other. This lack of integration in the design process represents a major challenge for green buildings to increase efficiency, ensure the comfort and safety of occupants, while ensure proper operation [7]. Moreover, regulatory framework is not adequate to promote their sustainable construction or refurbishment, energy requirements of such building typologies among with their related technical spaces are often not regulated in terms of energy efficiency, missing mandatory energy performance rating as other buildings typologies. To reduce energy consumption and improve passenger well-being, designers and stakeholders increasingly use voluntary sustainability protocols such as LEED [8], Airport Carbon Accreditation [9], etc., which have dedicated procedures for transit buildings [10]. However, despite these are often institutionally endorsed, they are adopted on a voluntary basis [11].

For further reduction in carbon emission and cost-saving, renewable energy sources should be taken into account after considerations of both passive and active measures on the envelope and the HVAC systems of the building. However, the integration of technology based on RES (Renewable Energy Sources) needs to be carefully assessed from the technical and the economic point of view. Ideally, modern RES-based energy systems should be designed to maximize the energy self-consumption and energy self-sufficiency while minimizing interaction with the national grid [12]. Among the available renewable energy systems, the solar-based ones are the most suitable for building applications due to the large availability of the solar source, especially in the countries of southern Europe and the Mediterranean regions, where high values of annual solar energy are recorded.

# Objectives and contents

This thesis aims to support the international goal of reducing the carbon footprint of **transport infrastructure buildings**; to learn and make use of advanced technologies in building energy management; to propose a methodology for the analysis and implementation of sustainable systems in transportation buildings; and to provide **design criteria** to ensure high energy-saving levels in transport facilities.

The research activity aims to critically analyse the state of the art of the current energy-saving solutions adopted in the design and the management of transport infrastructures, i.e. railway and maritime stations, airports, etc. The scope is also to identify **new technologies**, **innovative methodologies,** and **good practices** to be adopted in the design workflow of these buildings in order to minimize their environmental and economic impact.

Transport infrastructures are often high-consuming buildings or clusters of buildings. Hence, it is required to move from the concept of energy-intensive to that of **net zero or positive energy infrastructures**. To provide general guidelines and assess the suitability of innovative energy solutions, this dissertation focused on 4 types of buildings belonging to different categories: i) maritime stations (port buildings), ii) railway stations, iii) airport terminals, and iv) technical buildings for signaling equipment. The study carried out on each of these infrastructure categories is the subject of the chapters of this thesis (from Chapter 2 to Chapter 5). To analyse the performance of the energy-saving measures analysed, simulation models were developed on purpose by means of advanced *whole-building energy performance simulation tools*. Novel workflows based on *Building Information Modeling* to *Building Energy Modeling* (BIM2BEM) methodologies were adopted and developed (Chapter 1).

The chapter of this thesis are the result of distinct research activities carried out on several real case studies. Therefore, they have been organized to be stand-alone chapters but consistent with each other, according to the objectives of the thesis. Each of them provides an introduction section, where the state of the art and main contribution of the work is established, the methodology, the result, and discussion sections, as well as the conclusions according to modern publishing practices. Each chapter describes the literature and literature gaps that are relevant for the particular chapter. For this reason, this dissertation does not include a separate chapter for the literature review. As such, the readers can focus on the part of the thesis that is more relevant to them, since each chapter is a study in itself.

The thesis is structured as follow:

1. *Chapter 1* ***Building Information Modeling to Building Energy Modeling (BIM2BEM): a novel approach to improve infrastructure sustainability.***
   The chapter focuses on the methodology proposed and adopted to model the building case studies described in the following chapters. It identifies advantages that the BIM2BEM technique brings to the construction sector and propose a customized workflow to extrapolate model information for building energy analysis.
2. *Chapter 2* ***Improving the Efficiency of Maritime Infrastructures****.*
   The chapter focuses on the identification of suitable technologies and strategies to increase energy saving potential within harbour areas and port buildings.
3. *Chapter 3* ***Improving the Efficiency of Railway Building Stock****.*
   The chapter analyses the building stock of railway passenger stations. A bottom-up model of the entire Italian railway building stock was developed in order to define effective interventions to increase the efficiency of the stock.
4. *Chapter 4* ***Guidelines to reach the goal of highly efficient terminals: toward net zero energy airports****.*

The chapter focuses on the identification of suitable technologies and strategies to increase energy saving potential of airport facilities.

5. Chapter 5 ***Improving the efficiency of rail network service buildings: free cooling strategies for signaling equipment rooms***.
   The chapter presents the optimization of the air condition system for the cooling of signaling apparatuses of high-speed railway, providing important design criteria to systematically retrofit the air-conditioning equipment for wayside buildings.

A graphic overview describing the methodology adopted to carry out the study is reported in Figure 1.

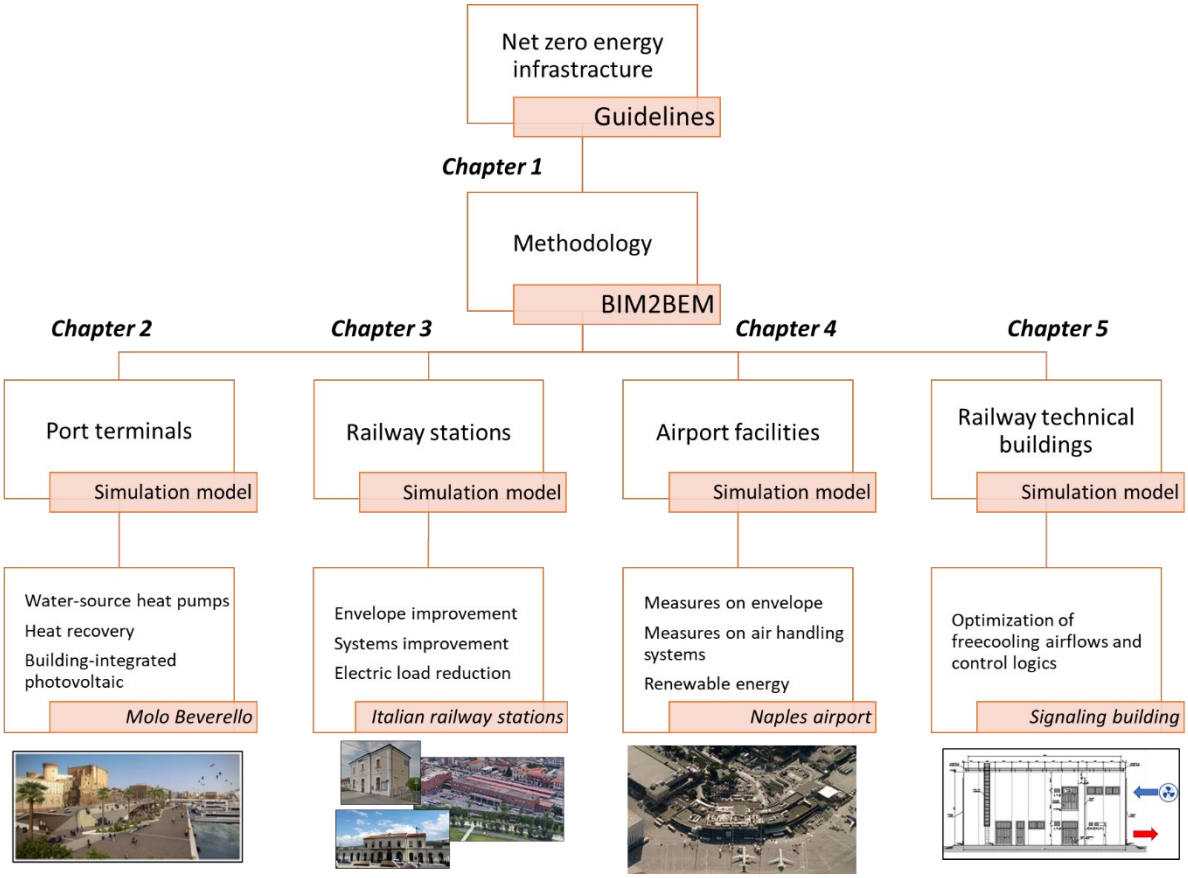


**Figure 1.** Description of the study and structure of the thesis.

The study presented in this thesis resulted from the research activity conducted at the **University of Naples Federico II** as part of an **industrial doctoral program** co-funded by the National Research Council (CNR) and Confindustria. The activity lasted 3 years, mainly used in research and training. Specifically, the scientific collaboration took place between the **Institute for Construction Technologies (ITC CNR)** and the **Brancaccio Costruzioni** company, with the aim of increasing the current knowledge on modelling, analysis, and design of the "*Zero Energy Infrastructures*", highly efficient buildings devoted to public uses. To the best of my knowledge, this is the first attempt in the available literature regarding the investigation of the energy performance of infrastructure buildings, conducted by means of innovative approaches and by developing a scalable methodology that could be hopefully applied by practitioners and further enhanced by researchers toward the sustainability of the transportation sector.

# Nomenclature

| | |
|---|---|
| AEC | Architecture, Engineering and Construction |
| AHU | Air Handling Units |
| ASHP | Air Source Heat Pump |
| BEM | Building Energy Modeling |
| BEST | Building Energy Software Tools |
| BIM | Building Information Modeling |
| BPS | whole-Building Performance Simulations |
| CFD | Computational Fluid Dynamics |
| DOE | Departement of Energy |
| ESPO | European Sea Ports Organisation |
| HVAC | Heating, Ventilation, and Air Conditioning |
| IDP | Integrated Design Process |
| IFC | Industry Foundation Classes |
| LCA | Life Cycle Assessment |
| MEP | Mechanical, Electrical, and Plumbing |
| nZEB | nearly Zero Energy Building |
| PDCA | Plan, Do, Check, Act |
| PERS | Port Environmental Review System |
| PLR | Part Load Ratio |
| PROP | Proposed Building |
| PS | Proposed System |
| REF | Reference Building |
| WSHP | Water Source Heat Pump |

| | |
|---|---|
| $\Delta C$ | Economic saving, M€ |
| $\Delta PE$ | Primary Energy Saved, kWh/year |
| ACH | Air Change per Hour |
| BEM | Building Energy Modeling |
| BIM | Building Information Modeling |
| CDD | Cooling Degree Days |
| End,c | Cooling needs, kWh/m$^2$ |
| End,el | Electricity demand, kWh/m$^2$ |
| End,h | Heating needs, kWh/m$^2$ |
| EUI | Energy Use Intensity, kWh/m$^2$ |
| GDP | Gross Domestic Product |
| GIS | Geographical Information System |
| HDD | Heating Degree Days |
| HVAC | Heating, Ventilation and Air Conditioning systems |
| $I_0$ | Investment cost, M€ |
| $I_{el,equipment}$ | Electric equipment load intensity, W/m$^2$ |
| $I_{el,lights}$ | Lights load intensity, W/m$^2$ |
| $I_{el,loads}$ | Total electric equipment load intensity of Service thermal |
| MLR | Multiple Linear Regression |
| N | time span, years |
| NPV | Net Present Value, M€ |
| P | interest rate, % |
| PE | Primary Energy, kWh/years |
| PES | Primary Energy Saving, % |
| PI | Profit index, (-) |

| | |
|---|---|
| RFI | Rete Ferroviaria Italiana |
| RI | Railway Infrastructure |
| SCOP | Seasonal Coefficient of Performance, (-) |
| SEER | Seasonal Energy Efficiency Ratio, (-) |
| SPB | Simple Pay Back, years |
| U | Heat transfer coefficient through building envelope, |
| UBEM | Urban Building Energy Modeling |
| Vc/V | Cooling volume to total volume ratio, (-) |
| Vh/V | Heated volume to total volume ratio, (-) |
| $\Delta E$ | Energy Consumption (Wh) |
| $\eta fan$ | Fan Efficiency (-) |
| $\Delta t$ | Timestep (h) |
| T | Temperature |
| U | Heat transfer coefficient ($W/m^2K$) |
| SHGF | Solar Heat Gain Factor (-) |
| PE | Primary Energy (kWh) |
| E | Energy required (kWh) |
| $\eta$ | Primary energy conversion factor (-) |

# Chapter 1
# Building Information Modeling to Building Energy Modeling (BIM2BEM): a novel approach to improve infrastructure sustainability

## Summary

Worldwide, the design, renovation, and sustainable management of buildings play a crucial role for sustainability. In this framework, a computer simulation of building's thermal behaviour is an almost mandatory tool for making informed decisions. However, the development of a building energy model is a challenging task that could discourage its adoption. A possible solution would be to exploit an existing Building Information Modeling (BIM) model to automatically generate an accurate and flexible Building Energy Modeling (BEM) one. Such a method, which can substantially improve decision-making and streamline the design-to-delivery processes, still presents some issues, and needs to be further investigated. In this framework, a novel workflow to extrapolate BIM data for energy simulation is proposed and analysed. The proposed methodology was adopted in this thesis to investigate several case studies and different strategies to reduce the annual primary energy consumption. Here, the BIM to BEM approach was tested as a useful tool for building infrastructures to improve the implementation of effective energy-saving measures.

In this chapter, the developed technique is presented and discussed, emphasizing its numerous benefits towards the achievements of the most modern sustainability standards. Furthermore, the optimal level of modelling detail required by a trustable building energy assessment is also discussed.

## 1.1 Introduction

Building Energy Modeling (BEM) has experienced significant growth in recent years [13]. Its application within the construction industry by architects and engineers allows building energy consumption reduction by supporting informed choices of effective low energy-consuming strategies [14]. There are several software that enable whole-building performance simulations (BPS), both commercial and open-source. To encourage their application, the U.S. Department of Energy (US DOE) hosts and maintains the BEST Directory, a list of recognised Building Energy Software Tools (BEST) which counts numerous software among BPS and other useful tools supporting the modelling of specific building physic aspects. In addition, many in-house BPS have been also developed within universities or scientific institutions for the purpose of more advanced researches [15], [16], or to enhance capabilities for complex simulations [17], [18]. Some authors also adopt Reduced Order Models (ROM) [19] of buildings to lower the modelling effort and computational cost with successful applications in district simulations. As a high number of building models may be required to simulate whole urban areas and perform multiple calculations, ROMs are very convenient for optimization purposes [2].

Physics-based building energy models require a high number of input parameters to carry out detailed dynamic calculations on an hourly or sub-hourly basis, i.e., hourly outdoor boundary conditions, building surface and space geometry, envelope thermal characteristics, occupancy and operation profiles, HVAC systems configurations, etc. [20]. The implementation of such building models is often complex and time-consuming, furthermore, design or construction firms use BEM only at an advanced stage of the project which reduces its potential benefits [21]. Indeed, BEM technologies have the capability of improving design from the point of view of the end-use energy consumption if adopted in the early phase of the design, following an Integrated Design Process (IDP) [22]. As shown in Figure 2, it is observed that the opportunity for simulation to influence design quickly decreases as the design advances. At the same

time, the cost related to the ongoing variants of the project increases as decision are taken and specifications are documented [23].

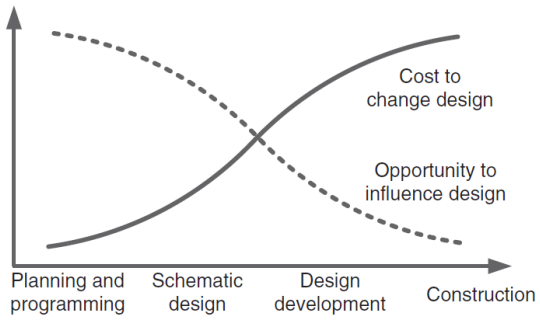


**Figure 2.** Opportunity to influence building design and related cost of changes. Figure from reference [23].

Building information modelling (BIM) is now the most effective strategy to streamline project management and integrate all the professionals and stakeholders involved in the project [24]. Digitalisation of the design information in a unique BIM model introduces an important simplification for interoperability between the different project areas, such as architects, civil and mechanical, electrical, and plumbing (MEP) engineers, general contractors, etc. Therefore, energy modelers may also benefit from a BIM database to develop BEM models, avoiding redundant building model creation and speed up the design [25]. This methodology, called BIM-based BEM, BIM to BEM or BIM2BEM, has been investigated in literature and is becoming a common practice in the industry. Nevertheless, it is still unperfect and can introduce geometry errors and loss of data during export/import procedures [26]. BIM to BEM relies on two transfer file formats: *IFC* (Industry Foundation Classes), developed by buildingSMART [27], and *gbXML* (Green Building XML) [28]. While the first one was purposely designed for exchanging data from BIM to BIM, *gbXML* embeds specific information allowing BEM models definition [29], [30]. Both are continuously updated to provide essential tools in the context of building energy modelling and to boost collaboration among practitioners.

The validity of the described approach is proven for various building types, such as industrial [31], educational [25], [32] and residential [33], [34]. The current trend is to increasingly improve the integration of energy simulations within the BIM software environment [35], which is particularly useful for preliminary sensitive analyses [36]. However, it is still incomplete and does not meet the user needs regarding flexibility [37]. In fact, availability of HVAC system layouts is still limited. Other authors studied and developed specific algorithms to join BIM and BEM capabilities, as in [38], where *gbXML* generated by different BIM authoring software were used to export geometry to custom metamodels for energy calculations. The authors also highlighted the need for the standardisation of data transfer schema, as several issues were encountered depending on the choice of the BIM software. This could also encourage the development of more complex workflows including multi-physics environment, such as advanced thermal and acoustic simulations [39], Life Cycle Assessment (LCA) analyses [40], Computational Fluid Dynamics (CFD) simulations [41], or daylighting and occupant thermal comfort assessments [42], [34, 43].

Aiming at boosting the adoption of the BIM to BEM technique in the context of building construction or refurbishment, a novel workflow, purposely conceived to extrapolate and convert BIM data into readable inputs for BEM, has been developed and here presented. Specifically, the proposed methodology is suitably conceived to provide detailed and accurate dynamic calculations of the thermal and electrical needs starting from a digital informative model of the building. The developed workflow is based on the use of widely used BIM and BEM software in the architecture, engineering and construction (AEC) industries, *Autodesk Revit* and *OpenStudio*. While *Autodesk Revit* is one of the most advanced BIM authoring software available on the market, *OpenStudio* is open source, designed, and developed to be a flexible and easy tool for energy modelling. This combination has the potential to become an attractive tool for both professionals in the building sector, who increasingly pay attention to energy saving in their projects, and researchers. Furthermore, facility managers might benefit from the usage of BIM2BEM techniques for management and

continuous improvement during the entire life cycle of the building. The methodology is a valuable instrument to implement energy-saving strategies within PDCA cycles (Plan, Do, Check, Act) that many standards (e.g. ISO 50001 [44]) require.

## 1.2 Materials and Methods

As previously specified, this thesis also aims to analyse a novel workflow based on the state-of-the-art practices of the BIM2BEM approach to be applied to the design and operation management of transit building facilities. The proposed workflow, based on the *Systems Analysis* features implemented within *Autodesk Revit*, one of the most used BIM authoring software, allows users to automatically export BIM-driven building and HVAC system data to *gbXML* that is consequently imported into *OpenStudio*, the building simulation software kit developed by the U.S. National Renewable Energy Laboratory (NREL). *OpenStudio* has the capability to create BEM models from a *gbXML* file, manipulate it programmatically or via its Graphical User Interface (GUI), and perform HVAC sizing and annual building energy simulations by means of *EnergyPlus*, the latest building simulation engine by the U.S. Department of Energy (DOE). *Revit* introduced *Systems Analysis* with the Autodesk Revit version 2020.1, providing a series of scripts, called *measures*, to extrapolate and process information from *gbXML*, set simulation parameters, and query the calculation engine to obtain specific outputs. Furthermore, custom *measures* can be implemented to boost modelling and extend the BIM to BEM capabilities.

The energy performance analyses carried out in the case studies presented in the next chapters were developed by means of Autodesk Revit 2022, OpenStudio CLI 3.2.0, and OpenStudio Application 1.1.0. A schematic diagram that reflects the methodology adopted is reported in Figure 3 which highlights the main tasks carried out during the process: data collection, BIM and BEM model development, model manipulation and review, simulation, and postprocessing.

Figure 3. Flowchart of the adopted methodology.

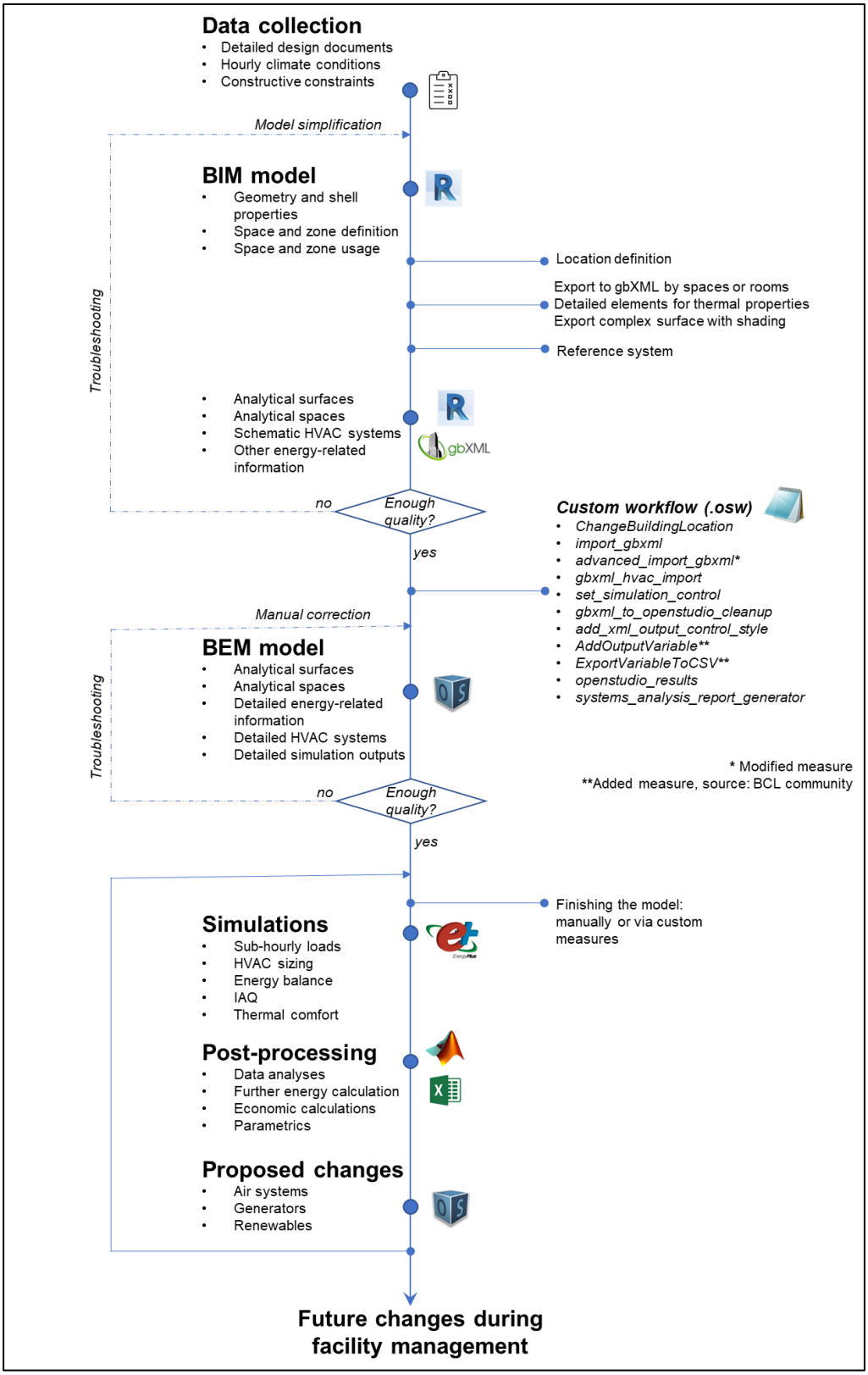

The entire process was carried out paying particular attention to the problems encountered along the way, to the operations necessary to eliminate such problems, and to the development of a real workflow able to optimize and speed up the whole process, including a postprocessing activity able to group, present and make easily analysable and usable the results provided by the software.

### 1.2.1 BIM Model Development

The level of detail, or level of development (LOD), is a parameter that indicates the level of detail and information of the graphical representation of the model. According to the American Institute of Architects (AIA) [45], the LOD is divided into 5 classes ranging from LOD 100, generic model poor of details, to LOD 500, a real model of the building [46].

From the experience gained during the building modelling carried out in the course of this study (described in detail in Chapters 2, 3, 4, and 5), the implementation of the BIM model carried out with a LOD between the LOD 200 and the LOD 300 ensures a faithful representation of each element of the building while provides accurate energy simulations when geometry is exported into BEM tools (model accuracy is further discussed in the next paragraph).

Particular attention needs to be paid to glass elements, which contribute in large part to the final thermal demand. Parameters representing thermal properties are set according to the information collected for the specific case study. The same is done for space information, such as occupancy, lighting and equipment schedules, ventilation, infiltration, thermostat and humidistat set-points, etc., by creating custom libraries in the BIM software. Afterward, spaces are grouped into thermal zones according to characteristics of HVAC systems and space boundary conditions. The entire modelling process is facilitated by the user-friendly tools integrated into the BIM environment which allow the users to develop their own object families

integrating the default libraries (refer to the complete software documentation [47]). Specifically, surface and space types are the main objects involved in the energy model. Each one needs to be characterised by means of all the above-mentioned information to represent the corresponding components in the actual building. However, complex projects still require significant commitment. Such input data have to be manually inserted, which involves a fair amount of time, especially when the number of spaces is high. Therefore, the need for time increases with the building complexity. Figure 4 provides the representation of the building as modelled in the Autodesk Revit environment as well as the information exchange flow of the BIM2BEM process.

### 1.2.2 BEM Model Development

The energy model is created by means of the suitable features of *Autodesk Revit* that allow the automatic generation of analytical spaces and surfaces. Such objects contain the information embedded in the BIM database, inputted during modelling, and then collected in the *gbXML*. The energy model was then reviewed to ensure the proper boundary conditions to spaces and surfaces. Whenever required, the BIM model was simplified in order to re-generate a more trustable energy model and correct the detected surface or space bugs.

HVAC systems are schematically defined as energy objects included in the *gbXML* by means of the plant templates of the new *Revit Systems Analysis* tools. Specifically, air loops, plant loops, and zone equipment are linked to each other and to zones in order to define the appropriate HVAC model. Often, those plant components available in the *Revit* library do not reflect the actual complexity of the HVAC systems of the specific case study, thus, they serve as the basis for more accurate modelling in *OpenStudio* environment. By performing a systems analysis simulation, a detailed *OpenStudio* model is generated from *gbXML* by means of a suitable script (*OpenStudio* workflow) including commands to automatically manipulate the model. The latter was purposely modified to include custom simulation settings and collect specific outputs. Furthermore, some default *OpenStudio*

measures were modified to reflect the modelling purposes. The graphical appearance of the energy model is depicted in Figure 4.

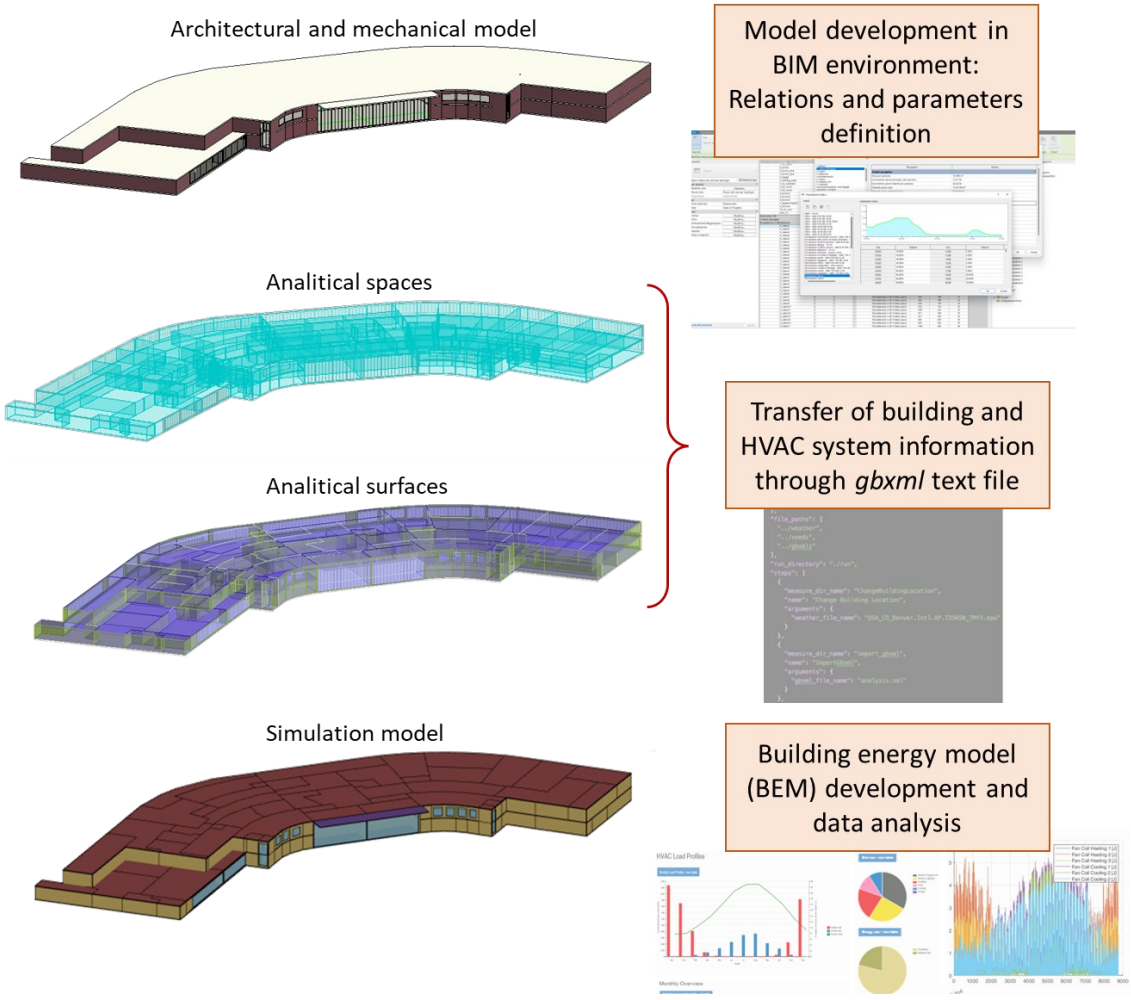


**Figure 4.** Representation of the process developed to obtain the building energy model starting from the BIM model, passing through the *gbxml* format to the *OpenStudio* and *EnergyPlus* software.

## 1.3 Discussion

Simulations provide useful insights and proofs for informed decisions. By means of energy consumption calculations, designers and facility managers have very important data for value engineering and sustainable management. The adopted approach has been found to be very convenient at an early stage of the project when energy analyses can guide concept design. BIM to BEM can also be successfully implemented in renovation projects by means of a comparison of different efficiency measures, as demonstrated in literature. Furthermore, the proposed method helps in the enhancement of the integrative design and to reduce project timing by avoiding the creation of redundant and time-consuming models, and by improving data management. However, some difficulties have been encountered during the process that are worth pointing out.

The building geometry may be very complex, so the building shell should be simplified to obtain a reliable yet accurate energy model. BIM tools allow a high degree of detail in geometry, providing advanced modelling tools. However, they have a lesser capability to model building materials or other energy-related parameters. BEM tools, in contrast, require a high degree of detail in building components but do not require as high a resolution for geometry. Inclusion of such details results in excessively complex models and may take an excessively long time to troubleshoot and perform calculations. Although the effort of simplifying the BIM model, the automatic generation of BEM model geometry can often present inaccuracies such as missing surfaces or their fragmentation. Those issues can occur at the *gbXML* definition within the BIM environment or during information transfer. Therefore, troubleshooting requires iterative geometry generation that can be very demanding and tedious. It is worth noticing that, as stated by Athienitis et al. in [22], evidence suggests that there are diminishing returns on model accuracy as model resolution increases. This entails the need to identify the best trade-off between the model’s reliability and the difficult to develop the energy model.

While the effort due to data collection is strictly linked to the progress of the project, the modelling phases require a significant cost in terms of time. Of course, this will depend greatly on geometry complexity and whether or not the HVAC systems, another time-consuming category of inputs, are modelled in detail. However, the time needed to generate an accurate building energy model might be halved by taking advantage of BIM modelling and advanced automation tools (e.g. *OpenStudio*), as redundant models are avoided. As also depicted in Figure 3 the time devoted to geometry and HVAC modelling comprise a significant period of time dedicated to debugging of building geometry and troubleshooting. Simulation, post-processing, and data analysis require a lower amount of time within the entire process.

Geometry export by *gbXML* is generally complete, however, HVAC systems still present many limitations regarding either plant configurations or working and control parameters. Customisation of HVAC components should be carried out afterwards by means of the BEM modelling tools or by creating custom BIM parameters and suitable *measures* parsing the *gbXML* and manipulating the existing plant templates. Although the latter is a consistent, sharable, and scalable solution, it requires specific modelling and programming skills which could discourage the adoption of advanced energy modelling.

In the next chapters, the analyses carried out prove the validity of the BIM to BEM methodologies for the design of transit buildings and other infrastructures in general. In addition, the methodology is suitable as a tool in facility management and continuous improvement processes. The major quality and energy management standards such as ISO 9001 and ISO 50001 suggest and encourage the adoption of the plan-do-check-act (PDCA) cycle which is the operating principle to guarantee effective improvement. The ISO scheme is depicted in Figure 5; here, the BIM to BEM approach fits within the PDCA cycle to support decision-makers with data retrieved by the whole-building dynamic energy simulations. After the actions to reach goals of energy reduction are defined, both the BIM and

BEM models should be continuously updated all over the cycle with newly added information to test the proposed energy–saving strategies and be aware of any unpredicted problems. Finally, when the cycle is abandoned because it has been successful, the new baseline is defined for future strategy planning considering the data and measurements collected during operation. In this way, the digital model accompanies the improvement process, facilitating the facility management and making the transition of transportation infrastructures toward reduction of air pollution and energy efficiency improvement easier and more effective.

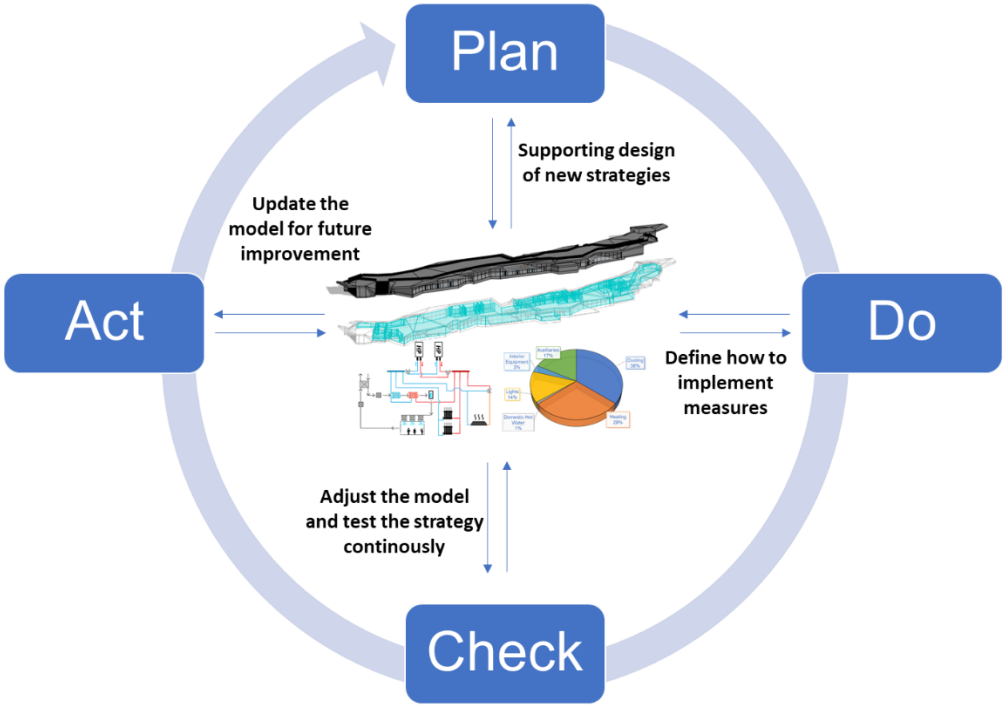


**Figure 5.** BIM to BEM within the continuous improvement (PDCA) cycle of ISO standards.

Moreover, it is also interesting to notice how the approach used fits with the needs of the sustainability of buildings, both in the planning and management phases.

Despite the enormous advantages that BIM2BEM brings, currently, the interoperability between BIM and BEM is low and highly software-

dependent. However, there is growing attention from the academic world given the continuous emergence of studies in this regard. BIM2BEM has various applications such as energy needs estimation, materials and solutions comparison, optimization, Nearly Zero-Energy Buildings (NZEB), life-cycle analysis (LCA), hygrothermal design, energy certification, thermal comfort analysis, etc. Software houses are gradually including even more tools and features within BIM environment to improve interoperability with BEM tools. Therefore, BIM2BEM is expected to become, from an innovative tool that is the prerogative of researchers and larger and more structured companies, a widely used tool and a standard in the construction sector to improve the sustainability of all sorts of projects.

## 1.4 Conclusions

In this chapter, it was critically analysed how BIM methodology coupled with whole-building energy modelling (BEM) and simulation can increase the effectiveness of sustainable design and management of buildings. In this framework, a novel workflow to extrapolate and convert BIM data into readable inputs for BEM has been developed and discussed. The technique is adopted in the next chapters as the main methodology framework to analyse the energy saving potential of several strategies suitable for passenger building infrastructures.

The adopted approach is found very important in the concept design phase when everything has to be decided. However, BIM2BEM can also be successfully implemented in renovation projects by means of a comparison of different efficiency measures. Specifically, the plan-do-check-act cycle suggested by international quality and energy management standards can be carried out with the auxiliary of this advanced tool.

At present, this approach is effective and reliable if a medium detailed model is developed (LOD 200/300). Therefore, future research and

developments are needed to limit the information losses that occur in the BIM to BEM exchange process.

# Chapter 2
# Improving the Efficiency of Maritime Infrastructures

## Summary

This chapter aims at exploring different strategies to reduce the energy consumption of port buildings and identifying best practices for effective efficiency measures.

The “Molo Beverello” maritime station in Naples was analysed by means of the BIM2BEM methodology to identify energy efficiency strategies and reduce the overall primary energy consumption of the facility. Specifically, a detailed BIM model of the building was developed in order to generate a reliable building energy simulation model. The optimal modelling level of development was chosen after an optimization procedure aimed at identifying the optimal trade-off between model accuracy and time costs of the whole simulation process.

Taking the current status of the project as a baseline, several energy-saving strategies were simulated by the developed workflow to evaluate their conveniences, such as: water-source heat pump, heat recovery from chiller condensers, replacement of window facade with special photovoltaic glass, and replacement of shading systems with photovoltaic canopies. The adoption of the selected measures always showed interesting outcomes from an energy, economic, and environmental points of view.

## 2.1 Introduction

Attention to ecological issues has increased significantly in the maritime sector. As stated in the 2020 Environmental Report, the European Sea Ports Organisation (ESPO) has ranked air quality, climate change, and energy efficiency as the top three of its ten environmental priorities [48]. The growing awareness about this topic has led many ports to plan concrete actions to reduce energy consumption that are often carried out in the framework of international standards such as ISO 50001 [44] and EN 16001 [49], or specific tools developed to support environmental management in ports, i.e., the Port Environmental Review System (PERS). The enhancement of the energy efficiency of ports can also be seen as part of the broader research trend regarding independent and semi-independent energy communities.

Among technological and operational energy-saving measures adopted in the European seaports, the improvement of building performance by means of innovative design and/or renovation of existing infrastructures has been considered as one of the key solutions to face ESPO (European Sea Ports Organisation) priorities, highlighted also by Sdoukopoulos et al. in their recent work [50]. They provided an overview of the main policies, technologies, and practices that European ports have adopted to-date for enhancing energy efficiency. The authors collected several cases of actual building renovations that were developed in harbour areas in the last years, mainly in the Baltic Sea. The survey addressed different building typologies such as offices and passengers terminals, as well as warehouse buildings [51], involving passive design concepts, innovative heating, ventilation, and air conditioning (HVAC) systems, and renewable energy technologies for the in-site electricity and thermal energy production. It is worth mentioning the significant examples of the office buildings of Värtahamnen port and the terminal passengers' building of the Port of Portsmouth. Both were designed following the most modern eco-building standards and their heating and cooling systems have been equipped with water source heat pumps exploiting the renewable thermal energy from seawater. Such a solution allows very high performance for hot and cold water production, however,

its application is limited by seawater temperatures [52]. The North Adriatic Sea Port Authority also recognises the importance of renovating port buildings [53]. After energy audits on buildings located in the harbour area of Venice and Marghera (office and artisan activity buildings), it was found that, although they were renovated in 2007, the investigated buildings have low thermal insulation, which causes high energy consumption, both in terms of fuel for winter heating and electricity for summer air conditioning. Acting through the insulation of walls and floors, the replacement of windows and doors and the replacement of the current methane heat generators with heat pump systems, it could be possible to significantly reduce energy consumption and related CO2 emissions.

An interesting report dealing with the energy planning of the Port Lands of Toronto provides useful guidelines for a net zero energy district [54]. The adopted approach involves the calculation of energy use, energy demand, and GHG emissions for different strategies of development, in order to understand the potential future energy needs of the Port Lands. In addition, current trends and practices in developing net zero communities were investigated by exploring existing and in-development case studies buildings such as Hammarby Sjostad, HafenCity, and Dockside Green (see Figure 6). The pillars that the author identified to reach the goal of net zero energy districts were: (i) improving the codes and standards, (ii) enhancing energy conservation in new buildings, (iii) adopting a building-scale local energy supply, and (iv) adopting block-scale energy sharing networks. In addition, other unique opportunities, such as creating synergies with the Portlands Energy Centre and the geography of the Port Lands itself within Toronto’s waterfront, were identified, and specific technologies were then evaluated to understand their potential contribution towards achieving net zero.

Furthermore, in a recent study of Vaher et al. [55], a review of the active and passive strategies adopted in large buildings (i.e., non-residential, museum, airports, and a cruise terminal) is reported with the aim of making the Tallinn cruise terminal a nearly Zero Energy Building (nZEB) and

providing useful guidelines for efficiency improvement of similar buildings in northern climates. From the experiences retrieved from other case studies and the modelling and simulation of the investigated one, the authors defined the pillars for the effective and sustainable operation of the Tallinn cruise terminal that may be also extended to other similar buildings. The solutions proposed were (i) reduction of window I solar factor and adoption of solar protections; (ii) increasing heating and cooling efficiency by seawater source heat pumps; (iii) adoption of demand-controlled devices for ventilation and lighting in order to avoid energy waste due to irregular occupancy; (iv) on-site electricity generation. The authors assessed the potential energy savings and indoor air conditions by means of a commercial dynamic simulation software, i.e., IDA Indoor Climate and Energy [56], which is one of several commercial design tools available for building energy modelling (BEM). Although the methodology of BEM is becoming a reference in the construction industry, as it represents the most effective state-of-the-art tool to predict building energy behaviour, the work of Vaher et al. is one of the few examples found in the scientific or technical literature that explicitly addresses BEM for building design in the maritime sector.


a) b) c)

**Figure 6. a)** Hammarby Sjostad, the industrial harbour of Stockholm, Sweden, redeveloped in 2004. **b)** HafenCity, Industrial harbour in central Hamburg, Germany, renovated to accommodate population growth without consuming more Land. **c)** Dockside Green, the waterfront brownfield redevelopment in Victoria, Canada, the first LEED Platinum community in the world [54].

To address the task of moving towards a zero energy future for port buildings, there is an urgent need to align research and innovation with

practice, identifying paths for the exploitation of strategies and technologies able to reduce the carbon footprints of port infrastructures.

In this chapter, with the twofold aims of supporting design decisions oriented to energy consumption reduction and providing a consistent tool for continuous improvement in facility management, the case study of the new “Molo Beverello” maritime station of Naples (a real building located in the South of Italy and currently under construction) is analysed. The considered case study project is part of a wider redevelopment plan of the port area and aims to achieve high standards of efficiency. A detailed BIM-based BEM model was developed to assess several innovative energy efficiency measures that suits the needs of buildings in the context of ports.

## 2.2 Case Study and modelling assumptions

The project of the *Molo Beverello* is part of a wider plan of “Redevelopment of the monumental area of the port of Naples” which follows the idea of improving the interaction and integration of the urban and port resources. Figure 7 shows a render of the project of the new terminal taken from the project documentation which was provided by the design and construction firm that is realizing the project.

The project, approved in 2018, consists of two parts:

1. The construction of a Commercial Area linked to the near metro station of “Piazza Municipio”;

2. The re-arrangement of the “Molo Beverello” area, directly connected to the Commercial Area and to the pedestrian tunnel coming from the adjacent subway station. This project includes the construction of a new passenger terminal station for the fast sea lines to the islands of the Gulf of Naples.

An energy survey was carried out to assess energy consumption and to size the thermal plants, however, advanced modelling and simulations were

carried out to propose new measures able to reduce consumption and promote energy efficiency.

**Figure 7.** The new “Molo Beverello” of the monumental area of the port of Naples.

### 2.2.1 Data Collection

All the information required to carry out the analysis were retrieved from the detailed design documentation, provided by the general contractor [57]. Furthermore, climate-related data of Naples were considered. Specifically, the Napoli Capodichino International Airport weather file from the IGDG collection was used for simulations. A 2D representation of the terminal within the context in which it is going to be built is provided in Figure 8. More detailed data related to the investigated facility design are omitted as they are intellectual property of the design engineering company [58].

With respect to the thermal properties of constructive elements such as walls, floors, ceiling, doors, and windows, the *U*-values and thermal capacities of the building components were calculated accounting for all materials they are made of. Specifically, the characteristics of the main envelope elements are summarised in Table 1. Please, note that these

values are those selected by the design firm following the current Italian normative which provides mandatory thresholds for each building component feature (e.g., U-value, thermal mass, etc.) depending on the considered weather zone [59].

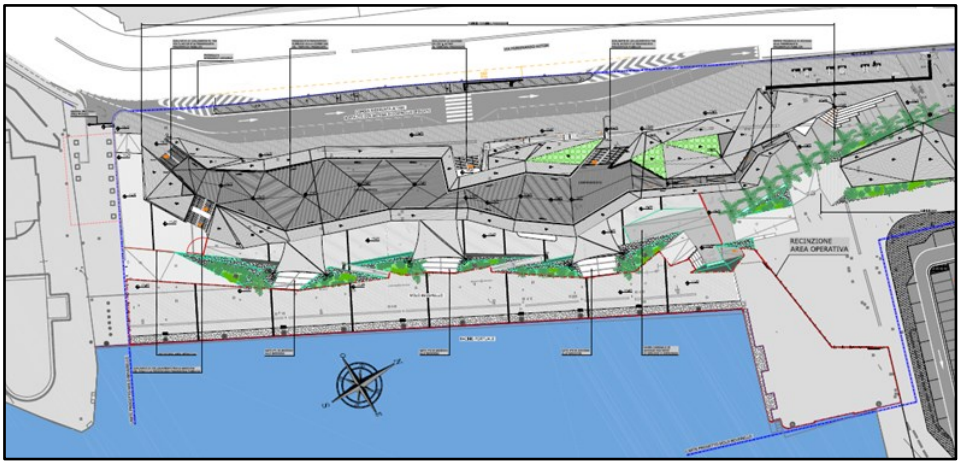

**Figure 8.** Site 2D drawing of the project.

**Table 1.** Characteristics of the main envelope components.

| Surface type | U value ($W/m^2K$) | Thermal mass ($kJ/ m^2K$) | SHGC (-) |
|---|---|---|---|
| **Window façade** | 1.25 | - | 0.2 |
| **External wall** | 0.36÷0.56 | 318÷544 | - |
| **Internal wall** | 0.36÷3.3 | 38÷544 | - |
| **Floor** | 0.28÷0.31 | 1197÷1243 | - |
| **Ceiling** | 0.31 | 877 | - |

**Table 2.** Space characteristics summary.

| Zone | Name | Type of space | Area ($m^2$) | Volume ($m^3$) | HVAC type |
|---|---|---|---|---|---|
| **North Bathroom** | T.33 W.C. | Toilets | 23 | 90.75 | Heating & Cooling; AHU; Radiant systems |
| | T.34 W.C. | Toilets | 23 | 96.12 | |
| | T.34_1 W.C. service | Toilets | 3 | 12.42 | |
| | T.35 W.C. | Toilets | 4 | 16.17 | |
| **Ovest Bathroom** | T.24 W.C. | Toilets | 8 | 31.42 | Heating & Cooling; AHU; Radiant systems |
| | T.25 W.C. | Toilets | 8 | 30.36 | |
| | T.26 W.C. | Toilets | 3 | 13.21 | |
| | T.27 W.C. | Toilets | 4 | 14.76 | |
| | T.27_1 Storage | Storage area | 4 | 11.29 | |
| **South Bathroom** | T.2 + T.5 W.C. | Toilets | 56 | 185.79 | Heating & Cooling; AHU; Radiant systems |
| | T.3 W.C. | Toilets | 3 | 11.19 | |
| | T.4 W.C. service | Toilets | 4 | 14.19 | |
| | T.7 W.C. | Dressing room | 7 | 25.33 | |
| **Rad. Ovest 1** | T.9 WC | Toilets | 4 | 17.23 | Heating & Cooling; AHU; Radiant systems |
| **Rad. Ovest 1** | T.12 WC | Toilets | 4 | 16.86 | Heating & Cooling; AHU; Radiant systems |
| | T.14 WC | Toilets | 4 | 16.91 | |

| | | | | | |
|---|---|---|---|---|---|
| **Terminal** | T.0 Terminal | Tickets | 1612 | 6252.23 | Heating & Cooling; AHU; Low temperature Radiant systems |
| | T.6 Bar | Commercial | 22 | 78.25 | |
| | T.8 Storage | Commercial | 18 | 75.32 | |
| | T.10 Storage | Storage area | 3 | 10.86 | |
| | T.11 Store | Commercial | 22 | 93.5 | |
| | T.13 Storage | Storage area | 2 | 10.61 | |
| | T.15 Storage | Storage area | 2 | 10.64 | |
| | T.16 Store | Commercial | 21 | 89.97 | |
| | T.17 Office | Office | 10 | 36.08 | |
| | T.18 Office | Office | 9 | 31.38 | |
| | T.19 Office | Office | 9 | 31.78 | |
| | T.20 Office | Office | 9 | 32.36 | |
| | T.21 Office | Office | 9 | 33.45 | |
| | T.22 Office | Office | 9 | 33.4 | |
| | T.23 Meeting | Meeting room | 16 | 60.53 | |
| | T.28 Office | Office | 18 | 68.26 | |
| | T.30 Infirmary | Infirmary | 9 | 32.3 | |
| - | T.0_1 Terminal | Entrance | 178 | 476.8 | AHU |
| - | T.1.B | Technical room | 7 | 15.62 | Unconditioned |

| | | | | | |
|---|---|---|---|---|---|
| - | T.1.C | Technical room | 16 | 34.79 | Unconditioned |
| - | T.29 Rack | Technical room | 4 | 12.26 | Unconditioned |
| - | T.31 | Technical room | 106 | 341.93 | Unconditioned |
| - | T.36 | Technical room | 1 | 1.84 | Unconditioned |
| - | T.37 | Technical room | 12 | 27.82 | Unconditioned |
| - | T.38 | Technical room | 2 | 7.58 | Unconditioned |
| - | T.39 | Technical room | 52 | 171.97 | Unconditioned |

The facility, with a total area of 2340 $m^2$ (2119 $m^2$ conditioned) and an overall volume of 8675 $m^3$, is expected to host a maximum number of 400 people during peak hours. The building consists of a total of 42 different spaces, grouped in 7 different thermal zones, while 7 not-conditioned spaces used as technical rooms are treated as single isolated thermal zones. Table 2 provides the information related to spaces and thermal zones as defined for energy modelling purposes. The HVAC system comprises two air handling units (AHU), balancing the latent and sensible (partially) heating and cooling loads, and a hydronic water loop to balance the remaining sensible loads by means of low temperature radiant systems. The generation system consists of two twin air source heat pumps/chillers that provide the thermal power required to keep thermal comfort (heating set-point 20° C; cooling set-point 26 °C; relative humidity 50%). The two heat pumps/chillers are sequentially activated to maximise operational performance under nominal conditions. They are managed by a

thermoregulation system that monitors the room temperature and relative humidity within the thermal zones.

The two heat pumps have a heating capacity of 157.8 kW (outdoor air condition 2 °C—wat–r 45 - 40 °C; COP = 2.82) and a cooling capacity of 147.2 kW (outdoor air conditions 35 °C—wa–er 7 - 12 °C; EER = 2.33). The maximum COP is recorded for a partial load ratio (PLR) of 25% which is equal to 4.60 at nominal conditions [58].

The zone equipment consists of radiant floors within the main zone (terminal one). On the other hand, the bathrooms of the perimetral area of the building are equipped with radiators. The hot water is sent to the radiators at 50 °C and to the radiant floor loop at 35 °C (according to the Italian standard UNI 1264 in order to limit the surface temperature of the floor to 29° C). During the summer season, the radiant floor receives water at 19° C to avoid surface condensation.

The two AHUs process only outdoor air and provide both the air needed for ventilation, as required by the UNI 10339 and EN 13779. The air circuit has a maximum flow rate of 14000 $m^3$/h and is equipped with an air heat exchanger to recover part of the exhaust air thermal energy. The air system treats the air by means of cooling coils, heating coils, re-heat coils, and humidifiers in order to supply the fresh air to the zones at 21.5 °C (relative humidity 45%) and 20.5 °C (relative humidity 55%) in heating and cooling mode respectively. It also allows free cooling when the outdoor air conditions are favourable.

The domestic hot water system consists of a air-water heat pump with a heating capacity of 18 kW that produces water at 60 °C and a 1500 L storage tank equipped with internal electrical resistance to ensure supply to all spaces of the building, such as toilets, shop, infirmary, and bar.

The waiting area of the terminal is open to the public from 7:00 a.m. to 9:00 p.m. Therefore, HVAC systems are operated when the terminal station is occupied. The occupancy schedule is supposed as maximum during the middle hours of the day, while the decrease in the number of passengers in

the hours of the late afternoon is considered as few departures and arrivals are planned in the evening.

### 2.2.2 BIM Model Development

As the building geometry is very complex, the building shell has been simplified to obtain a reliable yet accurate energy model.

The implementation of the BIM model was carried out with a LOD 200/300. Particular attention was paid to glass elements, which contribute in large part to the final thermal demand. Parameters representing thermal properties are set according to the information collected for the case study. The same was done for space information, such as occupancy, lighting and equipment schedules, ventilation, infiltration, thermostat and humidistat set-points, etc., by creating custom libraries in the BIM software. Afterward, spaces were grouped into thermal zones (see Table 2) according to characteristics of HVAC systems and space boundary conditions. Figure 9 provides the prospective representation of the building as modelled in Autodesk Revit environment.

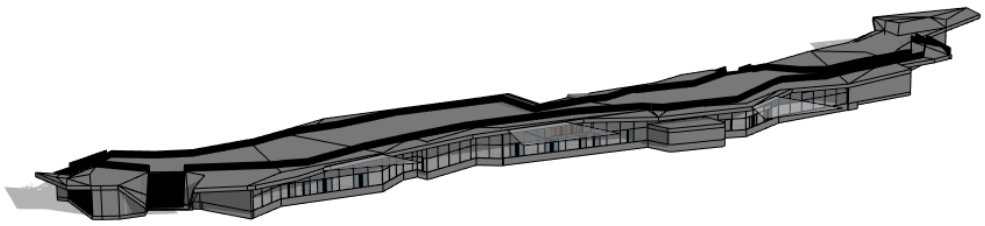

**Figure 9.** BIM model of the building**.**

### 2.2.3 BEM Model Development

The energy model was created by means of the suitable features of Autodesk Revit that allow the automatic generation of analytical spaces and surfaces leveraging data collected into the *gbxml*. The energy model was then reviewed to ensure the proper boundary conditions to spaces and surfaces. In Figure 10, both analytical spaces and surfaces are highlighted to show how the final building envelope model appears.

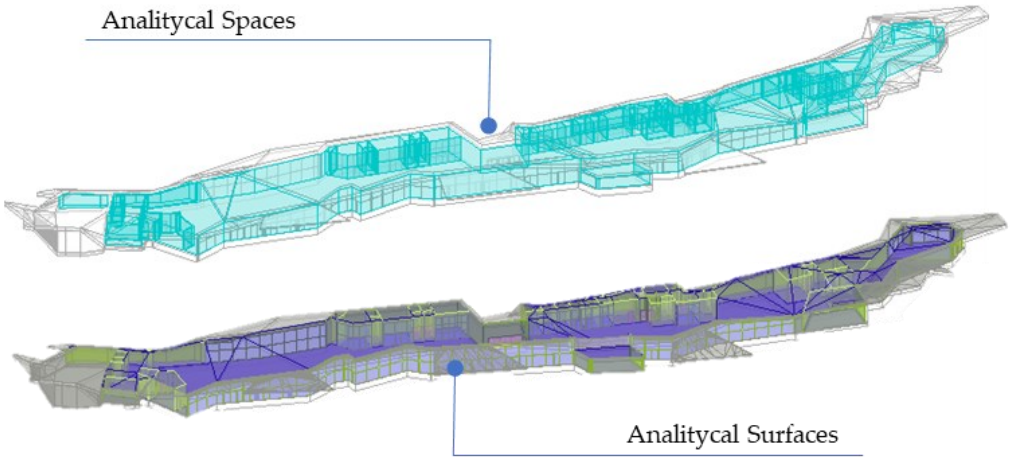


**Figure 10.** BEM model of the building, analytical spaces, and surfaces.

HVAC systems were schematically defined as energy objects included in the *gbXML* by means of the plant templates of the new *Revit Systems Analysis tools.* Specifically, air loops, and hot and cold water loops, were linked to radiant panel zone equipment. Those plant components do not reflect the actual complexity of the HVAC systems of the case study, however, they serve as the basis for more accurate modelling. Thus, after *gbXML* exporting, the HVAC system was rearranged to account for its higher complexity. Baseboard zone equipment were added to bathrooms and, two mixing valves were included in the piping system to mix supply and return water of radiant floor (Figure 11). Furthermore, an air-to-air heat exchanger was added to the air loop and, both air loop and water loop controllers were adapted to the operation strategies of the systems. Operation temperatures and the size of plant equipment were then adjusted to fully characterise them. All changes in the HVAC configuration were made with the help of *OpenStudio Application*, a user-friendly GUI to perform whole-building energy simulations by OpenStudio/EnergyPlus.

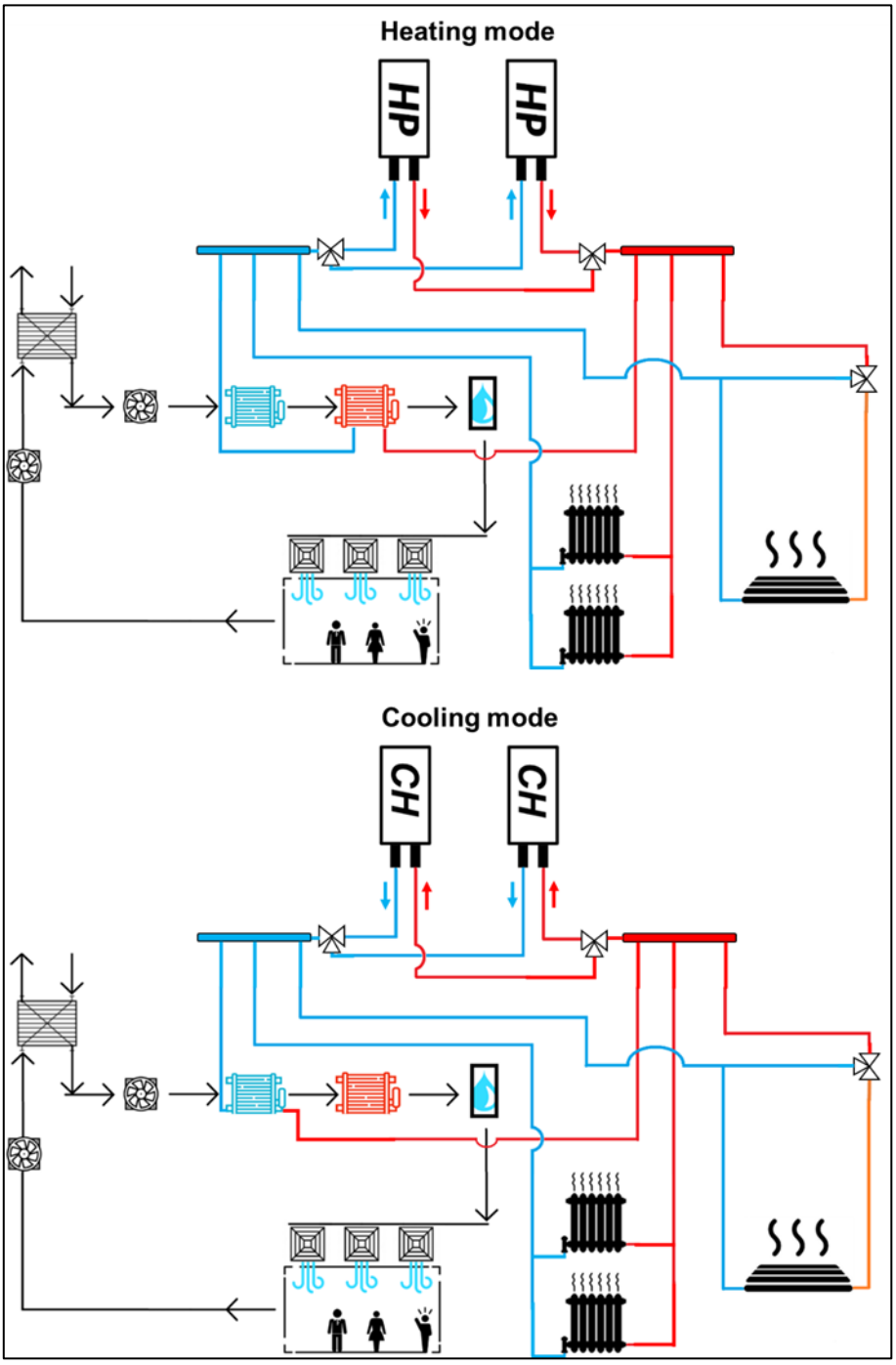


**Figure 11.** Schematic diagram of heating, cooling, and air treatment systems as modelled in OpenStudio.

## 2.2.4 Model Manipulation and Review

The energy model described so far is the one adopted as a reference for comparison with other energy-saving measures. Specifically, the following were considered as candidate strategies to enhance energy efficiency or reduce annual primary energy consumption:

- Proposed System 1 (PS1), water-source heat pump;
- Proposed System 2 (PS2), heat recovery from chiller condensers;
- Proposed System 3 (PS3), replacement of window facade with photovoltaic glass;
- Proposed System 4 (PS4), replacement of shading systems with photovoltaic canopies.

*2.2.4.1 Proposed System 1: Water-Source Heat Pump*

Water-source heat pumps (WSHP) are generally more efficient compared with equivalent air source ones (ASHP). As the analysed building is close to the sea, such a solution can reduce the electricity consumption of heating and cooling generation systems. The water-source heat pump exploiting the free thermal energy of seawater was modelled accounting for the seawater temperature variation. The water-source heat pump was selected among the products available on the market, chosen according to the system's needs. The characteristics of the machines at nominal conditions were provided by manufacturer: cooling capacity, 140.5 kW (use side 12–7 °C—source side 30–35 °C, EER: 5.147); heating capacity, 160.4 kW (use side 40–45 °C—source side 10–6.7 °C, COP: 4.493). The extra cost of the implementation of WSHPs compared to the ASHPs is EUR 40000.

Historical data of the average temperature of the seawater of the port of Naples (shown in Figure 11) were used to evaluate the improved performance of the HVAC system [60].

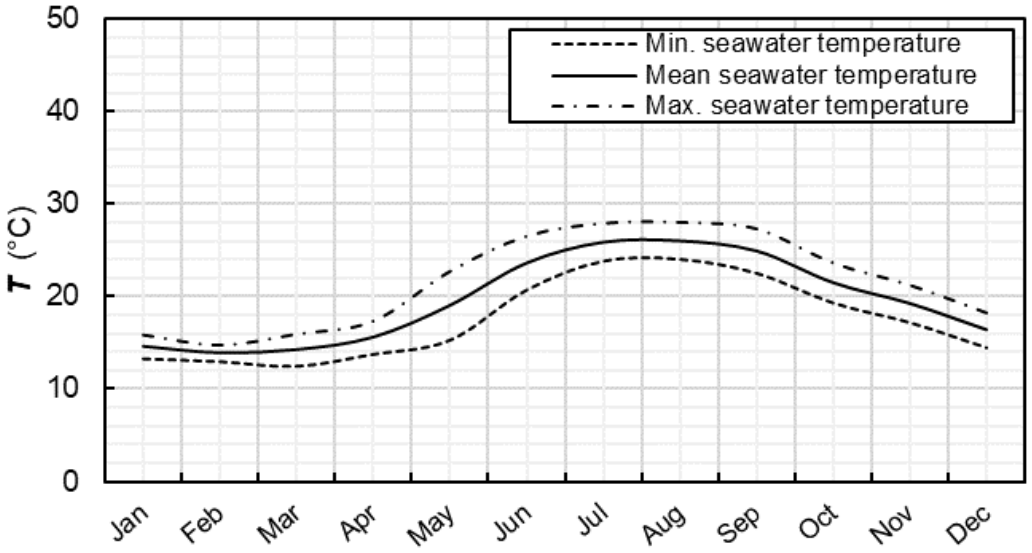


**Figure 12.** Minimum, maximum and average sea water temperature profile of the Gulf of Naples.

*2.2.4.2 Proposed System 2: Heat Recovery from Chiller Condenser*

As during summer operation both cooling and reheat coils work at fixed temperatures, chillers work to simultaneously provide hot and cold water. The recovery of the chiller condensing heat can be used to fully or partially heat the water that feeds the reheat coils of the AHU. However, chiller heat recovery can involve a performance drop depending on condensing temperature. Thus, a parametric analysis of system operation was carried out accordingly, to identify the optimal recovery temperature providing the least final electricity consumption. Specifically, recovery temperatures ranging from 25 °C to 50 °C were simulated and three characteristic parameters were used for evaluation:

- Electricity for heating is expected to decrease, as the higher the recovery temperature, the lower the thermal power required for reheat coil;
- Electricity for cooling is expected to increase, as the higher the recovery temperature, thus condensing temperature, the lower is the efficiency of the machines;

- Total electricity for heating and cooling is the total electricity required by chillers and is the parameter to optimise.

The modifications to the system to allow the condensation heat recovery have an estimated cost of around EUR 2000.

### *2.2.4.3 Proposed System 3: Replacement of Window Façade*

The terminal presents a large window façade on the south-east side that can be used to produce electricity through photovoltaic technologies.

The analysed glass is an amorphous silicon photovoltaic glass with two 6 mm low-emission glass and a 12 mm Argon chamber, its characteristics for three different types are shown in Table 3.

**Table 3.** Summary of PV window characteristics.

| | SHGC (%) | U-Value ($W/m^2K$) | Efficiency (%) | Transparency (%) | Cost ($EUR/m^2$) |
|---|---|---|---|---|---|
| **Low transparency** | 9% | 1.2 | 4% | 10% | 107 |
| **Medium transparency** | 12% | 1.2 | 3.4% | 20% | 110 |
| **High transparency** | 17% | 1.2 | 2.8% | 30% | 115 |

The choice of replacing the glass facades with photovoltaic glass is due to the fact that installation of a large number of photovoltaic panels on the building roof is not possible since the roof is also used for pedestrian transit. In order to not compromise the lighting conditions inside the building, the selected photovoltaic panels are made of amorphous transparent or semi-

transparent silicon, in order to allow enough daylighting. However, these types of photovoltaic panels have relatively low efficiency (3–4%) and therefore in order to make the investment affordable from both an economic and an energy point of view, a multi-objective optimisation was carried out in order to evaluate the most viable solution. Several types of photovoltaic panels with different efficiencies, SHGCs, U-values, and transparency conditions were considered.

In addition, to maximise the produced electricity, the shading surfaces outside the building have been removed. The window façade was divided into 3 zones in order to select the most effective amount of photovoltaic glass. The sectors of the façade that would be replaced are shown in Figure 13. For each type of glass, the replacement of Zone C (area of 109.4 $m^2$), Zone B+C (area of 278 $m^2$), and Zone A + B + C (area of 414.27 $m^2$) were respectively investigated.

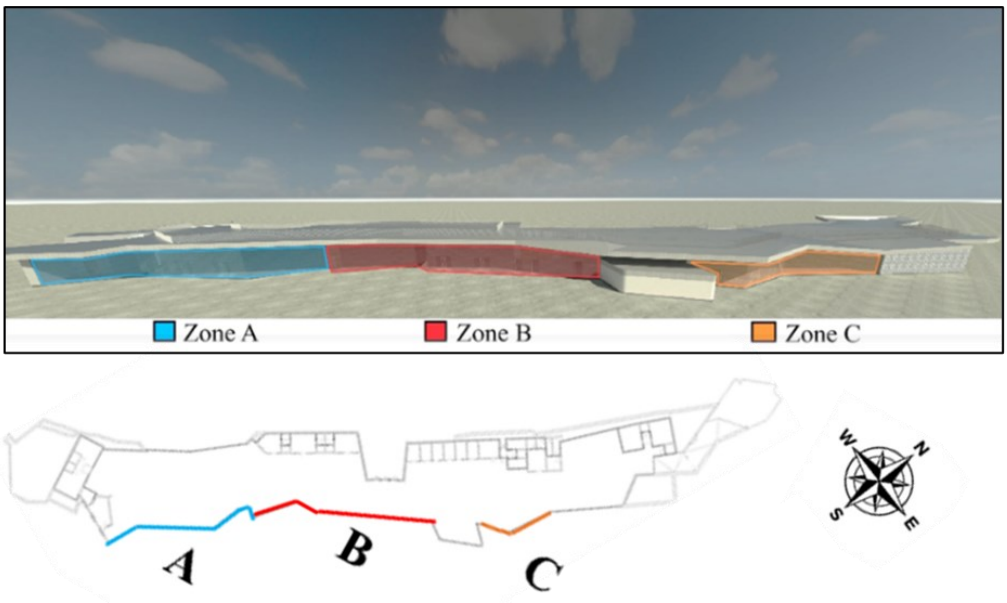


**Figure 13.** Façade sections for implementation of PV glass.

The first combination involves only zone C as it is the area that receives the most incident solar radiation. Thus, the optimisation involved a total of 9 combinations. The study carried out was a multi-objective optimisation with

the aim of identifying the most advantageous solution both from the energy and economic point of view. The objective functions considered for optimisation were the net present value (NPV), calculated by Equation (6), and the primary energy saving (PES), calculated by Equation (3) (see next section). These parameters also assessed the difference in heating and cooling loads due to the installation of new photovoltaic glass. Although there are interesting contributions due to electricity generation, installation of such systems may lead to an increase in thermal needs due to their different solar heat gain coefficients (SHGC) and U-values compared to the reference system. Specifically, the increase of heating loads may occur since new glasses allow lower free solar gains. Vice versa, this can lead to a decrease in cooling loads.

To assess the productivity of photovoltaic glass, the incident and diffuse solar radiation on each panel have been evaluated, accounting for any possible shadings. The considered amorphous photovoltaic glasses have capital costs in the range of 104 - 109 EUR/$m^2$ depending on transparency degree, applied to conduct the economic analysis.

#### *2.2.4.4 Proposed System 4: Photovoltaic Canopies*

At the end of the study of energy efficiency solutions, the hypothesis of the installation of photovoltaic canopies was evaluated. These structures have been inserted in place of the tarpaulins outside the building so as not to vary much the structure and ensure the same solar shading, the coloured surfaces in Figure 14.

Monocrystalline silicon panels with nominal efficiency of 18.4% and a rated power of 300 W were selected. The overall extension of the canopies is 366 $m^2$, so 230 photovoltaic modules were installed for a total rated power of 69 kW. A capital cost of ~250 EUR/$m^2$ was considered, accounting for all the necessary technologies that comprises the plant.

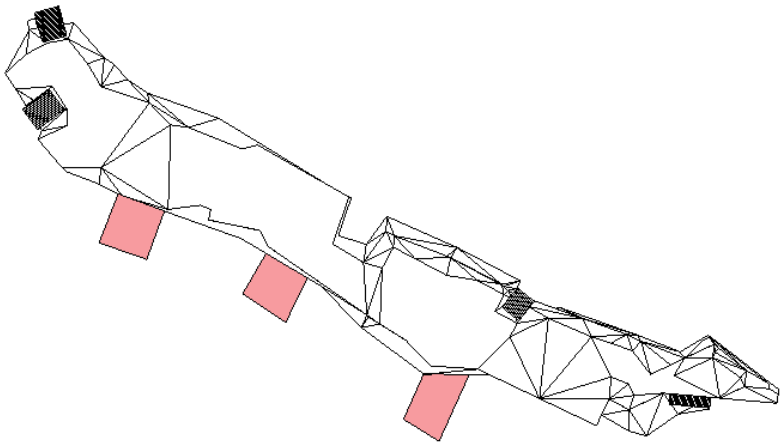

**Figure 14.** Site view of building station showing photovoltaic canopies.

## 2.2.5 Simulation and Post Processing

The simulations were carried out by means of the *EnergyPlus* built-in features with a timestep of 15 min, providing detailed outputs to analyse the building behaviour, as well as the performances of the systems. *Variables* and *Meters* that refer to zone air conditions, thermal gains, heating and cooling system capacity rates, and electricity consumptions were processed to evaluate the project from an energy and economic point of view. Each proposed strategy (*prop*) was compared to the baseline, also called Reference building (*ref*), in order to calculate the indices for decision-making that are described below.

The conversion of calculated electricity into primary energy was carried out by means of the factor $\eta_{el}$ representing the average efficiency of the entire Italian generation system ($\eta_{el}$ = 0.46)

$$E_p = \frac{E_{el}}{\eta_{el}} \quad (1)$$

The primary energy saved ($\Delta E_p$) and the primary energy saving (*PES*) related to the proposed scenarios with respect to the reference case, are calculated as:

$$\Delta E_p = E_{p,ref} - E_{p,prop} \tag{2}$$

$$PES = 1 - \frac{E_{p,prop}}{E_{p,ref}} \tag{3}$$

Similarly, the avoided carbon dioxide emissions are evaluated by Equation (4) considering the emission factor $f_{CO2}$ equal to 0.2.

$$\Delta E_{CO_2} = \Delta E_p \cdot \mathrm{f}_{CO_2} \tag{4}$$

Finally, to assess the economic profitability, the simple payback period (*SPB*) is calculated as:

$$SPB = \frac{I_0}{\Delta C} \tag{5}$$

where $I_0$ is the investment cost and $\Delta C$ are the cost differences between reference and proposed scenarios. At last, net present value (*NPV*) and profit index (*PI*) are also evaluated as:

$$NPV = \Delta C \cdot \left\{ \frac{1}{p} \cdot \left[ 1 - \frac{1}{(1+p)^N} \right] \right\} - I_0 \tag{6}$$

*p* is the interest rate and *N* is the life time span. In this study, NPV was calculated taking into account an interest rate and a useful life of 5% and 20 years, respectively.

$$PI = \frac{NPV}{I_0} \tag{7}$$

The procedure adopted to account for the variability of EER in different working conditions follows the procedure suggested by the Italian standard UNI TS 11300 [61], indicated hereinafter. It is important to note that EER is calculated at each simulation timestep, indicated in the following equations by the index *i*. The same procedure was carried out for the COP calculation to assess electricity demand for space heating.

The calculation involves the normalized efficiency curves of the considered generators $EER_{n,PLR}$ depending on heat pump/chiller PLR and that was obtained from the real operating curve provided by manufacturers, the maximum $EER_{max}$ calculated by Equation (8), and the exergetic efficiency $\eta_{ex}$ calculated by Equation (9).

$$EER_{\max} = \frac{T_{ev,nom} - \Delta T_{ev}}{(T_{co,nom} + \Delta T_{co}) - (T_{ev,nom} + \Delta T_{ev})} \tag{8}$$

$$\eta_{ex} = \frac{EER_{100\%}}{EER_{\max}} \tag{9}$$

Here, $T_{ev,nom,}$ and $T_{co,nom}$ are the evaporator and condenser temperatures respectively, while $\Delta T_{ev}$ and $\Delta T_{co}$ are the average heat exchanger temperature differences at the evaporator and condenser. The latter are equal to 5 or 10 °C, depending on whether the heat exchange occurs with water or air.

Therefore, the actual *EER* at specific outdoor conditions is defined by Equation (10).

$$EER_i = \frac{T_{ev,i} - \Delta T_{ev,i}}{(T_{co,i} + \Delta T_{co,i}) - (T_{ev,i} + \Delta T_{ev,i})} \cdot EER_{n,PLR} \cdot \eta_{ex} \tag{10}$$

The price of electricity used to evaluate economic savings was 0.20 EUR/kWh.

## 2.3 Results and Discussion

This section provides the simulation results of the energy-saving measures investigated to improve the efficiency of the selected building and to analyse the suitability of the BIM to BEM methodology in the maritime sector.

### 2.3.1 Reference Building

The building-plant system, as described in the previous sections, has been taken as a baseline for comparison purposes. At the same time, the BEM model of the Reference Building (REF) was thoroughly revised to test the accuracy of the simulation results.

It is worth noting that an optimization of the model LOD was made during the modelling process in order to achieve a trade-off between accuracy and time for the entire simulation procedure. Although more detailed models (LOD > 300) achieve more accurate calculations, longer process times are obtained due to complex modelling problems and higher computational load (greater number of building envelope surfaces or thermal zones). Conversely, LODs that are too low (< 200) would speed up the process and lose the reliability of the simulation results. Therefore, an intermediate LOD between 200 and 300 was selected to obtain an optimal compromise to apply to the considered design procedure.

Indoor air conditions compared to outdoor temperature are depicted in Figure 15, showing the model capability to reflect the actual system operating strategies. The chart also highlights the correct operation of the system that keeps temperature and humidity within the acceptability range, i.e., 20 - 26 °C and 40 - 60% for indoor temperature and relative humidity respectively.

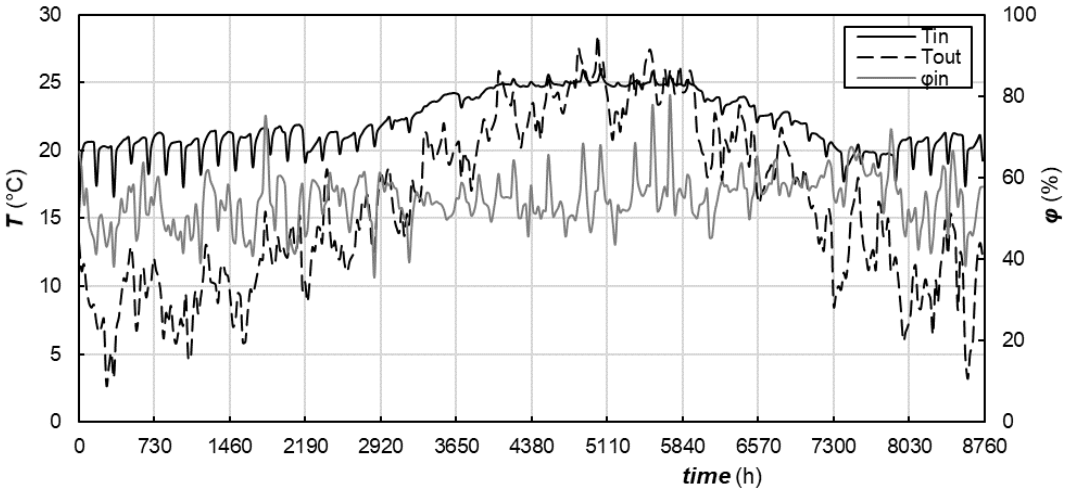


**Figure 15.** Average indoor air conditions.

The overall energy consumption shares of the reference building were calculated and are reported in Figure 16, while baseline values such as thermal energy, electricity, and primary energy usage are summarized in Table 4. Space heating and cooling were the main facility energy needs, followed by lighting, and air conditioning auxiliary equipment. The proposed solutions, described in the next paragraphs were chosen to significantly reduce both energy demand and primary energy consumption.

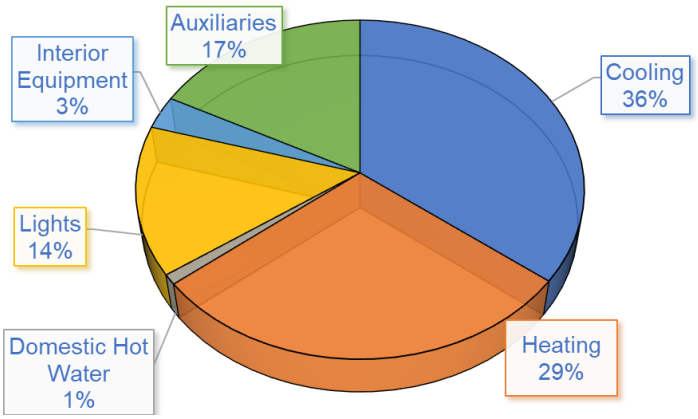


**Figure 16.** Energy consumption shares of reference building.

**Table 4.** Summary of energy consumption of reference building.

| | Thermal Energy (MWh/year) | Electricity (MWh/year) | Primary Energy (MWh/year) |
|---|---|---|---|
| **Heating** | 108.7 | 26.9 | 27.6 |
| **Cooling** | 127.1 | 34.9 | 35.8 |
| **Domestic hot water** | 4.1 | 0.9 | 0.9 |
| **Himidifier** | - | 3.4 | 3.5 |
| **Lights** | - | 13.4 | 13.7 |
| **Interior equipment** | - | 2.9 | 2.9 |
| **Fans** | - | 14.3 | 14.7 |
| **Pumps** | - | 2.4 | 2.5 |
| **Total** | 239.9 | 99.1 | 101.6 |

### 2.3.2 Water Source Heat Pump

A WSHP requires lower energy intensity than an ASHP to meet the thermal loads for space heating and cooling in Naples. Indeed, the seawater temperature is particularly favourable, being less variable and, on average, lower during summer and higher during winter than the ambient temperature (see Figure 12).

The highest performance is observed during the summer season, when the Coefficient of Performance (COP) is higher, and both cooling and heating services are required. The convenience of adopting WSHP instead of ASHP for the project is demonstrated in Figure 17, where the electricity demand for the reference and proposed cases are compared.

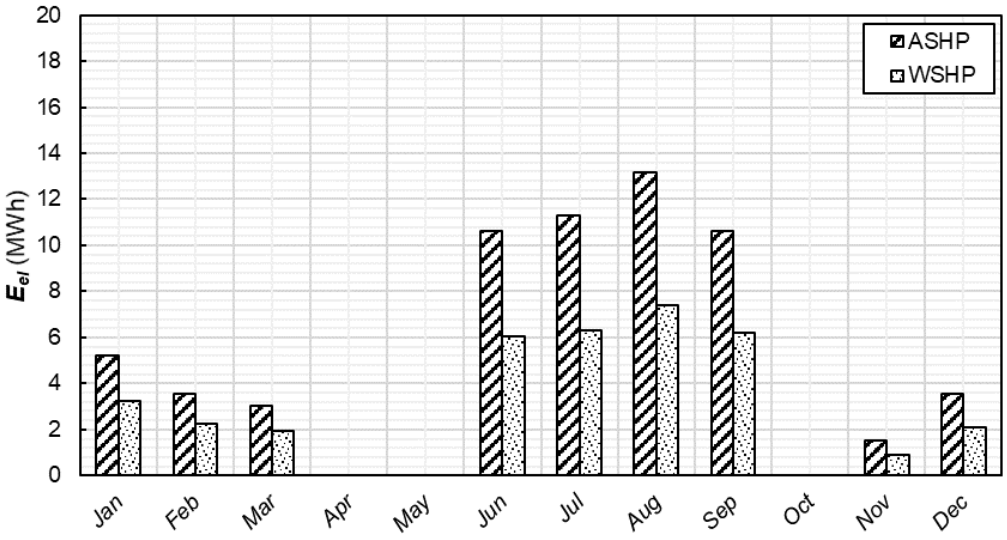


**Figure 17.** Comparison of monthly electricity usage between ASHP and WSHP.

The proposal allows a saving of 42% of the total primary energy consumed by the building in one year. Further metrics related to the measure of WSHP, such as actual $CO_2$ emissions and total primary energy consumption are summarised in Table 5.

**Table 5.** Metrics related to the implementation of water-source heat pumps.

| | Electricity (MWh/year) | Primary Energy (MWh/year) | $CO_2$ Emission (t/year) | PES (%) |
|---|---|---|---|---|
| **REF** | 62.7 | 136.3 | 27.2 | - |
| **PS1** | 36.6 | 79.6 | 15.9 | 41.6 |

### 2.3.3 Heat Recovery from Chiller Condenser

As expected, while heat recovery involves a lower electricity consumption for heating, cooling results in a lower performance at the higher heat recovery temperature. The increase in electricity demands for cooling prevails over the decrease in electricity demands for heating, which

leads to a slight rise in the total electricity curve. The behaviour of the new plant configuration, in terms of electricity consumed to produce the required thermal energy, is shown in Figure 18.

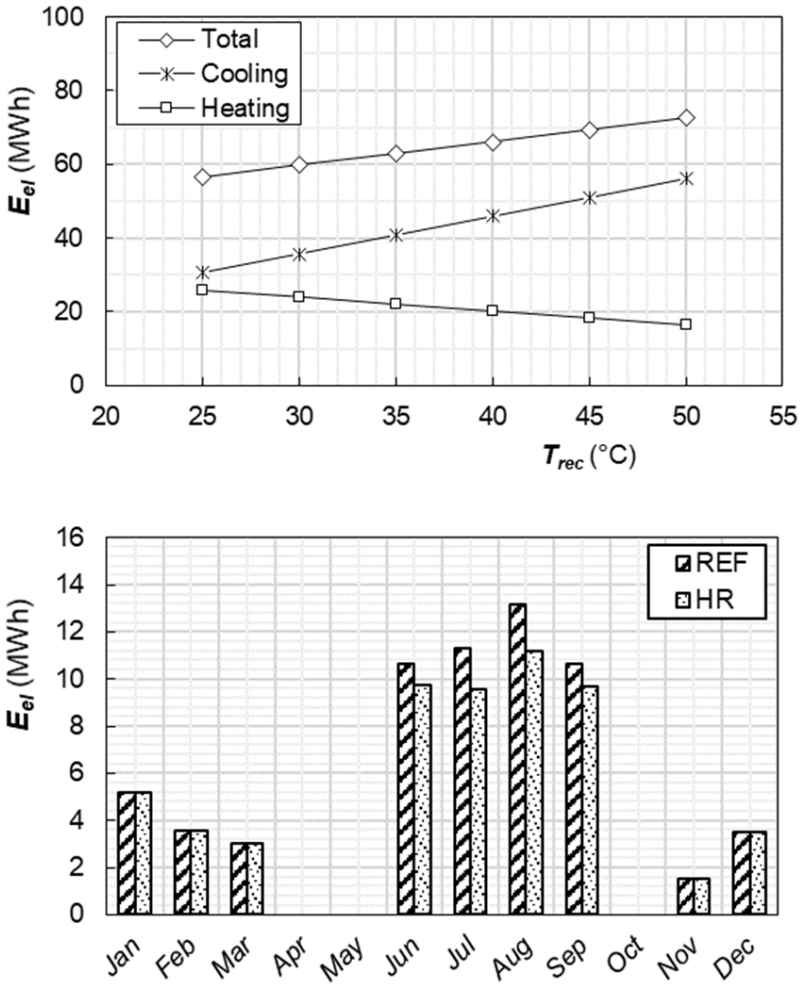


**Figure 18.** Electricity consumption against HR temperature and comparison between reference and chosen systems.

Therefore, the result of the optimisation indicates overall energy savings at low heat recovery temperatures, the highest performance is obtained by preheating the reheat coil water at 25 °C. Furthermore, while a deterioration in the performance of chillers is registered, the performance of the second

heat pump in the heating operation improved as it works at lower part-load factors with higher energy efficiency. The effects discussed so far make optimisation necessary as they are in contrast to each other.

Figure 18 also shows the monthly electricity consumption of the system equipped with the heat recovery (HR) at 25 °C compared to the reference one. This measure is interesting as it provides significant savings (up to 10.2%) in terms of primary energy against very low investment costs for piping works and additional heat exchangers. The annual electricity and primary energy consumption, as well as carbon dioxide emissions, are reported in Table 6.

**Table 6.** Metrics related to the implementation of heat recovery.

| | Electricity (MWh/year) | Primary Energy (MWh/year) | $CO_2$ Emission (tons/year) | PES (%) |
|---|---|---|---|---|
| **REF** | 62.7 | 136.3 | 27.2 | - |
| **PS2** | 56.3 | 122.4 | 22.5 | 10.2 |

### 2.3.4 Replacement of Window Façade

Among the configurations described in the methodology section, the implementation of the low transparency glazing over the entire available surface (A + B + C) is the most profitable solution, both from an economic and energy point of view. The results of the multi-objective optimisation conducted are summarised in Figure 19. Here, it is also possible to note that the low transparency technology always provides better performance compared to medium or high transparency ones. However, low transparency glass can significantly affect daylighting and the visual comfort of occupants. Therefore, the medium transparent configuration (20% of visual transparency) on the whole façade (A + B + C) has been also considered as a valuable solution in terms of NPV and PES.

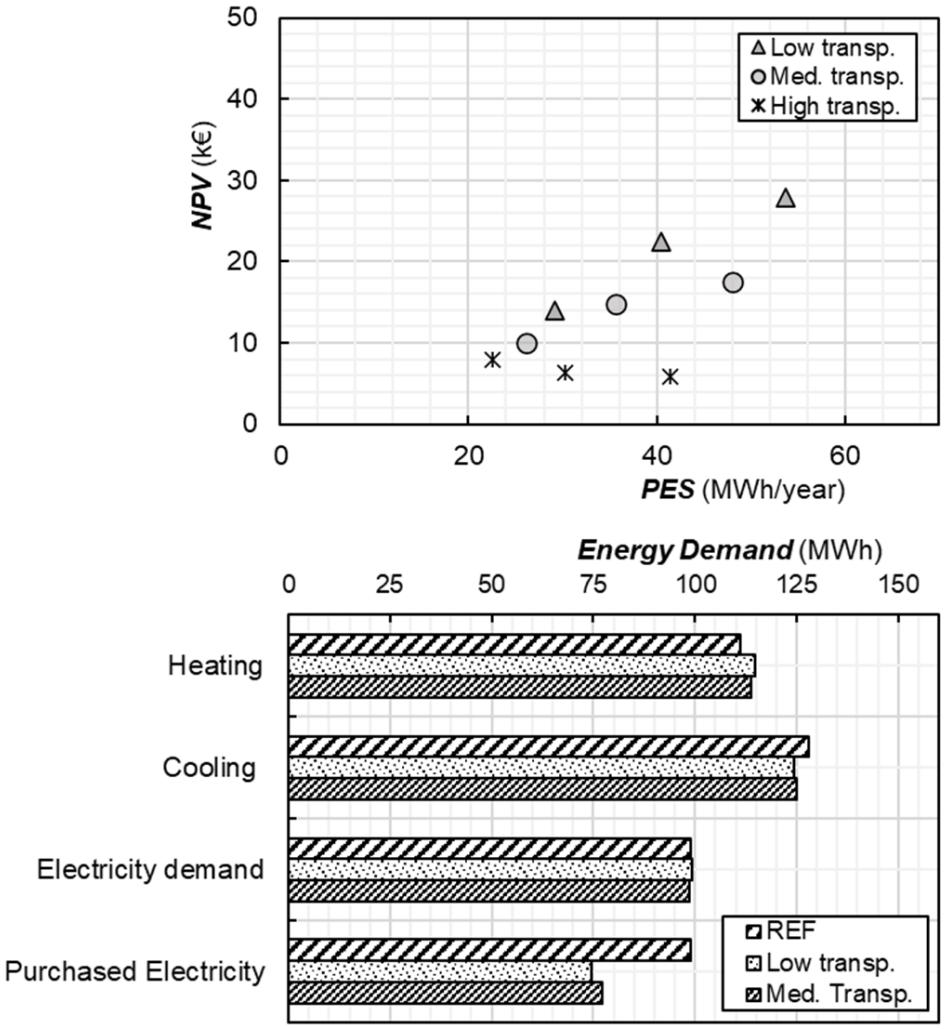


**Figure 19.** Optimal configuration selections and effect on thermal demand of PV glass.

Figure 19 also shows the effects that the adoption of the two selected configurations have on the heating and cooling needs, as well as the electricity demands of the building. As the photovoltaic glass has a very low SHGC, the winter solar gains result is lower than traditional glazing systems which causes the increase of heating loads. However, summertime solar gains are lower with the consequent decrease of cooling loads. The sum of these two effects leads to a slight increase in electricity demand with low-

transparent glasses (99.2 versus 99.1 MWh/year), in contrast, medium-transparent glass entails a slight reduction in electricity demand (99.0 versus 99.1 MWh/year).

Obviously, the main advantage is due to the remarkable reduction in electricity purchased from the grid which leads to ~25% of PES values. The savings of electricity, primary energy, and $CO_2$ are presented in Table 7.

**Table 7.** Metrics related to the implementation of PV glazing.

| | Electricity demand (MWh/year) | Purchased Electricity (MWh/year) | Primary Energy (MWh/year) | $CO_2$ Emission (tons/year) | PES (%) |
|---|---|---|---|---|---|
| **REF** | 99.1 | 99.1 | 215.4 | 43.1 | - |
| **PS3 Low-T** | 99.2 | 74.6 | 162.2 | 32.4 | 24.7 |
| **PS3 Medium-T** | 99.0 | 77.3 | 168.1 | 33.6 | 24.3 |

### 2.3.5 Photovoltaic Canopies

The proposal to install a photovoltaic system, such as the one described, allows a PES value of about 40%. The dynamic analysis conducted on the incoming and outgoing energy fluxes shows a substantial saving of the energy required from the grid. The monthly electricity that is effectively purchased from the power operator is reported in Figure 20. As for previous analyses, further metrics, useful for decision-making, are provided in Table 8.

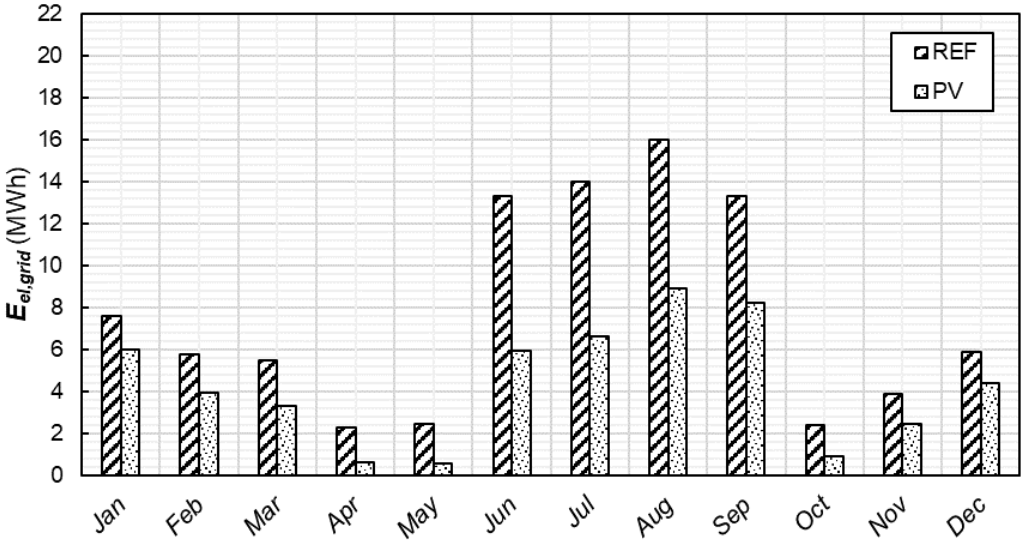


**Figure 20.** Comparison of electricity consumption between reference and proposed systems.

**Table 8.** Metrics related to the implementation of PV canopies.

| | Electricity Demand (MWh/year) | Purchased Electricity (MWh/year) | Primary Energy (MWh/year) | $CO_2$ Emission (tons/year) | PES (%) |
|---|---|---|---|---|---|
| **REF** | 99.1 | 99.1 | 215.4 | 43.1 | - |
| **PS4** | 99.1 | 58.7 | 127.6 | 25.5 | 40.7 |

## 2.3.6 Economic Assessment of Proposed Systems

The analysed energy-saving solutions, shown in Table 9, were also assessed from the economic point of view, taking into account both the energy market prize and capital costs of the considered systems that are provided in the previous sections. All measures lead to significant savings

and attractive returns on investments, among which, the HR provides the highest PI, equal to 7. Although it has the lowest NPV after 20 years, the very low capital costs and the simplicity of the technology make the HR the most profitable solution. More in detail, concerning the thermal power plant, the PS1 provides the highest rate of primary energy saving, nevertheless, such a solution requires substantial investment costs that lead to a SPB value of circa 8 years. Given the possibility of exploiting sea water, a system based on the WSHP is certainly a very efficient solution to take into consideration, despite the higher costs. Indeed, all the alternatives investigated to reduce electricity demand from the power grid are viable from the economic point of view. While both low- and medium-transparency photovoltaic glass (PS3) are less impacting and do not require dedicated supporting structures, traditional PVs (PS4) are more efficient and return major savings (8.1 k EUR/year). However, traditional PVs are more expensive returning higher SPB (~10 years) with PI equal to 0.3.

**Table 9.** Summary of the economic value of considered energy-saving measures.

| | Savings (k EUR/year) | $E_{el}$ Sold (k EUR/year) | SPB (year) | NPV (k EUR) | PI (-) |
|---|---|---|---|---|---|
| **PS1: WSHP** | 5.2 | - | 7.6 | 25.1 | 0.6 |
| **PS2: Heat recovery** | 1.3 | - | 1.6 | 13.9 | 7.0 |
| **PS3: Low-T PVs** | 4.9 | 0.8 | 7.6 | 27.9 | 0.6 |
| **PS3: Medium-T PVs** | 4.3 | 0.7 | 9 | 17.5 | 0.4 |
| **PS4: PV canopies** | 8.1 | 1.3 | 9.8 | 25.0 | 0.3 |

## 2.4 Conclusions

The “Molo Beverello” maritime station in Naples was numerically analysed by means of the developed methodology (described and discussed in Chapter 1) to identify energy efficiency strategies and reduce the overall primary energy consumption of the facility. Specifically, a detailed BIM model of the building was developed in order to automatically generate a reliable energy model exploiting the information included in the BIM database. The optimal modelling level of development (LOD) was chosen after an optimization procedure aimed at identifying the optimal trade-off between model accuracy and time costs of the whole simulation process.

Taking the current status of the project as a baseline, several energy-saving strategies were simulated by the developed workflow to evaluate their conveniences, such as: water-source heat pump, heat recovery from chiller condensers, replacement of window facade with special photovoltaic glass, and replacement of shading systems with photovoltaic canopies. The adoption of the selected measures always showed interesting outcomes from an energy, economic, and environmental points of view. Moreover, it is also interesting to notice how the approach used fits with the needs of the sustainability of buildings, both in the planning and management phases. Both RES-based technologies and advanced HVAC strategies are demonstrated to be fundamentals to increase decarbonisation potential and achieve the goal of net zero of large facilities as the one analysed in this chapter.

# Chapter 3
# Assessing the energy consumption of building stock in railway infrastructures

## Summary

This chapter presents the potential energy consumption reduction due to envelope improvement, increase in system efficiency, and the electrical load reduction in the railway building stock. To this aim, a simulation tool is developed to assess the energy footprint and potential savings of railway buildings, intended to support railway infrastructure operators and decision-makers in planning systematic energy retrofits.

The developed methodology is applied to the Italian railway building stock, modelled with a bottom-up approach, identifying several groups of similar stations (*archetypes*) that are clustered according to real data collected. Afterward, a data-driven model is derived from the detailed dynamic simulations of physics-based models representing the whole building heritage. To provide guidelines for railway operators, a comprehensive analysis is conducted on the considered case study.

The surrogate data-driven model shows $R^2$ coefficients always above 0.93 compared to physics-based model in predicting heating, cooling and electricity demand. Depending on the size of the stations, the mean relative error is in the range 5.9-15.0%. Furthermore, the surrogate model turns out to be an easy-to-use tool to analyse retrofit scenarios and take informed decisions, while the methodology is easily extensible and scalable to other contexts. As proved, the most impactful measure among the ones investigated is the adoption of high-performance lighting systems which entail an overall primary energy saving up to 26%, with very low pay back periods (~1 year).

## 3.1 Introduction

Despite train is the first modern mobility system, rail infrastructures still provide one of the cleanest and most convenient transport modes. Rail infrastructures are responsible for 3% of the global transports energy demand [2], a modest value compared with the share that railways take in the entire transport activity.

Between 2005 and 2015, the European passenger rail activity increased by 8.9%, of which high-speed rail is responsible for 84%. In the same period, China registered a huge increase in railway traffic, passing from 7 billion of passengers per km in 2005 to 386 billion passengers per km in 2015 [62]. This rapid development led to a higher attention to the carbon footprint related to the whole rail industry. Consequently, energy efficiency of non-traction infrastructures such as station buildings, depots and sub-stations are also gaining importance to reduce their energy demand. This segment of the entire rail industry accounts for the 10% of the total energy used in the sector [63] which is even higher within urban areas [64]. At the same time, with the increase of living standards, passengers are demanding increased comfort and greater services in building stations, representing a difficult challenge for the railway industry and transportation sector in general [5]. Accommodating passengers' needs, providing comfortable environment in waiting halls and high quality services can significantly encourage the adoption of rail transports, with significant benefits for the environment [65]. Several scientific works focused on the passengers' comfort aspect [66], and the related energy consumption due to the Heating, Ventilation and Air Conditioning systems (HVAC) [67-70] or electrical equipment [71]. However, while new stations are being built to high standards and very efficiently, the existing building stock of the railway infrastructure is often outdated and does not meet the most modern efficiency standards.

Improving services for passengers in a significant way requires important renovations that can also contribute to reduce the carbon footprint

of railway stations. Of course, energy retrofits enable significant cost savings as well, allowing money to be directed back into improving customer experience and overall company performance [63]. For this reason the railway operators plan to renew their facilities; it is the case of the Italian company Rete Ferroviaria Italiana RFI that planned important investments on the infrastructure between 2022 and 2026 exploiting funds allocated by means of the National Recovery and Resilience Plan (Piano Nazionale di Ripresa e Resilienza, PNRR) by the Italian government [72]. In this framework, benchmarking activities of building stations energy consumption are of significant to railways authorities to develop informed energy efficiency plans.

### 3.1.1 Studies on energy consumption of railway stations

Unlike other building typologies such as residential or commercial [73], train station energy consumptions are poorly investigated on medium or large scale. Moreover, the overall impact of stations on the entire regional or national rail network energy use is rarely considered even in precise studies of the sector, mainly focused on train energy consumption [20, 74]. The assessment of their energy/environmental footprint strongly depends on availability of detailed data of both construction and technological plants. As an example, within a study on the carbon footprint and environmental impact of a Railway-Infrastructure (RI) [75], a synthetic and fast estimation of energy consumption and other environmental indices are provided for 5 relevant building typologies, without providing details about calculation assumptions and building features. Similarly, a large energy consumption survey on traffic buildings in China was conducted in ref. [76]. The authors analysed airports, railway and subway stations. As regards railway stations, the ones located in the hot summer and cold winter areas are the most consuming buildings with an average Energy Use Intensity (EUI) of 147 kWh/m$^2$year, followed by the hot and warm winter area with an EUI of 122 kWh/m$^2$year.

With the aim of identifying the most impacting parameters on energy consumption and provide a benchmarking tool, a Multiple Linear Regression

(MLR) was applied for the energy consumption data collected from 80 large stations in China [77]. Both for heating and cooling energy consumption, the authors identified the building area, number of passenger and regional Gross Domestic Product (GDP), as well as other construction characteristics, as the main influencing factors. With $R^2$ values greater than 0.609, their model was found to be reliable and applicable. The study, however, mainly focuses on large railway stations and does not consider small or medium ones, which could limit the model applicability in such circumstances. Train station complexes are also analysed in ref. [78], where the multiple variable dependent regression model (similar to [77]) was developed to provide a design tool. In addition, the impact of the user typologies in the station complex was also considered adopting both measured and simulation data of typical building usages. Wang et al. report A methodology used to estimate both the energy consumption and the $CO_2$ emission of the Chinese High-Speed Railway infrastructure (HSR) during its life cycle was presented in [79]. The proposed model consists of 3 blocks: Infrastructure cycle, HSR train cycle and operation cycle. It also accounts for the buildings and stations of the network since, "*the energy consumption and carbon emissions during the HSR operation cycle mainly come from the operation of HSR and daily operation of HSR stations"*. The study proves that accurate models are fundamental to reliable Life Cycle Analysis (LCA) in this field.

### 3.1.2 Modelling approaches of building stock

In general, simplified models to evaluate energy consumption of buildings are recognised as useful tools to adopt in the early design stage [80, 81]. Moreover, they are of great importance in decision-making processes since accurate models may provide technical support and data evidence to define informed plans for construction and/or renovation of the entire building stock, including railway stations. Nevertheless, models estimating performance of buildings on large scale rely on availability of on-site measurements or precise energy-related information that are often

inadequate [82]. Several and different approaches to represent performance of building stocks and overcame the lack of energy consumption data have been developed either at urban or national level [83, 84]. The most adopted one is the bottom-up analysis that is based on identification of representative buildings to reflect a large population of buildings [60, 85]. Otherwise, using a top-down approach, groups of buildings are treated as an aggregated energy entity, where energy consumption is correlated to some top-level variables (GDP or other economic indices, weather etc.) [86]. Between the two approaches, the bottom-up analysis better reflects the spatial distribution of energy consumption and allows more accurate and detailed calculation. Nevertheless, the effort to develop the model is higher due to the need of defining a number of building *archetypes* that will be simulated and allocated in predefined building set. Usually, single *archetypes* are simulated by physics-based models to dynamically calculate their energy consumption [87, 88].

In this context, several urban building energy modelling procedures and tools based on the most used state-of-the-art Building Energy Modelling (BEM) software (i.e. *EnergyPlus*, *Modelica*, *TRNSYS*, etc.) have been developed [89, 90]. Such tools require building geometry, location, construction types, HVAC system and operation patterns, and weather data as input [91] and provide hourly or sub-hourly energy consumption profiles [16]. By parametrization of *archetypes*, urban BEM tools has the capability of good representing the building diversity, thus, investigating energy management strategies and retrofit plans for cities or districts. To support the spread of the urban BEM methodology, new data format such as *CityGML* [92] or *GeoJSON* [93] have been developed to facilitate urban building modelling and create standards for 3D building shape implementation [94]. However, although open-source Geographical Information Systems (GIS) databases are rich of information, they lack comprehensive building data. Therefore, it is still required a big effort for urban modellers to define geometry and physical properties of *archetypes* [95]. In order to bridge this gap, some projects aiming at identify and classify

building typologies of European countries were developed to support building experts [96, 97].

### 3.1.3 Considerations and aim of the work

As reported in [98], the majority of the current studies in the field of building stock energy analysis focus on residential sector. Only few studies addressed office buildings or non-residential buildings, which is understandable since homes represent most of the built environment. Furthermore, according to the literature review, no studies were carried out by considering a whole building stock, and specifically the railway stations building stock, and none of them proposes a combined approach based on BEM and archetypes to derive data driven models [99]. Defining a baseline and benchmarking stations energy demand - whether these are small regional stations or large terminal for national or international traffic - is fundamental for railway authorities to develop a sustainable plan and reduce both expensive waste of energy and harmful greenhouse gas emission.

In this framework, this chapter focuses on a novel approach proposed to assess the energy consumption and the potential energy retrofit actions for the railway stations building heritage. The approach adopted is based on the dynamic simulation of detailed physics-based building models, conducted by means of a BEM tool. The investigated stations are owned by the main Italian railway operator, Rete Ferroviaria Italiana (RFI), that manages more than 2000 stations spread throughout the Italian peninsula. According to the available data, several *archetypes* are defined by clustering similar stations, following a bottom-up approach. The developed physic-based model was then used to develop a *surrogate* mathematical model to provide an easy-to-use tool for the interested stakeholders to estimate the end-use energy consumption of the station buildings.

The developed tool was adopted to analyse some retrofit scenarios such as envelope or HVAC system improvement, and reduction of electric loads. A comprehensive energy and economic analysis of the Italian railway building stock is also presented. The analysis has a twofold aim, such as: i)

proving the feasibility and scalability of the methodology to be applied to other cases and building stocks, and ii) supporting the investment planning of the Italian railway operator (RFI) as part of the National Recovery and Resilience Plan (Piano Nazionale di Ripresa e Resilienza, PNRR) which amounts to 24 billion of euros.

## 3.2 Materials and method

This section includes the description of the key steps of the proposed methodology, structured by following the actual workflow adopted to carry out the study. Starting from the analysis of the selected railway infrastructure, the simulation model was built with a bottom-up approach involving building *archetypes,* extrapolated from the available data [57], [100]. All those phases are schematically summarized in Figure 21 and described in detail in the following subsections.

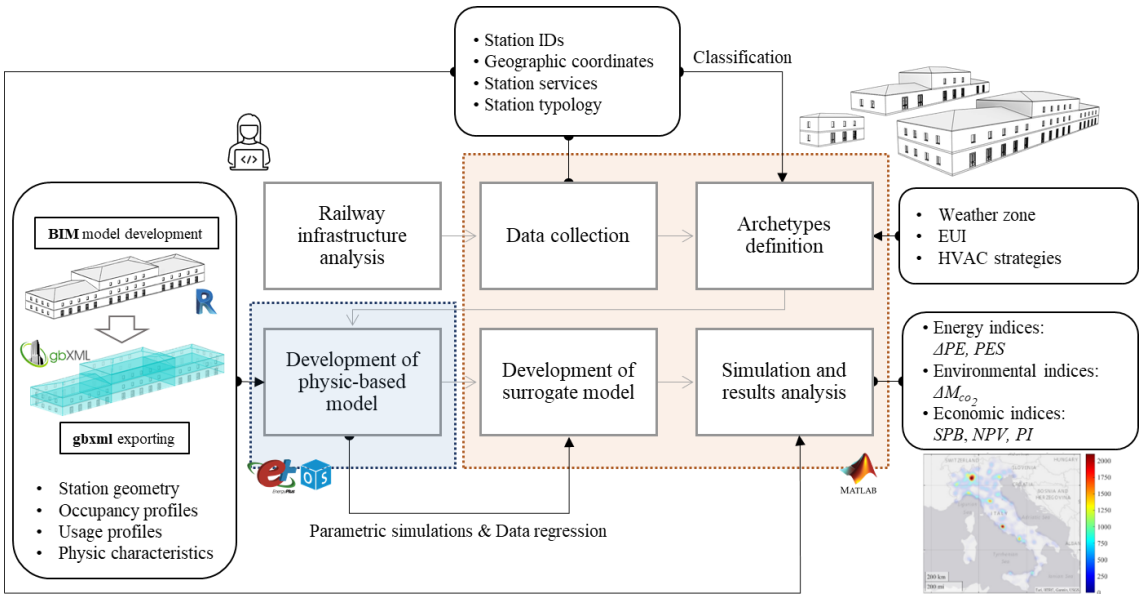


**Figure 21.** Schematic workflow of the methodology adopted

In sections 3.2.1, the analysed case of the Italian passenger stations and the procedure to gather the available data and classify the stations are respectively presented. Afterword, building *archetypes* modelling and mathematical formulation of the developed surrogate model are described in sections 3.2.2 and 3.2.3, while the economic and energy performance assessment method is reported in section 3.2.4. The proposed methodology was exploited to also provide a graphical visualization of energy indexes, by showing the geographical distribution of the impact of the renovation measures.

### 3.2.1 Case study: the Italian railway building stock

The main Italian national railway network is entirely managed by RFI and runs through all the Italian regions and their provinces. In 2020, RFI registered 16782 km of active rail lines (mostly electrified, 72%), of which 1467 km of high-speed rails [101].

Circa 2200 passenger stations serve the rail network. As shown in Figure 22, Italian stations are distributed throughout the national territory, however, a higher concentration is recorded in the north side or near the most populated cities, i.e. Rome, Milan, Naples and Turin. RFI owns and operates over 2000 stations, while the rest are operated by regional or local authorities. Due to the lack of data, stations of regional or local operators are excluded from the analysis.

Although there are several modern stations from an architectural point of view, most of them have a typical style and construction typology that have been reproduced when built since the 20$^{th}$ century.

Currently, the Italian railway authority is involved in an innovation process and places its commitment against climate change and waste energy reduction as one of the priority objectives of its business model.


**Figure 22.** Geographic distribution of Italian railway stations. Data from [62], [63].

Data availability is one of the main challenges of building stock analyses and urban energy modelling. This study is based on the official information provided by RFI and other public databases [62], [63]. Specifically, data related to each of the 2070 considered stations are retrieved by an automated procedure. Specifically, a Matlab routine was suitably developed to query the abovementioned open databases, reducing the time and effort

of data collection. The following data were collected: station ID, geographic coordinates, and the types of services provided to passengers.

The information available allowed to define a clusterization criteria to group stations in order to also provide results and graphical visualization of energy indexes, by showing the geographical distribution of the impact of the renovation measures. The aggregation of similar stations was defined according with the official administrative subdivision of the Italian territory [102].

Moreover, RFI identifies stations on the basis of a classification system that is based on passengers traffic, station attraction, interchange capacity and commercial services quality [103]. Four categories are defined:

- *Bronze*. The facilities consist of small stations and stops that may be unstaffed, with the passenger building closed to public, and equipped with services only for regional or local traffic. Generally, the average number of users is <500 daily users.
- *Silver*. Medium-to-small facilities that may be unattended, equipped only with urban, sub-urban or metropolitan services. The average number of users is >2500 daily users (sometimes >4000 daily users).
- *Gold.* Medium or large plants equipped with high quality services to travellers for long, medium and short distances. Specific services for non-travelling visitors are generally guaranteed. The average number of users is >10000 daily users.
- *Platinum*. Large plants equipped with high quality passenger services for long, medium and short distances and High Speed train. Specific services for non-travelling visitors are always guaranteed. The average number of users is >25000 daily users.

It should be underlined that the classification system adopted by the Italian railway operator does not account for any energy or sustainability indices or protocols. The sole grouping criteria adopted are the relevance

and the size of the stations. Hereinafter, the same nomenclature adopted by RFI is considered for the classification in the proposed methodology. Specifically, the four considered categories are referred to as stops (*Bronze*), small stations (*Silver*), medium stations (*Gold*), and large stations (*Platinum*). The geographic distribution of the railway stations as classified by RFI is provided in Figure 23.


**Figure 23.** Geographic distribution of RFI railway stations, classified in *Bronze*, *Silver*, *Gold* and *Platinum* stations. Data from [62], [63].

As mentioned above, stations services (reported in Table 10) are also provided for each station of the network. This information reflects the importance of the considered facility and is useful to define its specific energy consumption.

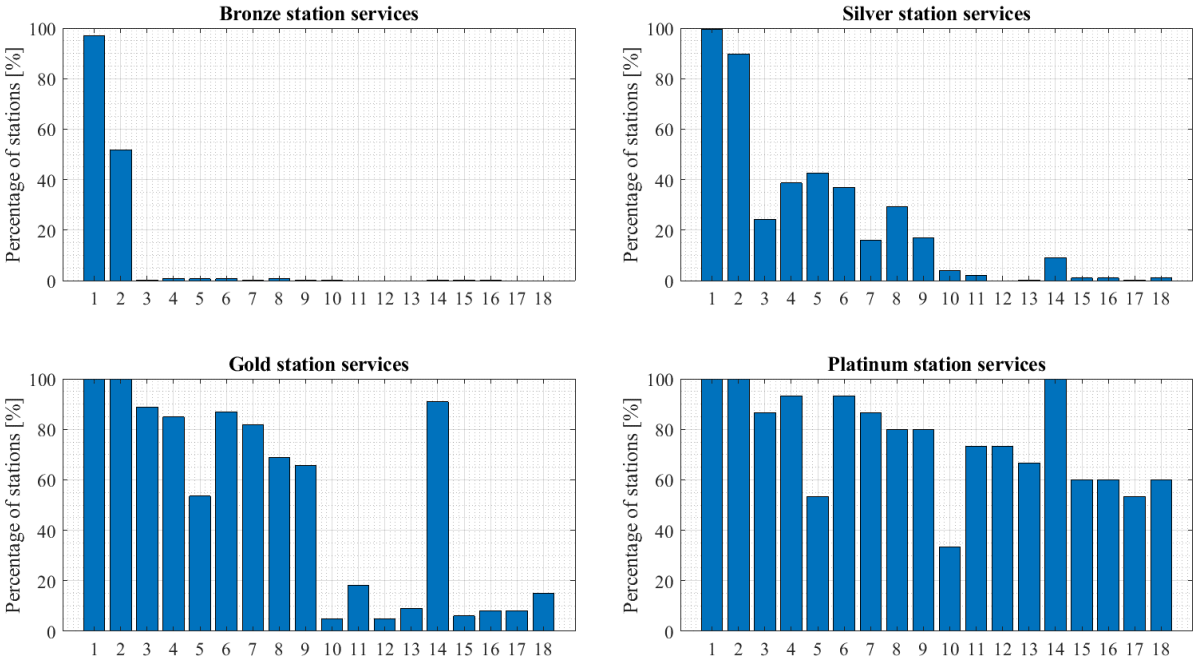


**Figure 24.** Services of stations (the corresponding ID number of services is reported in Table 10).

It is worth noticing that in Figure 22 the marker size of RFI stations is proportional to the number of services provided by the station facilities. Furthermore, the number of stations facilities that offers specific services are reported in Figure 24. Services are also marked with the symbols E (Energy consuming services) and C (Commercial services) for classification purpose which will help assessment of energy consumption.

**Table 10.** Services provided by the station facility.

| | *Services* | *ID number and typology* | |
|---|---|---|---|
| **Accessibility** | Track accessibility | - | - |
| | Assistance services for people with disabilities | - | - |
| | Accessible toilets | - | - |
| | Parking with reserved places | - | - |
| | Sound public information systems | 1 | E |
| | Visual public information systems | 2 | E |
| | Accessible ticket office | - | - |
| **Services** | Ticket office | 3 | E |
| | Toilet | 4 | E |
| | Spaces for waiting | 5 | - |
| | Bar, cafeteria, restaurant | 6 | C, E |
| | Vending machines for snacks and drinks | 7 | E |
| | Tobacco | 8 | C, E |
| | Newsstand | 9 | C, E |
| | Tourist / cultural information points | 10 | C, E |
| | Shopping | 11 | C, E |
| | Travel services | 12 | C, E |
| | Luggage storage | 13 | E |
| | Security | 14 | C, E |
| | Supermarkets, groceries, minimarkets | 15 | C, E |
| | Pharmacy | 16 | C, E |
| | Library | 17 | C, E |
| | Financial and postal services | 18 | C, E |
| **Integrated mobility** | Local public transport | - | - |
| | Bike | - | - |
| | Auto Motorcycle | - | - |
| | Direct connection with the airport | - | - |

A reliable modelling of station *archetypes* needs detailed data about construction typologies, building size and facility operation in order to derive typical stations that represent a larger group of stations. However, as no GIS data about size and characteristics of the stations are provided, the procedure to define *archetypes* was made by observations of satellite images. Specifically, due to the large population of buildings considered in the study (*Bronze (Stops)*, 1043; *Silver (Small)*, 802; *Gold (Medium)*, 99; *Platinum (Large)*, 15), the 10% of each station category has been randomly sampled to statistically represent the entire population of the category (*Bronze (Stops)*, 104; *Silver (Small)*, 80; *Gold (Medium)*, 10; *Platinum (Large)*, -). Then, satellite images of the station sample were detailed analysed to identify one or more common building prototypes which may faithfully feature the station category. Their volumes were evaluated by measuring both the footprint areas and the building elevations. Three building prototypes were identified to respectively represent the *Bronze*, *Silver* and *Gold* stations. They have been built based on the average volumes estimated respectively as high as 1200 $m^3$, 3000 $m^3$ and 15000 $m^3$ for the *Bronze (Stops)*, *Silver (Small)* and *Gold (Medium)* stations. It is worth noticing that *Platinum (Large)* stations were excluded from the analysis because they are extremely heterogeneous and require careful considerations. Based on the three selected building prototypes, different *archetypes* are identified by considering the following assumptions:

1. 5 climatic conditions according to Italian weather zones, classified by Heating Degree Days (*HDD*) and Cooling Degree Days (*CDD*): Zone B, *600≤ HDD≤ 900*; Zone C, *901≤ HDD ≤ 1400*; Zone D, *1401≤ HDD≤2100*; Zone E, *2101≤ HDD≤3000*; Zone F, *HDD>3000*);
2. 4 heating and cooling strategies (no HVAC systems, HVAC only in waiting halls, HVAC only in workplaces/services room, HVAC both in waiting halls and in workplaces/services rooms);
3. 4 different electric load intensities (5, 10, 15, 20 W/m$^2$).

By combining these parameters, 80 different archetypes are generated starting from each building *prototype*. In Figure 25, the 3D models of the selected prototypes, as well as a logical scheme of the described workflow are reported.

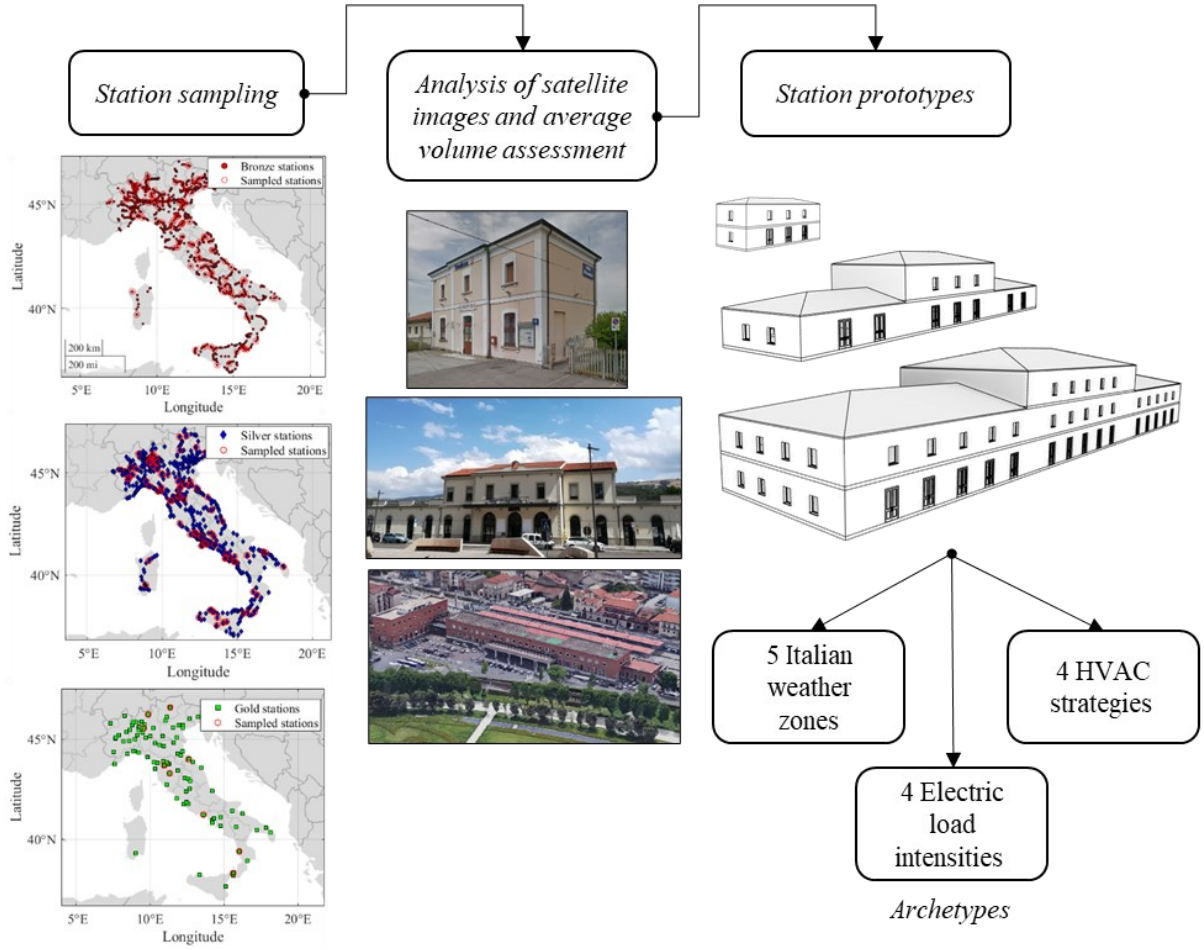


**Figure 25.** Archetypes identification workflow.

## 3.2.2 Energy modelling of *archetypes*

Once defined both station prototypes and all *archetypes,* the physic-based energy models are developed. The three-dimensional models were carried out by means of the BIM (Building Information Modeling) software Autodesk Revit. It allows to create, and export through *gbxml* format [104], a detailed energy model leveraging all the energy-related information inputted in the BIM model, such as geometry, construction materials, zones, occupancy schedules, lighting, set-point temperatures, ventilations, etc. So, after the three station prototypes (*Bronze (Stops)*, *Silver (Small)* and *Gold*

*(Medium)*) are modelled, the energy models of the prototype were exported in *OpenStudio* environment to further manipulate the model and define the basis for *archetypes* simulations in EnergyPlus. The data transfer from BIM to BEM software relying on *gbxml* format is a completely automated process performed by means of the *Revit Systems Analysis*, which is a built-in feature of *Autodesk Revit 2021* [68].

In Figure 26, the BIM and BEM models of the *Gold* stations are shown. Here, it is also possible to see the space types that have been considered. For simulation purposes, each space has been defined as an independent thermal zone. According to building *archetypes* defined in the previous section, the thermal zones conditioned by HVAC systems are Offices, Waiting hall and Services. *Bronze* and *Silver* stations are not reported for the sake of brevity since their modelling is quite similar. As concern thermal zones, the only difference in the *Gold* stations is the presence of office spaces on the upper floor that are not considered in the other building prototypes. The parameters inputted in the energy model for conditioned thermal zones are summarised in Table 11, Table 12 and Table 13. Please note that other space types/thermal zones shown in Figure 26 are not conditioned, however, they are occupied so lighting and equipment power densities are also considered.

As regards to the air-conditioning plants modelling, the simulations are performed by considering the station buildings equipped with ideal HVAC systems to estimate the heating and cooling energy demands. Then, the primary energy required is calculated by means of performance coefficients of real systems such as heating boilers or heat pumps/chillers, according to equation (16). Given the purpose of the research study and to keep the analysis as less case specific as possible, the HVAC systems is not modelled in detail, whereas the surrogate model is derived from the physics-based building heating and cooling demands (as described in section 3.2.3). The developed model is intended to be a general tool for analyses in a wider domain than that of a single building, useful in planning and life cycle analysis.

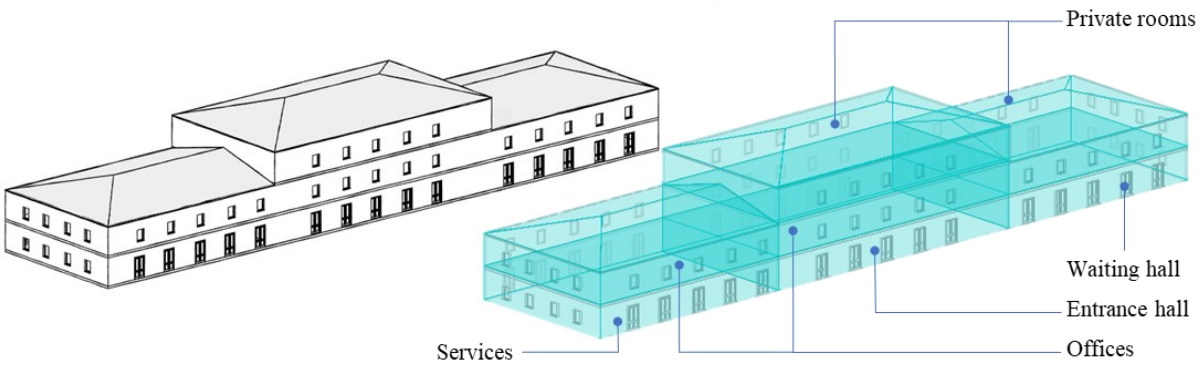


**Figure 26.** Energy model and zoning.

**Table 11.** Input parameters of energy model for *Bronze* stations.

| | | *Services* | | *Waiting hall* | | *Offices* | |
|---|---|---|---|---|---|---|---|
| | **Parameter** | **Settings** | **Value** | **Settings** | **Value** | **Settings** | **Value** |
| **Bronze (Stops)** | Occupancy schedule [h] | 6:00 – 21:00 | 1 [people/m2] | 6:00 – 21:00 | 1 [people/m2] | - | - |
| | Lighting schedule [h] | 18:00 – 9:00 | 12 [W/m2] | 18:00 – 9:00 | 12 [W/m2] | - | - |
| | Appliances schedule [h] | 0:00 – 24:00 | 5, 10, 15, 20 [W/m2] | 0:00 – 24:00 | 6 [W/m2] | - | - |
| | HVAC system | Ideal loads air system | ON; OFF | Ideal loads air system | ON; OFF | - | - |
| | Heating set-point [h] | 6:00 – 21:00 | 20 [°C] | 6:00 – 21:00 | 20 [°C] | - | - |
| | Cooling set-point [h] | 6:00 – 21:00 | 26 [°C] | 6:00 – 21:00 | 26 [°C] | - | - |
| | Ventilation | Outdoor air flow air changes per hour | 8 [ACH] | Outdoor air flow air changes per hour | 8 [ACH] | - | - |

**Table 12.** Input parameters of energy model for *Silver* stations.

| | | *Services* | | *Waiting hall* | | *Offices* | |
|---|---|---|---|---|---|---|---|
| | **Parameter** | **Settings** | **Value** | **Settings** | **Value** | **Settings** | **Value** |
| **Silver (Small)** | Occupancy schedule [h] | 6:00 – 21:00 | 1 [people/m2] | 6:00 – 21:00 | 1 [people/m2] | - | - |
| | Lighting schedule [h] | 18:00 – 9:00 | 12 [W/m$^2$] | 18:00 – 9:00 | 12 [W/m2] | - | - |
| | Appliances schedule [h] | 0:00 – 24:00 | 5, 10, 15, 20 [W/m2] | 0:00 – 24:00 | 6 [W/m2] | - | - |
| | HVAC system | Ideal loads air system | ON; OFF | Ideal loads air system | ON; OFF | - | - |
| | Heating set-point [h] | 6:00 – 21:00 | 20 [°C] | 6:00 – 21:00 | 20 [°C] | - | - |
| | Cooling set-point [h] | 6:00 – 21:00 | 26 [°C] | 6:00 – 21:00 | 26 [°C] | - | - |
| | Ventilation | Outdoor air flow air changes per hour | 8 [ACH] | Outdoor air flow air changes per hour | 8 [ACH] | - | - |

**Table 13.** Input parameters of energy model for *Gold* stations.

| | | *Services* | | *Waiting hall* | | *Offices* | |
|---|---|---|---|---|---|---|---|
| | **Parameter** | **Settings** | **Value** | **Settings** | **Value** | **Settings** | **Value** |
| **Gold (Medium)** | Occupancy schedule [h] | 6:00 – 21:00 | 1 [people/m2] | 6:00 – 21:00 | 1 [people/m2] | 6:00 – 21:00 | 0.12 [people/m2] |
| | Lighting schedule [h] | 18:00 – 9:00 | 12 [W/m$^2$] | 18:00 – 9:00 | 12 [W/m2] | 18:00 – 9:00 | 12 [W/m2] |
| | Appliances schedule [h] | 0:00 – 24:00 | 5, 10, 15, 20 [W/m2] | 0:00 – 24:00 | 6 [W/m2] | 0:00 – 24:00 | 6 [W/m2] |
| | HVAC system | Ideal loads air system | ON; OFF | Ideal loads air system | ON; OFF | Ideal loads air system | ON |
| | Heating set-point [h] | 6:00 – 21:00 | 20 [°C] | 6:00 – 21:00 | 20 [°C] | 6:00 – 21:00 | 20 [°C] |
| | Cooling set-point [h] | 6:00 – 21:00 | 26 [°C] | 6:00 – 21:00 | 26 [°C] | 6:00 – 21:00 | 26 [°C] |
| | Ventilation | Outdoor air flow air changes per hour | 8 [ACH] | Outdoor air flow air changes per hour | 8 [ACH] | Outdoor air flow air changes per hour | 8 [ACH] |

As said, *archetypes* are generated by varying HVAC operation strategies, electric load intensities and weather conditions. A suitable algorithm developed in Matlab programmatically modified the *EnergyPlus*

input data file (*idf*). To do so, the *idf* generated from the *OpenStudio* models were manually modified to define the varying parameters (e.g. U-value and internal thermal loads) that are then parsed by the purposely developed *Matlab* routine. The 5 weather files that represents the considered weather zones are collected from the public repository “Gianni De Giorgio” (IGDG). Specifically, the weather files of Palermo, Bari, Roma, Milano and Tarvisio were used for the weather zones B, C, D, E and F, respectively.

Finally, dynamic simulations of all the *archetypes* are performed with a timestep of 0.25 hours, providing accurate results of building energy needs. The outputs of the dynamic simulations are then integrated on annual basis obtaining the heating $E_{nd,h}$, cooling $E_{nd,c}$, and electricity $E_{nd,el}$ demands. As *archetypes* are derived from the simplification of the entire station building stock, the $E_{nd,h}$, $E_{nd,c}$, and $E_{nd,el}$ indices, which refer to a specific *archetype,* are assumed to represent all the stations with similar characteristics (same *archetype*), as typically occurs in bottom-up modelling approaches.

It worth of noticing that *archetypes* are simulated according to the prescriptions of the Appendix G of ASHRAE Standard 90.1 to provide building energy consumptions that are neutral to building orientation.

### 3.2.3 Surrogate model

Detailed physics-based building energy models require a high number of input parameters and it is a very time-consuming task. Therefore, simplified models based on data regression may be useful tools for designers and benchmark purposes [105, 106].

To define a reliable and a simple surrogate model to be used as an alternative to the detailed model, a linear regression approach was adopted. Heating and cooling needs of *archetypes*, $E_{nd,h}$ and $E_{nd,c}$, resulted from the physics-based model, were fitted by a first-order equation function of *HDD* and *CDD*. Afterwards, correlation coefficients were adjusted to take into account the effect of fraction of conditioned volume (heated and cooled

volume to total volume ratios, $V_h/V$ and $V_c/V$), the wall *U-value*, and the electric equipment load intensity ($I_{el,loads}$). Furthermore, a linear equation depending on total electric light load intensity $I_{el,lights}$ and the total electric equipment load intensity $I_{el,equipment}$ is derived to calculate the total electricity demand $E_{nd,el}$. The progressive steps of the data regression procedure, which leads to equations (11), (12) and (13), are summarised in Figure 27. Curve fitting was carried out by the curve fitting tool in Matlab environment.

$$E_{nd,el} = a_{el} \cdot I_{el,lights} + b_{el} \cdot I_{el,equipment} \tag{11}$$

$$E_{nd,h} = \left(\left(c_{h,1} + c_{h,2} \cdot \frac{V_h}{V}\right) \cdot \left(c_{h,3} + c_{h,4} \cdot U\right) + \left(c_{h,5} + c_{h,6} \cdot \frac{V_h}{V}\right) \cdot \left(c_{h,7} + c_{h,8} \cdot U\right) \cdot HDD\right) \cdot \left(c_{h,9} + c_{h,10} \cdot I_{el,loads}\right) \tag{12}$$

$$E_{nd,c} = \left(\left(c_{c,1} + c_{c,2} \cdot \frac{V_c}{V}\right) \cdot \left(c_{c,3} + c_{c,4} \cdot U\right) + \left(c_{c,5} + c_{c,6} \cdot \frac{V_c}{V}\right) \cdot \left(c_{c,7} + c_{c,8} \cdot U\right) \cdot CDD\right) \cdot \left(c_{c,9} + c_{c,10} \cdot I_{el,loads}\right) \tag{13}$$

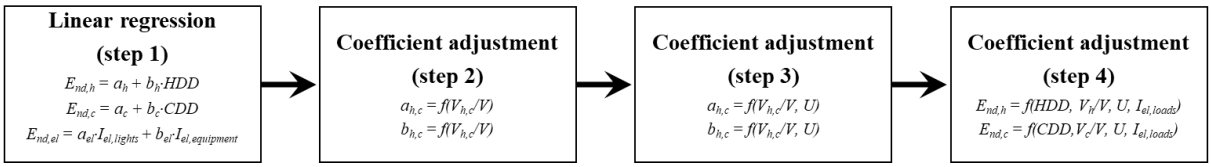


**Figure 27.** Schematic procedure of the surrogate model development.

The accuracy of the surrogate model was evaluated by the coefficient of determination ($R^2$) which is an index of the goodness of how the surrogate model approximates observations [107]. $R^2$ is function of the *i-th* expected output $x_i$, the *i-th* predicted output $y_i$, and the average value of all the expected output $\bar{x}$. It is calculated by equation (14).

$$R^2 = 1 - \frac{\sum_i \left(x_i - y_i\right)^2}{\sum_i \left(x_i - \bar{x}\right)^2} \tag{14}$$

The surrogate model will be used to calculate energy consumption of the entire Italian stations building stock according to the available data described so far. In addition, the mean relative error *e* was calculated according to equation (15), which is the mean percentage deviation between surrogate and physic-based models:

$$e = \frac{1}{N}\sum_i \frac{\left(x_i - y_i\right)}{x_i} \tag{15}$$

### 3.2.4 Energy, economic and environmental assessment

To calculate the energy and economic performance of the system, several indices are calculated for both the proposed system and the reference one [108].

The primary energy (*PE*) is calculated by considering the primary energy conversion factors $\eta_{el}$, $\eta_h$ and $\eta_c$ for electricity, heating, and cooling, as:

$$PE = \frac{E_{nd,el}}{\eta_{el}} + \frac{E_{nd,h}}{\eta_h} + \frac{E_{nd,c}}{\eta_c} \tag{16}$$

The primary energy saved ($\Delta PE$) and the primary energy saving (*PES*) of the proposed scenarios respect to the reference case, are calculated as:

$$\Delta PE = PE_{reference} - PE_{proposed} \tag{17}$$

$$PES = 1 - \frac{PE_{proposed}}{PE_{reference}} \tag{18}$$

To assess the economic profitability the Simple Pay Back period (*SPB*) is calculated as:

$$SPB = \frac{I_0}{\Delta C} \tag{19}$$

where $I_0$ is the investment cost and $\Delta C$ are the cost difference between reference and proposed scenarios. At last, net present value (*NPV*) and profit index (*PI*) are also evaluated as:

$$NPV = \Delta C \cdot \left\{ \frac{1}{p} \cdot \left[ 1 - \frac{1}{(1+p)^N} \right] \right\} - I_0 \tag{20}$$

here $p$ is the interest rate and $N$ is the time span.

$$PI = \frac{NPV}{I_0} \tag{21}$$

Finally, the environmental performance is assessed by the $\Delta M_{CO_2}$ index that represents the total equivalent $CO_2$ emitted. The indicator is calculated by:

$$\Delta M_{CO_2} = E_{el} \cdot F_{el} + E_g \cdot F_{ng} \tag{22}$$

Equation (11) involves the energy consumption provided by electricity $E_{el}$ and natural gas $E_g$, as well as the related emission factors $F_{el}$ and $F_{ng}$.

## 3.3 Results and discussion

In this section, both the data regression procedure and simulation results of the carried analysis are presented and discussed.

The surrogate model is defined by equations (11), (12) and (13) that are fully characterised by means of several constant coefficients for each station category, reported in Table 14. Users are required to input 3 input variables to calculate heating and cooling needs, and 2 input variables for electricity demand, which are much fewer inputs compared to detailed physics models such as the ones developed for *archetypes*.

**Table 14.** Surrogate model coefficients.

| | | Bronze | | Silver | | Gold |
|---|---|---|---|---|---|---|
| **Heating demand** | $c_{h,1}$ | -0.134 | $c_{h,1}$ | 0.366 | $c_{h,1}$ | 4.896 |
| | $c_{h,2}$ | -33.808 | $c_{h,2}$ | -10.052 | $c_{h,2}$ | 18.507 |
| | $c_{h,3}$ | 1.056 | $c_{h,3}$ | 1.137 | $c_{h,3}$ | 0.908 |
| | $c_{h,4}$ | -0.058 | $c_{h,4}$ | -0.164 | $c_{h,4}$ | 0.123 |
| | $c_{h,5}$ | 0.000 | $c_{h,5}$ | 0.000 | $c_{h,5}$ | 0.011 |
| | $c_{h,6}$ | 0.171 | $c_{h,6}$ | 0.209 | $c_{h,6}$ | 0.194 |
| | $c_{h,7}$ | 0.911 | $c_{h,7}$ | 0.970 | $c_{h,7}$ | 0.971 |
| | $c_{h,8}$ | 0.093 | $c_{h,8}$ | 0.036 | $c_{h,8}$ | 0.039 |
| | $c_{h,9}$ | 1.073 | $c_{h,9}$ | 1.054 | $c_{h,9}$ | 1.015 |
| | $c_{h,10}$ | -0.006 | $c_{h,10}$ | -0.004 | $c_{h,10}$ | -0.001 |
| **Cooling demand** | $c_{c,1}$ | 0.044 | $c_{c,1}$ | -0.209 | $c_{c,1}$ | -1.072 |
| | $c_{c,2}$ | -6.789 | $c_{c,2}$ | -2.659 | $c_{c,2}$ | -3.669 |
| | $c_{c,3}$ | 0.908 | $c_{c,3}$ | 0.908 | $c_{c,3}$ | 0.946 |
| | $c_{c,4}$ | 0.096 | $c_{c,4}$ | 0.096 | $c_{c,4}$ | 0.073 |
| | $c_{c,5}$ | 0.001 | $c_{c,5}$ | 0.001 | $c_{c,5}$ | -0.008 |
| | $c_{c,6}$ | 0.423 | $c_{c,6}$ | 0.336 | $c_{c,6}$ | 0.201 |
| | $c_{c,7}$ | 0.910 | $c_{c,7}$ | 0.910 | $c_{c,7}$ | 1.011 |
| | $c_{c,8}$ | 0.094 | $c_{c,8}$ | 0.094 | $c_{c,8}$ | 0.015 |
| | $c_{c,9}$ | 0.797 | $c_{c,9}$ | 0.807 | $c_{c,9}$ | 0.974 |
| | $c_{c,10}$ | 0.016 | $c_{c,10}$ | 0.015 | $c_{c,10}$ | 0.002 |
| **Electricity demand** | $a_{el}$ | 3.968 | $a_{el}$ | 3.968 | $a_{el}$ | 3.968 |
| | $b_{el}$ | 6.308 | $b_{el}$ | 6.308 | $b_{el}$ | 6.308 |

The surrogate model provides very accurate results and reflects with good agreement the outputs of the physics-based model as shown in the charts of Figure 28, Figure 29, and Figure 30.

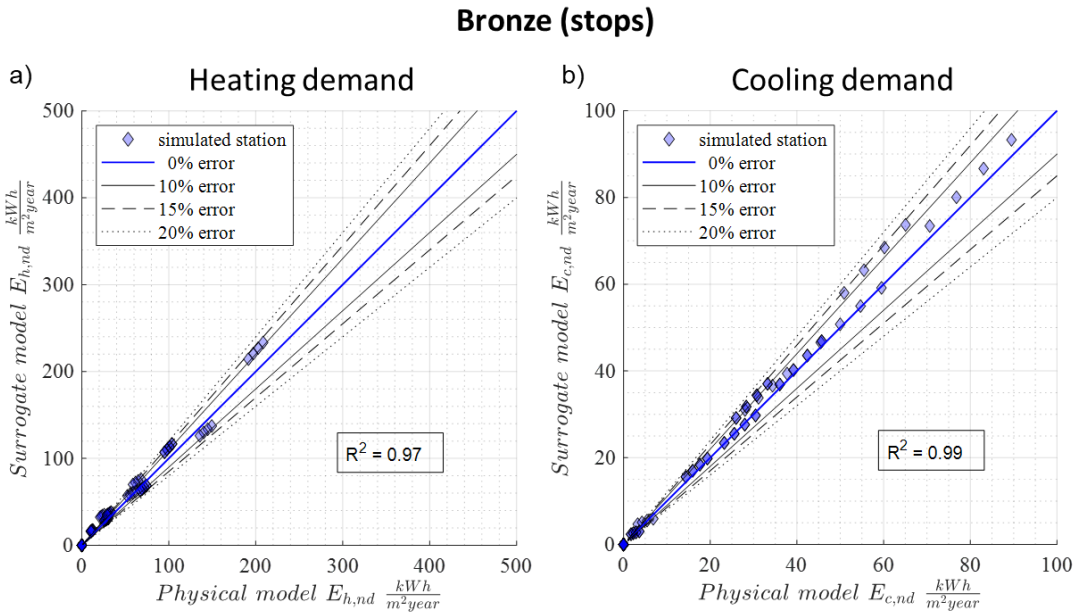


**Figure 28.** Model accuracy comparison for Bronze stations, a) heating needs and b) cooling needs.

Specifically, in the figures both the heating (a) and cooling needs (b) calculated by the surrogate model for different station *archetypes* are plotted against the same outputs of the physic model. The relative errors are mostly within the range ±20% with some exceptions for low $E_{h,nd}$ and $E_{c,nd}$ values. However, the mean relative errors, calculated by means of equation (15) taking into account all the *archetypes* of the considered station typologies (*Bronze (Stops)*, *Silver (Small)*, *Gold (Medium)*), are equal to 15.0 %, 6.7%, and 5.9% for $E_{h,nd}$, while 6.2%, 7.7%, and 9.8% for $E_{h,nd}$. As expected, the higher error is registered for *Bronze (Stops)* stations as $E_{h,nd}$ values are lower compared to the other station categories. The determination coefficient $R^2$, calculated by equation (14), is also reported for each station category. It should be noted that $R^2$ is greater than 0.97 in case of *Bronze (Stops)* and *Silver (Small)* stations, while it is equal to 0.93 in predicting the cooling demand of *Gold (Medium)* stations.

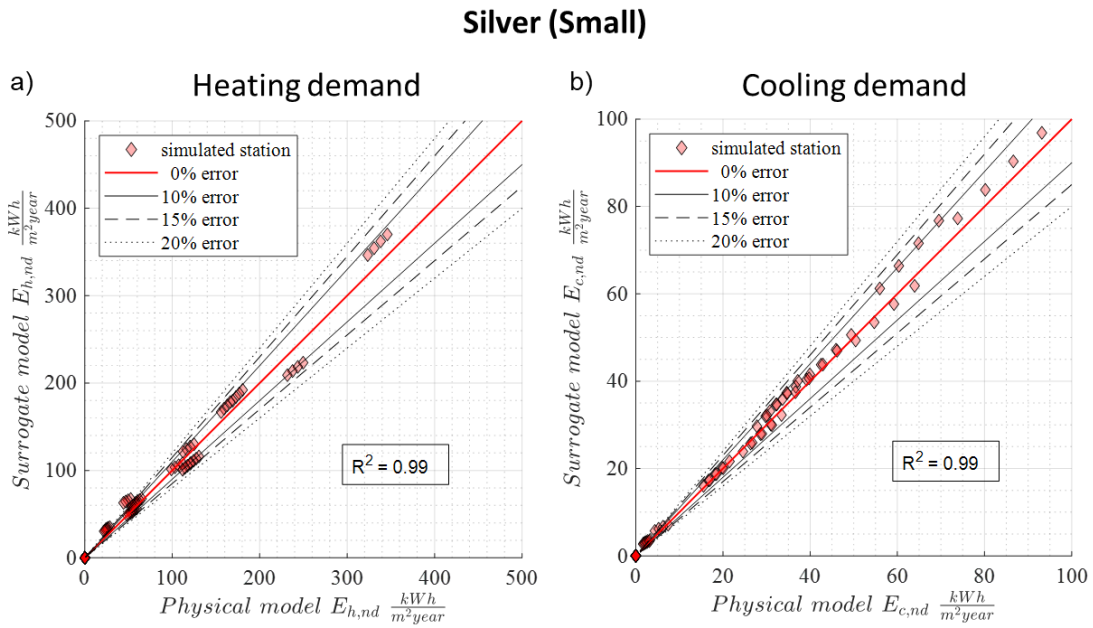


**Figure 29.** Model accuracy comparison for Silver stations, a) heating needs and b) cooling needs.

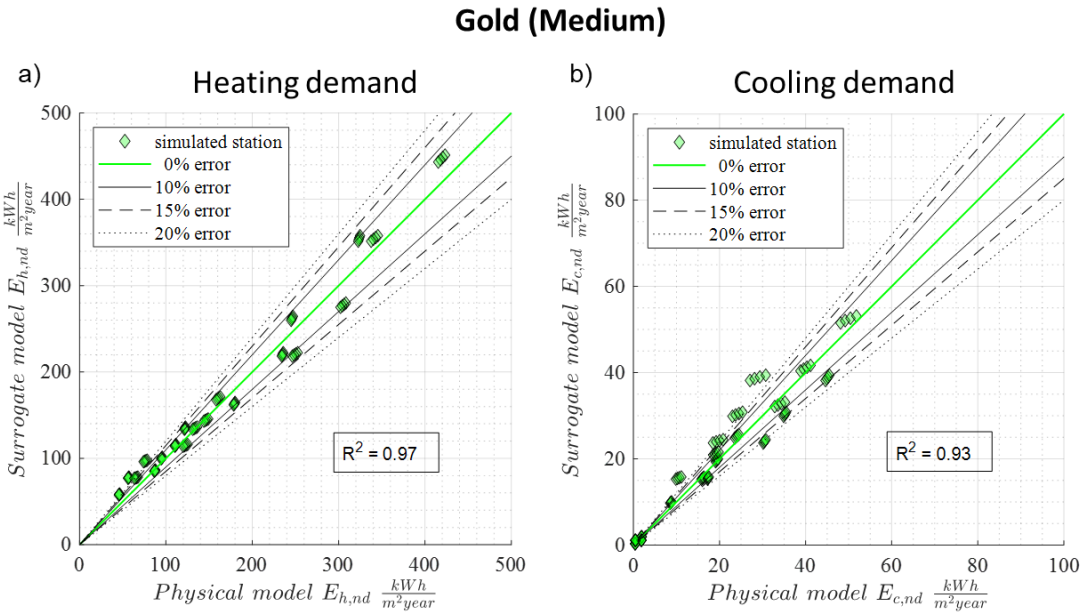


**Figure 30.** Model accuracy comparison for Gold stations, a) heating needs and b) cooling needs.

In this case, the lower value of determination coefficient is due to the increasing complexity of the station building compared to the simplicity of the surrogate model.

The high values of $R^2$ obtained prove the validity of the proposed approach. As also mentioned in the introductory section of this chapter, regression models with even lower values of the coefficient of determination ($R^2$) have been obtained and applied in the literature. However, it must be considered that these models are derived through a *top-down* approach using consumption data and available indices of the buildings investigated. As regards the approach used in this study (i.e., the *bottom-up*), the greatest uncertainty lies in the input data, i.e., in the selection and physical modelling of the archetypes, as well as in their ability to represent the stock of buildings under study. Therefore, given the wide consensus and trust that building energy modelling experts place in BEM tools, this methodology is considered, if based on reliable data and consistent models, suitable and coherent for carrying out a large-scale analysis of the building heritage of railway stations.

The simplified calculation method is not intended to replace neither detailed building energy models nor dynamic simulations of HVAC systems in the design process. BEM is still the most convenient state-of-the-art method to investigate passive and active energy saving strategies for complex buildings. However, it requires significant efforts, so that a surrogate model can be successfully adopted as decision support tool to analyse building energy demand on a large scale. Its viability is demonstrated by a suitable analysis of retrofit actions on the over 2000 Italian railway stations. Specifically, three different systematic energy retrofit actions have been analysed: the envelope performance improvement, the renovation of HVAC systems, and the implementation of more efficient lighting systems. Such interventions have been individually investigated both on the entire building stock and on part of it. They consist in the reduction of U-value factor to 0.60 (*Bronze*), 0.51 (*Silver*) and 0.44 (*Gold*),

the switching to highly efficient heat pumps (*SCOP*=4.0) and chillers (*SEER*=4.0), and the reduction of lighting power density to 3.4 W/m$^2$.

The potential benefit of the investigated strategies has been evaluated by comparing their related energy consumptions to the one of the baseline. The latter is calculated according to the following assumptions:

- *HDDs* and *CDDs* are taken by the Italian regulation (Allegato A of DPR 412/93 [109]);
- $V_h/V$ is calculated by the number of conditioned thermal zones defined in station *archetypes.* It depends on whether stations provide commercial services (marked as C in Table 10), or waiting halls, or both;
- *U* is as high as 1.8, 1.6 and 1.4 respectively for *Bronze*, *Silver* and *Gold* stations.
- $I_{el,loads}$ depends on the total number of energy-consuming services $N_{services}$ (marked as E in Table 10): if $N_{services}\leq 2$ then $I_{el,loads}$=5 W/m$^2$; if $2<N_{services}\leq 6$ then $I_{el,loads}$=10 W/m$^2$;
  if $6<N_{services}\leq 12$ then $I_{el,loads}$=15 W/m$^2$; if $N_{services}>12$ then $I_{el,loads}$=20 W/m$^2$;
- Heating system: Gas Boiler ($\eta_{gb}$=0.9); Cooling system: Split System (*SEER*=3.0);
- Primary energy consumption calculation is performed taking into account the average Italian electricity conversion efficiency of $\eta_{ce}=0.46$.

A graphical visualization of primary energy consumption is reported in Figure 31, where all contributions due to electricity, heating and cooling are compared for both baseline and renovation scenarios. This figure also shows how the proposed methodology can be exploited to provide a graphical visualization of energy indexes, by showing the geographical distribution of the impact of the renovation measures.

The Electric loads reduction strategy turns out to be the most impactful solution from an energy point of view, providing a *PES* of ~26.0%, followed by the System efficiency improvement (14.3%) and Envelope improvement (1.2%) strategies. The building stock of railway stations is mainly composed of small or medium passenger buildings, which are often unconditioned. Therefore, the overall greater impact of electricity consumption compared to the one related to air conditioning is understandable. However, this might not be true for the specific stations within the stock and, especially, for the *Platinum (Large)* stations that should be investigated by means of customized analyses.

System improvements show significant effect on the stations energy performance mostly during the heating season due to the higher efficiency enhancement of heating generators compared to the cooling ones. Only 3.5% of the annual *PES* is due to higher *SEER* of chillers while the heat pumps are responsible for the rest of primary energy reduction.

Building envelope improvement such as insulation of external walls or substitution of low-performance windows enable a minor reduction in primary energy consumption, resulting to be the less interesting energy efficiency measure to implement on the investigated building stock. Indeed, station buildings are modelled with high air change rates (8 ACH according to Italian standard UNI 10339 [110]) to reflect intrinsic characteristics of terminals, i.e. high infiltrations, high outdoor air requirement, etc. As a result, the impact on thermal loads and demands due to the heat transfer through the envelope is low if compared to the ventilation. As expected, the different station typologies have different impacts in terms of potential energy savings. Although there are fewer *Gold (Medium)* stations, these contribute more to limit primary energy consumption in case of retrofitting envelope (75%) and plants (79%). *Silver (Small)* stations cover a smaller share instead, as high as 24% and 20% for the envelope and system efficiency improvement respectively. These solutions have no impact (1%) on *Bronze*-type stations since only a very small number of stations were considered air-conditioned. This behaviour is also depicted in Figure 32 where the shares of primary energy saved for station types are shown.

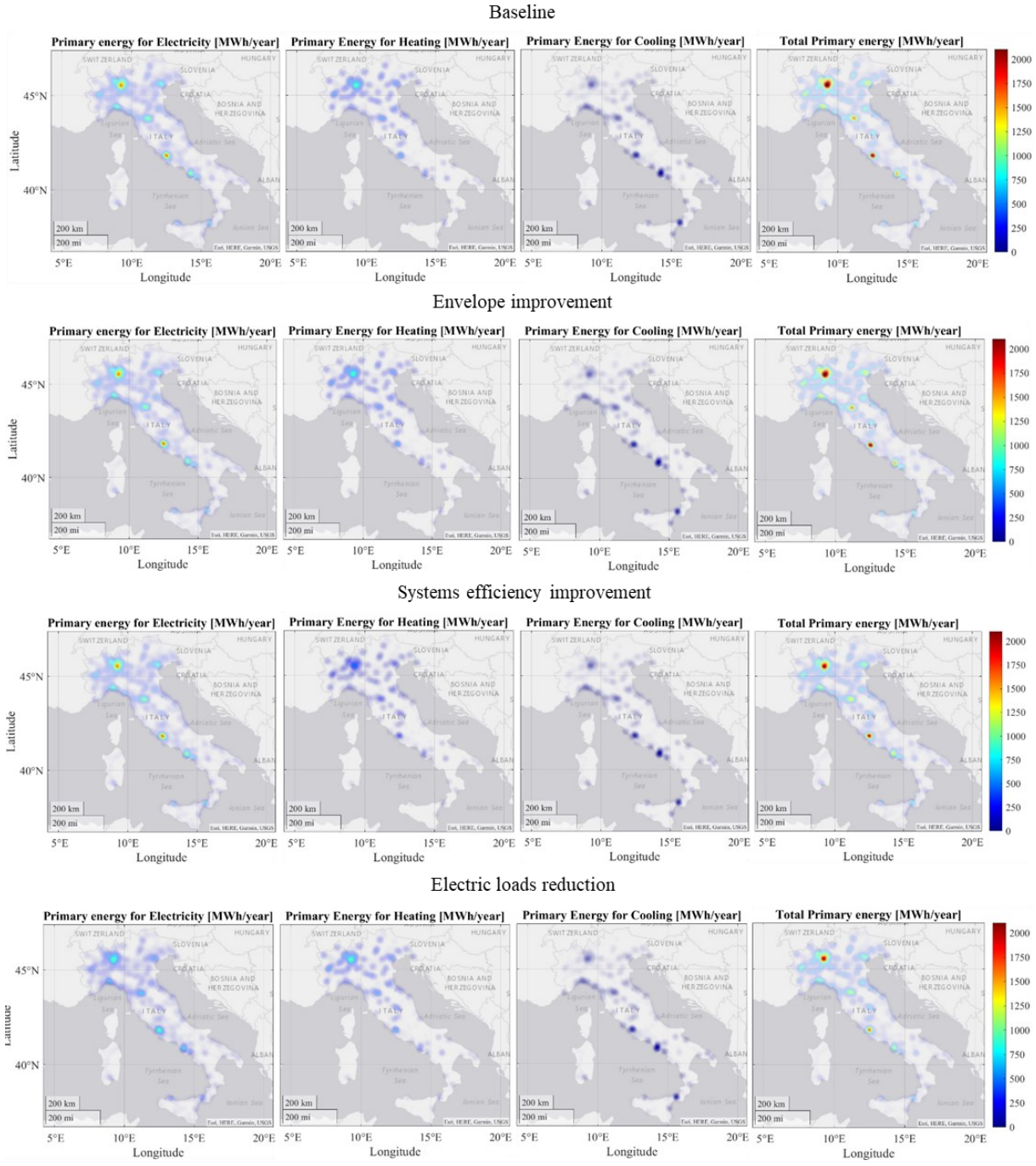


**Figure 31.** Overall impact of systematic energy retrofit actions.

Furthermore, the figure also reports the station typology contributions in case of the electric load reduction. Here, *Bronze (Stops)* stations gain

importance (22%). Nevertheless, the *Silver (Medium)* stations bring the greatest savings accounting for 48%.

A similar analysis was also carried out for geographical sub-areas which is shown in Figure 33. While improvements on stations implemented in northern and central Italy reflect the performance at national level, in the South the weight of the small and medium stations is higher. Specifically, in Sicily and Sardinia, the share of primary energy saved of *Silver (Small)* stations reach 48, 35, and 57% respectively for the investigated scenarios, against 49, 64, and 16% of *Gold (Medium)* stations. Moreover, *Bronze (Stops)* stations in the South of the peninsula contribute for 26% when electric loads for lighting are reduced.

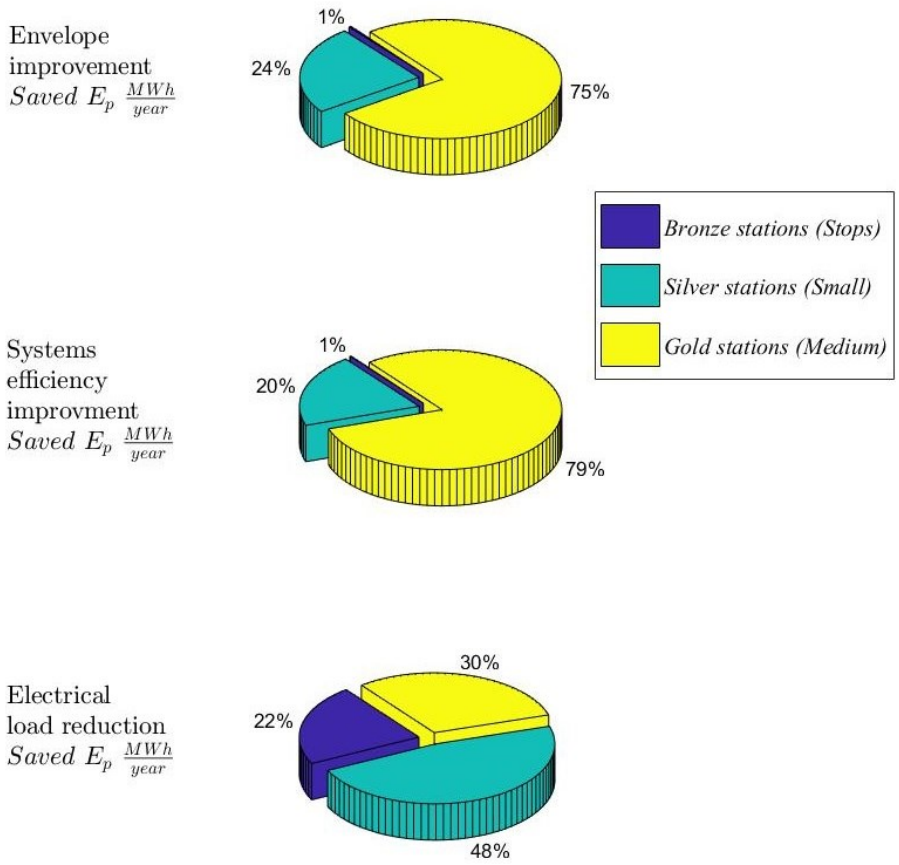


**Figure 32.** Impact of systematic energy retrofit actions by station typologies.

The primary energy saving (*PES*) strongly depends on the number of refurbished stations. However, only a limited number of stations should undergo renovation. Figure 34 showing the *PES* value for different percentages of refurbished stations is provided as guidance for the reader. The index adopted is also useful to quickly obtain information on the percentage of avoided carbon dioxide emission since the two indexes are proportional. The results of a sensitivity analysis of the model are also reported in Figure 34. Different values of parameters such as envelope heat transfer coefficients (*U*), system energy efficiency factors (*SCOP* and *SEER*), and lighting power densities ($I_{el,light}$) were considered. Specifically, the explored solutions are summarised in Table 15 reporting the value of the affecting variables as well as the unitary costs adopted for the economic assessment.

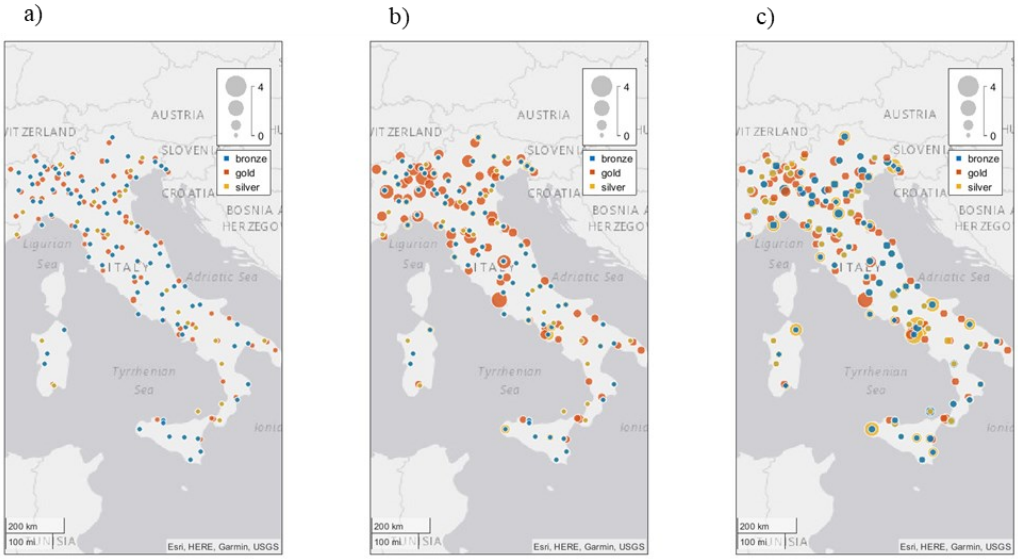


**Figure 33.** Potential primary energy (GWh) saving by regional areas: a) Envelope improvement; b) System efficiency improvement; and c) Electric load reduction.

It is worth noticing that *PES* is always an increasing function of the number of stations refurbished in all the investigated scenarios (see Figure 34). However, interventions such as Env.1, Env.2, and Env.3 or Sys.1, Sys.2, and Sys.3 do not entail further reductions of *PES* over certain percentages of renovation. This is evident in the case of the *Silver* stations since the maximum *PES* value occurs for an intervention on about 30% of the stock of the medium stations. As already mentioned, the savings of the smaller stations are negligible. On the other hand, Eui.1, Eui.2, and Eui.3 are the most interesting solutions as all building typologies have significant potential energy savings, regardless of the number of stations considered. Furthermore, due to the large number of small stations compared to medium and large ones, the *PES* values are higher if we consider the redevelopment of the *Bronze (Stops)* stations alone. It should be underlined that *PES* values are calculated considering the primary energy consumption of each building category instead of the entire stock (*Bronze PE*: 52.6 GWh; *Silver PE*: 148.3 GWh; *Gold PE*: 174.3 GWh).

**Table 15.** Investigated interventions on station building stock.

| | | Bronze (Stops) | | Silver (Small) | | Gold (Medium) | |
|---|---|---|---|---|---|---|---|
| | ***Intervention Code*** | ***Unitary cost*** €/m$^2$ | ***Affecting variable*** *U-value* W/m$^2$K | ***Unitary cost*** €/m$^2$ | ***Affecting variable*** *U-value* W/m$^2$K | ***Unitary cost*** €/m$^2$ | ***Affecting variable*** *U-value* W/m$^2$K |
| **Envelope improvement** | Env.1 | 60 | *0.60* | 60 | *0.50* | 60 | *0.44* |
| | Env.2 | 80 | *0.30* | 80 | *0.25* | 80 | *0.22* |
| | Env.3 | 40 | *0.90* | 40 | *0.75* | 40 | *0.66* |
| | ***Intervention Code*** | ***Unitary cost*** €/kW | ***Affecting variable*** SCOP/SEER | ***Unitary cost*** €/kW | ***Affecting variable*** SCOP/SEER | ***Unitary cost*** €/kW | ***Affecting variable*** SCOP/SEER |
| **System efficiency improvement** | Sys.1 | 130 | 4 | 130 | 4 | 130 | 4 |
| | Sys.2 | 150 | 5 | 150 | 5 | 150 | 5 |
| | Sys.3 | 170 | 6 | 170 | 6 | 170 | 6 |

| | ***Intervention Code*** | ***Unitary cost*** €/m² | ***Affecting variable*** $I_{el,lights}$ W/m² | ***Unitary cost*** €/m² | ***Affecting variable*** $I_{el,lights}$ W/m² | ***Unitary cost*** €/m² | ***Affecting variable*** $I_{el,lights}$ W/m² |
|---|---|---|---|---|---|---|---|
| **Electric load reduction** | Eui.1 | 7.7 | *3.4* | 7.7 | *3.4* | 7.7 | *3.4* |
| | Eui.2 | 5.3 | *5.7* | 5.3 | *5.7* | 5.3 | *5.7* |
| | Eui.3 | 3.6 | *7.9* | 3.6 | *7.9* | 3.6 | *7.9* |

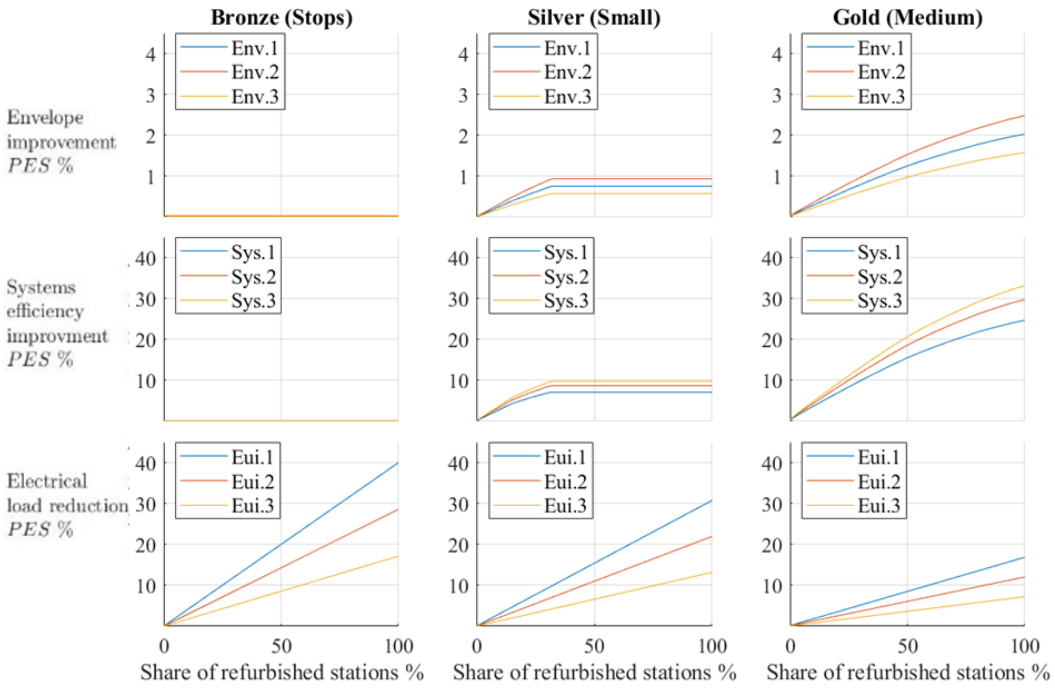


**Figure 34.** Impact of systematic energy retrofit actions for different share of refurbished stations.

The proposed strategies are analysed from the financial point of view as well. The most relevant energy/environmental and economic indices that are calculated (i.e. $\Delta PE$, *PES*, $\Delta M_{CO_2}$, *SPB*, *NPV*, and *PI*) are summarised in Table 16. Investment costs are evaluated by means of average unitary

costs (shown in Table 15) such as insulation, heat pumps/chiller, and efficient lamps [111, 112]. Similarly, running costs calculation involves the average cost of electricity (0.22 €/kWh) and natural gas (0.2 €/$Sm^3$), while the total equivalent $CO_2$ emissions are evaluated by means of the emission factors $F_e$ and $F_{ng}$, respectively equal to 0.480 and 0.202 $tCO_2$/MWh for electricity and natural gas [113].

**Table 16.** Summary of economic assessment of energy saving strategies.

| | Code | ΔPE [GWh/y] | PES [%] | $\Delta M_{CO2}$ [$tCO_2 \times 10^3$/y] | $M_{CO2}$ [%] | Economic savings [M€/y] | SPB [y] | NPV [M€] | PI [%] |
|---|---|---|---|---|---|---|---|---|---|
| **Envelope improvement** | Env.1 | 4.7 | 1.2 | 0.95 | 1.2 | 0.13 | ~170 | -19.7 | -92 |
| | Env.2 | 5.7 | 1.5 | 1.17 | 1.4 | 0.16 | ~184 | -26.4 | -92 |
| | Env.3 | 3.6 | 1.0 | 0.74 | 0.9 | 0.10 | ~146 | -12.9 | -90 |
| **System efficiency improvement** | Sys.1 | 53.6 | 14.3 | 10.0 | 12.3 | -2.6 | - | -59.0 | -272.6 |
| | Sys.2 | 64.8 | 17.3 | 12.4 | 15.3 | -1.5 | - | -46.3 | -185.6 |
| | Sys.3 | 72.3 | 19.3 | 14.1 | 17.4 | -0.8 | - | -39.0 | -137.8 |
| **Electric load reduction** | Eui.1 | 96.1 | 25.6 | 21.2 | 26.2 | 9.7 | ~1.1 | 126.7 | 1225 |
| | Eui.2 | 68.6 | 18.3 | 15.2 | 18.7 | 6.9 | ~1.0 | 90.7 | 1267 |
| | Eui.3 | 41.2 | 11.0 | 9.1 | 11.2 | 4.2 | ~1.1 | 54.0 | 1130 |

Finally, thanks to the proposed methodology, it is clear that systematic renovation of the envelope from an energy point of view is certainly not convenient. The high cost of investment and the low impact on energy consumption leads to a very high return of investment periods (from 146 to 170 years). Similarly, renovation of HVAC systems provides negative *NPVs* with no return of investment. However, this type of strategy could be taken into consideration at the end of the plant life cycle since it leads to significant energy savings and avoided equivalent $CO_2$ emissions. Railway authorities should certainly focus on reducing the electrical loads of lights and appliances, the adoption of highly-efficient lamps all over the stations is the

cheapest and most impacting strategies of our analysis, providing a NPV up to 127 million euros after 25 years and preventing the emission of circa $21 \times 10^3$ $tCO_2$ per year.

## 3.4 Conclusions

In this chapter of the thesis, a novel approach based on large building stock energy modelling is presented. It has been adopted to analyse the energy use intensity of railway stations heritage. The study was conducted on the case study of the Italian passenger stations (> 2000 units), spread along the Italian peninsula. Furthermore, a simplified model was carried out to provide an easy-to-use tool for design and decision-making purposes. Aiming at proving the effectiveness and potentials of the adopted methodology, some easy to implement energy retrofit actions were investigated to deduce useful insights, and potential energy and economic savings on the entire stations building stock.

The simplified model has been developed by linear regression of data obtained from simulations of detailed physic-based building models, developed by the BEM approach, which have been deduced from a randomly generated sample of real station buildings and data provided by the Italian railway operator. Several station archetypes were modelled and simulated by means of both BIM and BEM software such as *Autodesk Revit* and *OpenStudio/Energyplus*. Conditioned volume to total volume ratio, electric load intensity, envelope quality and weather conditions are the variable defining the station *archetypes*. The derived surrogate model for each *archetype* provides results that are in good agreement with physic-based building models which demonstrates the validity of the proposed approach. Useful insights can be extrapolated that can serve as guidance for railway operators:

- the major energy and economic benefits are obtained by the reduction of electric load intensities that are the most impacting

energy consumptions. As demonstrated, an overall primary energy saving of 26% can be reached by adopting highly-efficient lighting systems (e.g. LED lamps) with very low pay back periods (~1 year);

- energy measures such as envelope improvement and replacement of HVAC with more efficient systems have a lower impact on the station heritage as only a limited number of stations are equipped with air conditioning systems. In these scenarios, the primary energy savings are estimated as high as 1.2% for envelope improvement and 14.3% for HVAC system renovations. Nevertheless, it should be highlighted that negative net present values over 25 years were calculated;
- if partial actions on the building stock are taken into consideration, small and medium-sized stations have a greater impact on reducing electricity consumption (not related to air conditioning) given their higher number, while interventions on large stations provide the highest primary energy savings when envelope and system improvements are considered. Furthermore, contrary to what happens in northern and central Italy where large stations count more, in the South and on the islands the medium stations have greater potential energy savings;
- the renovation of the entire building stock of the Italian stations can avoid the emission of $21 \times 10^3$ t of equivalent carbon dioxide per year.

The accuracy of both detailed and simplified models are limited by the lack of data on stations geometry and physical characteristics, as well as other energy-related information. The major uncertainty is due to the poor information on actual electric loads and operating schedules of stations, both affecting electricity consumption and thermal needs. Thus, the applicability of the model is limited in schematic or detailed design workflows. Nevertheless, the proposed methodology could result as a useful

tool for railway operators in the planning of refurbishment measures on medium or large scale.

Open-source data would foster the development of more complex models, capable to provide high flexibility and greater accuracy of predictive tools as the one developed in this study.

# Chapter 4
# Guidelines to reach the goal of highly efficient terminals: toward net zero energy airports


## Summary

This study aims at identifying valuable solutions to reduce the energy consumption of airport terminals and providing guidelines to stakeholders to implement important efficiency measures to make airport facilities zero impact and face the challenges that national legislations and international directives impose for energy saving.

A comprehensive study of a wide range of energy-saving actions was carried out employing a detailed building energy simulation model of a two-story terminal building comprising 91 thermal zones. Specifically, the *Naples International Airport* was modelled by accounting for real information gathered from previous energy audits on the facility. Several energy-saving strategies, such as envelope improvement, HVAC systems enhancement, and renewable energy adoption, were analysed. The carried-out analyses highlight a significant savings potential and show how airports can become important *green* hubs for producing energy from renewable sources. Design criteria can be obtained by the simulation results and exported to other airports facilities.

## 4.1 Introduction

Aviation is the fastest transport mode, essential to the world economy. However, the sector needs to move towards sustainability to support both pollutant reduction and economic growth.

Despite the unprecedented decline in passenger and cargo volumes due to the Covid-19 pandemic, they will rise more in the coming decades with the consequent increase of related energy consumption [114]. The total Greenhouse Gas (GHG) emissions linked to the aviation industry, which accounted for approximately 2.5% of the global GHG emissions in 2018, are divided into 85% due to air-side aircraft operations and 15% due to land-side operations, including airports [115]. Indeed, airport facilities are rapidly developing and represent key infrastructures with high energy consumption levels due to their intense operation. Although HVAC systems are the main consumers within terminal buildings, airports also require significant amounts of energy to provide services to both passengers and airlines, with energy consumption comparable to small cities [116]. Therefore, it is necessary to implement important efficiency measures to turn airport facilities to zero-carbon footprints and facing the challenges that national legislations and international directives impose concerning energy savings and pollution.

Airports worldwide are gradually adopting new strategies and technologies to reduce energy consumption since sustainability is an emerging interest in the sector. As reported in ref. [117], a great interest emerged few years ago on building “Energy Management” systems and procedures. Strategies such as centralized operations monitoring, additional metering for controlling major consumption points, and remote control of energy-use devices, etc., are considered valuable ways to achieve the goal of sustainability and cost savings. Building Management Systems (*BMS*) are fundamentals in the context of large facilities where the energy consumption of terminal buildings is the highest share of the total energy consumed in the airport district. Many studies conducted on several

airports revealed that HVAC operation is the largest share of energy used in terminal buildings, followed by lighting and electric devices for information technology and communications, and handling systems [118]. Typical amount of energy for air conditioning and heating is approximately 70% of the building energy use according to ref. [119]. This rate could be higher in cold climates, given the higher demand for heating. Therefore, improving performance operations of HVAC can lead to significant energy and cost reduction, as well as to other social-environmental benefits

The characterization of energy demand pattern is a key factor to reduce energy consumption at airports and implement cost-effective energy saving measures [120], [121]. They are mandatory preliminary steps for those airports that aspire to obtain sustainability certifications from independent accreditation bodies, e.g. Airport Carbon Accreditation (ACA) [122], LEED rating system [123], or energy management schemes such ISO 50001, etc. Newly airport-specific rating tools were also proposed to assess the *“greenery”* of such infrastructures [11], however

Furthermore, benchmarking activities are essential in designing new constructions or in extensive airport refurbishment. Adopting metrics derived from historical data such as Energy Use Intensity (EUI), along with energy modelling tools, can help designer in making the right choice in terms of energy consumption [124], [125]. With this aim, 9 of the busiest airports in the world in terms of passenger volume have been assessed through the Sustainability Ranking of Airports Index (RSA) developed by the authors of ref. [126]. The SRA index takes into account many performance indicators and spans the domains of sustainable development of energy, water, and environment systems. The results show the need to also move toward more efficient ground operation of airports.

Sustainability metrics and multi-domain assessment approaches are of fundamental importance at the beginning of huge projects. Kılkış highlights this aspect in his work [127], analysing the impact of a new airport planned for the city of Istanbul. It is reported that the project is not feasible from the environmental point of view. The study was carried-out comparing several “*green*” airport scenarios. Since a massive deforestation has to be done to

build the airport, none of the scenarios would offset the $CO_2$ emissions associated with the implementation of the project.

Energy-saving strategies for airports are widely investigated; useful case studies that analyse how airport terminals improved energy efficiency were found in the literature [128], [129], [130], [131], [132]. It is clear that high reductions of energy consumption can be achieved only with actions based on a holistic approach. In this context, HVAC and Renewable Energy sources (RES) systems play a crucial role in demand reduction and avoiding usage of fossil-fuels [133].

Authors of ref. [134] analysed the impact of natural ventilation in an airport located in the south of China adopting CFD computing methods. It is demonstrated that natural ventilation in the building analysed can significantly reduce the operation hours of HAVC operation. The paper was written when SARS increased attention on indoor air quality, which is a situation very similar to the current COVID-19 pandemic. Ventilation strategies such as activation of fans during night and variable air volume systems are also investigated in ref. [118] where different measures to improve efficiency of HVAC systems in airports are explored. The proposed changes in the HVAC system of the Erzurum Airport terminal led to a $CO_2$ reduction of 50% compared to the baseline building. Abdallah et al. [135] monitored the indoor environmental condition of the Assiut International Airport and stated that by increasing cooling indoor temperature setpoints from 25 to 27°C energy demand can be reduced to 25% during month with more severe external conditions.

In cold climates, air infiltration might significantly affect both energy consumption and thermal comfort in airports. It is found in ref. [136] that air infiltration can impact 18-71% of total heat loss since high air infiltration rates up to 0.56 h-1 can occur in airports due to frequent gate openings. The authors of the study conducted field measurements and general analyses in eighteen Chinese airports terminal, mainly located in cold winter climate zones. Another study [137] proposes to exploit radiant heating

systems to reduce air infiltration loss and proved that, in certain cases, air infiltration can guarantees the necessary outdoor air in the breathing zone with no need for mechanical ventilation.

On the contrary, thermal discomfort is sometimes due to the overheating that occurs in airports with very large glazed surfaces. These architectural features could lead to savings for improving daylighting, however, if not well designed glazed surfaces can significantly burden air conditioning systems, hence the growing need to effectively couple architecturally appealing solutions with energy saving needs [138].

Despite the high potential for energy savings due to improved HVAC, the goal of *net-zero emissions* or *net-zero energy* airports cannot be separated from the exploitation of renewable energy [9]. The large spaces available to the airport districts are well suited to the implementation of large photovoltaic systems [139], [140], [141], [142]. However, PV power generation plants should be carefully designed since glare may affect air navigation safety and pilots`s eye glare [143]. The implementation of RES-based technologies may be also be limited from other obstacle regulation in landing areas.

The *net-zero* goals require synergies among strategies to increase infrastructure self-sufficiency by a higher rate of renewable energy self-consumption [144]. Energy storage systems such as battery or electrolyzer-hydrogen tank plants have been investigated as interesting solutions in the field of airports [145]. Indeed, air-side operation of airport may also benefit from green hydrogen production to supply fuel to aircrafts [146].

While PV implementation feasibility is widely investigate, no studies about wind energy exploitation have been found, except the one carried out at Leonardo da Vinci International Airport, where both mini and micro wind power plants are analysed [133].

It is worth noticing that the available literature lacks comprehensive studies on airport facilities. Each of the mentioned works, which analyses interesting case studies and provides useful insights to improve airport energy efficiency, focuses on one or a few strategies suitable for terminal

buildings, exploring solutions restricted to an isolated domain, e.g. HVAC, building envelope, or RES.

How can the goal of net-zero energy (emission) airports be achieved? The answer is not trivial. This research aims to provide guidelines to stakeholders and information on potential savings resulting from the implementation of different strategies and technologies in the context of airport districts. An innovative approach based on the coupling of Building Information Modelling (BIM) and Building Energy Modelling (BEM) was adopted to model and simulate the building energy performance.

A comprehensive study of a wide range of energy-saving actions was carried out by means of a detailed building energy simulation model of a two-story terminal building comprising 91 thermal zones. Taking the Naples International Airport as a representative airport located in Mediterranean area, the building was modelled accounting for real information gathered from previous energy audits on the facility. The explored solutions were chosen according to their capacity to reduce airport energy demand, HVAC system efficiency, and increase renewable energy production. Dynamic energy performance simulations allowed studying both passive and active behaviour of the building and the complexity of plants interaction after the strategies implementation. Finally, sensitivity analyses of the main influencing parameters are provided for comparison purposes. The analyses carried out highlight a significant saving potential and show the pathway that airports should take to reach the goal of *net zero energy*, switching the current paradigm based on the consumption of fossil fuels.

## 4.2 Material and Methods

This section includes the description of the key steps of the proposed methodology, structured by following the actual workflow adopted to carry out the study. Starting from the analysis of the selected airport infrastructure, the simulation model of the reference building, as well as all the energy-saving measures investigated, was built with a BIM to BEM methodology. All those phases are described in the following subsection. Specifically, in section 4.2.1 the terminal building of the International Airport of Naples is described. In section 4.2.2 and 4.2.3, the modelling of the reference building and a wide range of energy-saving measures are presented. The strategies explored range from passive strategies on the envelope to reduce thermal loads to the implementation of RES-based systems, passing through efficiency solutions on the HVAC system.

### 4.2.1 Description of the building

All the information required to carry out the analysis were retrieved from the documentation provided by the airport operator company (GESAC, Gestione Servizi Aeroporti Campani). Furthermore, the climate-related data of Naples were considered. Specifically, the Napoli Capodichino International Airport weather file [123] from the IWEC collection was used for simulations. A 2D representation of the terminal is provided in Figure 35.

*U-values* of opaque building structures are calculated according to component materials which range from 0.5 to 1 W/m$^2$K. The considered airport terminal building has a total area of 25610 m² and overall volume of 81390 m³ that grows in 2 stories. In 2011, the recorded transit volume was over 5’700’000 passengers with a peak of 2’850 concurrent presences, which occurred in the month of August. The passenger data retrieved in the past years along with information on flight schedules were used to derive the occupancy profile of the terminal, which is shown in Figure 36. The airport is open to the public for 19 hours per day, 7 days a week. The HVAC system operates only when the airport is opened, from 4:00am to 12:00pm.

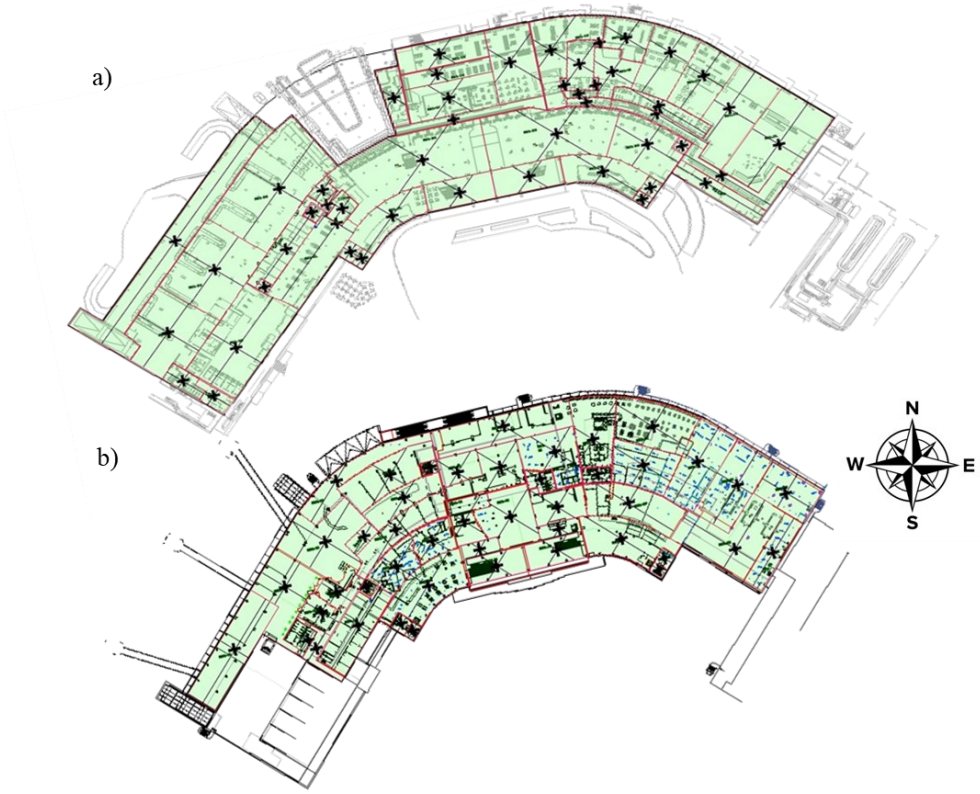


**Figure 35.** Plan view of the ground and first floors of the International Airport of Naples Capodichino.

4 space types characterised by different crowding indices: passenger transits (0.2 people/m$^2$), offices (0.1 people/m$^2$), baggage drop off (0.4 people/m$^2$), and check-in (0.5 people/m$^2$) have been identified. Furthermore, different power densities are considered according to space typology: passenger areas (10 W/m$^2$), passenger areas with control equipment (30 W/m$^2$), commercial areas (120 W/m$^2$), and offices (25 W/m$^2$).

The HVAC system of the terminal comprises over 50 rooftop Air Handling Units (AHU) capable of balancing both latent and sensible thermal loads. The air distribution system provides a constant airflow volume to heat up/cool down the airport spaces and ensure the minimum outdoor air flow

rate to the breathing zone (30 $m^3$/h per person). AHUs are equipped with outdoor air mixers that allow zone air recirculation.

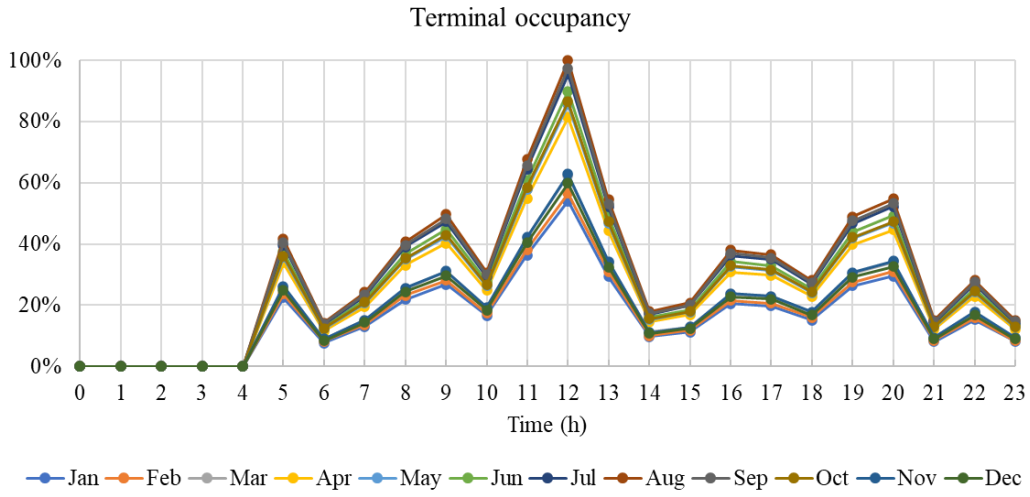


**Figure 36.** Occupancy schedule of the terminal.

The generation system consists of about 30 air-source heat pumps/chillers (HPs/CHs) with an overall installed thermal power of approximately 8.5 MW that provide hot or chilled water required by the air-conditioning system (Indoor Heating set-point 20° C; Indoor Cooling set-point 25°C; Relative humidity 50±10%). The heat pumps/chillers are grouped in 4 main thermal power plants (10 HPs/CHs) and over 20 activated single HPs/CHs, They are managed by a thermoregulation system that monitors the room temperature and relative humidity within the thermal zones. The rated COPs of the considered heat pumps and chillers are in the range 2.5-3.0 and 2.2-2.8 respectively in heating and cooling mode. Please note that rated COP values refer to standard condition of outdoor air condition 2 °C and water 45 - 40 °C, and outdoor air conditions 35 °C and water 7 - 12 °C.

Since in the reference building no electricity renewable energy systems are considered, electricity exclusively comes from national power grid (average efficiency of the entire Italian generation system $\eta_{el}$ = 0.46). In the

same regard, the $CO_2$ emission factor used in the calculation is 0.483 (see equation (25) and (26)).

Domestic Hot Water (DHW) is produced by means of 2 15 kW boilers coupled with 1 1500 L water tank heated up with a heat pump coil. Water is stored at 60°C. Poor information is provided about DHW systems. Presumably, the commercial areas of the airport are equipped with their own boilers for the production of DHW. However, the power consumption due to DHW is estimated as high as 0.3% of the total airport energy consumption, which is a little share of the total energy consumption of the terminal building.

### 4.2.2 Building modelling

Airport buildings are very large and complex facilities. The modelling of such complicated structures might be a very intensive and time-consuming task. The existing terminal building was modelled in detail using *Autodesk Revit 2022* according to available building documentation. Henceforth, the existing terminal building will be referred to as the “reference building”. The building model faithfully represents the geometry and plant zoning of the terminal. Where necessary, appropriate simplifications have been made, however, the BIM model differs from the actual extension of the building by only 2.8% on the total area and 1.1% on the total volume.

Afterward, the energy model of the reference building was generated by means of the automated BIM-to-gbxml-to-OpenStudio import routine of Autodesk Revit, *Revit Systems Analysis*. The data transfer workflow was purposely modified to include custom simulation settings and collect specific outputs (the BIM2BEM methodology is described in detail in Chapter 1). The terminal building model as rendered by Revit is shown in Figure 37.

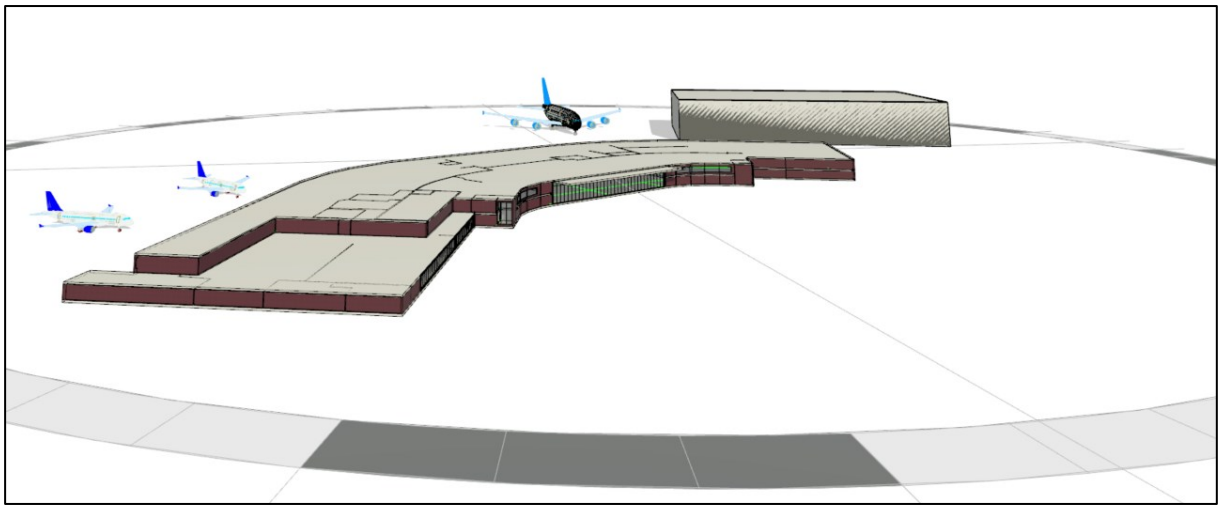

**Figure 37.** BIM model of the airport facility of the International Airport of Naples Capodichino.

The resulting energy model is comprised of 62 conditioned and 29 non-conditioned zones, assumed as well-mixed air node zones. The building is equipped with the air systems described in section 4.2.1 capable to provide the required amount of mixed air airflow to the zone and the necessary thermal energy to keep the temperature setpoints. The HVAC system also guarantees the minimum specified outdoor airflow rate.

The influence of people, lighting and electrical equipment on the heat balance algorithm is accounted by means of characteristic heat gains parameters such as sensible and latent heat fraction per person ($g_{s,p}$ and $g_{l,p}$, *W/person*), lighting power load intensity ($g_l$, $W/m^2$) and electrical equipment power load intensity ($g_{ee}$, $W/m^2$). The appropriate schedules complete the model to take into account the actual operating regime of the buildings under investigation. Parameters adopted are described in the case study section 4.2.1. More details on modelling and simulation assumption can be found on the complete *EnergyPlus* documentation [93].

### 4.2.3 Modelling of energy efficiency strategies

The energy model described so far is adopted as a reference for comparison with other energy-saving measures which consists of retrofit on HVAC systems, building envelope, and energy generation systems from RES. Specifically, the following were considered as candidate strategies to enhance energy efficiency or reduce annual primary energy consumption:

- Air Heat Recovery systems (AHR);
- Demand Controlled Ventilation (DCV);
- Differential Enthalpy Economizer (DEE);
- Demand Controlled Ventilation and Differential Enthalpy Economizer (DCV & DEE);
- Variable Air Volume (VAV);
- Wall Insulation (WI);
- Glazing Replacement (GR);
- Lighting Efficiency Improvement (LEI);
- Photovoltaic Glazing Façades (PVGF);
- Photovoltaic Façades (PVF);
- Large Photovoltaic (LPV);
- Combined Cooling Heat and Power (CCHP).

#### *4.2.3.1 Retrofit of HVAC systems*

The improvements to the HVAC system mainly concerned the air distribution system and ventilation. However, more efficient cooling and heat generation systems were also evaluated.

The AHR measure consists of the implementation of an air-to-air heat exchanger on each independent air distribution circuit in order to recover

the sensible waste thermal energy of exhaust air. AHRs, with an average recovery efficiency of 70%, might reduce the need of thermal energy from coils, mostly during winter because of higher temperature difference between indoor and outdoor temperature. Higher pressure drops ($\Delta p$, 200 Pa) due to AHR are also accounted according to equation (23) evaluating major energy consumption $\Delta E$.

$$\Delta E = \frac{\dot{m} \cdot \Delta p}{\eta_{fan}} \cdot \Delta t \tag{23}$$

With $\dot{m}$, air mass flow rate, and $\eta_{fan}$, fan efficiency, and $\Delta t$ the timestep. The fan efficiency value assumed for calculation is 0.7, which also includes the motor efficiency. Please note that the simulation model considers heat gains due to unideal equipment within the air distribution systems, so that any major energy consumption is taken into account.

DCV, as opposite to the constant ventilation, provides the exact need of outdoor airflow according to the actual occupancy level of the zone. Outdoor air flow rate is reduced proportionally by controlling the opening and closing of exhaust and outdoor air dampers. DCV could be a valuable ventilation strategy to adopt when outdoor temperature is not favourable. On the other hand, higher outdoor airflow volume could be useful in reducing cooling demand when outside temperature is lower than airport spaces setpoints. That happens with DEE, suitable controls are implemented in order to supply higher outdoor ventilation to zones. Whenever $T_{out} < T_{in}$, the outdoor air damper is proportionally opened to meet the zone cooling thermal load.

The CCHP strategy is adopted to both provide electricity and thermal energy to airport plants. Two 750 kW engines are considered in order to meet part of the total electricity request of the terminal. The engines are equipped with a cogeneration system to recover the high-temperature thermal energy from the engine jackets (80/90°C). The performance curve provided by the engines manufacturer was used to calculate the power production and the available recovered thermal energy rate according to partial loads of the engines. Similarly, the yield of the absorption chiller is

assessed by means of empirical correlations derived by field test on the machines.

Hot water is used to first meet the heating demand. The remaining thermal energy is conveyed to a 450-kW absorption chiller to produce refrigerated water serving the HVAC system of the terminal. Any integration of electricity or thermal energy is provided by the national power grid and existing HVAC systems. The impact in terms of fuel consumption and carbon emissions of the CCHP strategy is assessed for different fuels: biogas ($LHV$=8.3 kWh/kg, $F_{bg}$=0 $tCO_2/MWh_e$), biodiesel ($LHV$=10.4 kWh/kg, $F_{bd}$=0 $tCO_2/MWh_e$), natural gas ($LHV$=13.1 kWh/kg, $F_{ng}$=0.202 $tCO_2/MWh_e$), and LPG ($LHV$=12.6 kWh/kg, $F_{LPG}$=0.220 $tCO_2/MWh_e$).

#### *4.2.3.2 Retrofit of building envelope*

Since the terminal outermost areas may be affected by higher heat loss during winter, as well as undesirable heat gains in summer, the reduction of building wall heat transfer coefficients and increasing of glazed façade performances have been investigated. Such strategies can affect thermal behaviour of the building in different ways depending on exterior boundary condition. Specifically, the WI measure was carried out by applying an insulation layer to ensure the external walls' U-value of approximately 0.32 $W/m^2K$. The insulation panel adopted are wood fibre boards characterised by a 0.04 W/mK conduction coefficient and a density of 180 $kg/m^3$.

Windows are also renovated by means of replacement of existing glazing surfaces. Specifically, the south side transparent façade is replaced with special windows to control the entering solar radiation ($U$ = 2.00 $W/m^2K$; $SHGF$ = 0.20), while the north side windows are replaced with low-E glasses ($U$ = 1.80 $W/m^2K$; $SHGF$ = 0.66) to ensure lower heat losses.

#### *4.2.3.3 Exploitation of renewable energy sources*

The terminal presents a large window façade (420 $m^2$ large) on the south side that can be used to produce electricity through photovoltaic technologies.

Glass facades are replaced with photovoltaic glass made of amorphous transparent or semi-transparent silicon (PVGF measure). These types of photovoltaic panels have relatively low efficiency (3–4%), however, installation of such a system can overcome the lack of available space for photovoltaics. The analysed glass is an amorphous silicon photovoltaic glass with two 6 mm low-emission glass and a 12 mm Argon chamber ($U$ = 1.20 W/$m^2$K; $SHGF$ = 0.12; $\eta_{pv}$=4%). Similarly, the PVF solution consists of a number of photovoltaic panels attached to the south façade of the terminal so that all the opaque surfaces are covered by PVs. The total area affected by the PV façade implementation is about 400 $m^2$, with a total installed power of 77 kWp. As regards the LPV, a large photovoltaic field has been considered to produce a high amount of electricity from RES. Specifically, a photovoltaic plant with a peak power of 5 MW spread over an area of 25600 $m^2$ has been modelled. For this purpose, 4 neighbouring buildings belonging to the airport have been identified as valuable locations to install rooftop PVs.

Please note that all projects that involve PV panels must undergo ENAC evaluation (Ente Nazionale per l'Aviazione Civile) which is the Italian civil aviation authority. It is in charge to assess if PVs and related solar reflection entail a risk for air traffic. Therefore, since similar PV plants have been installed in the past years in the close areas of the airport, it was assumed that such a measure is feasible for the specific site analyzed.

#### *4.2.3.4 Simulation and key performance parameters*

The simulations were carried out by means of the *EnergyPlus* built-in features with a timestep of 15 min, providing detailed outputs to analyse the building behaviour, as well as the performances of the systems. *Output*

*Variables* referring to zone air conditions, thermal gains, heating and cooling systems' capacity rates, and electricity consumptions were processed to evaluate the project from an energy point of view. Each proposed strategy was compared to the baseline, also called Reference Building (RB), in order to calculate the Primary Energy Saving (*PES*) index for decision-making purpose (equation (24)). It should be underlined that all the energy-saving strategies analysed are assessed only on the basis of an energy balance calculation. Therefore, the indirect $CO_2$ emissions due to exergy destruction are not considered in this analysis, although such index can be an important tool to assess the goodness of renewable energy systems or other nearly-zero carbon applications [147].

$$PES = 1 - \frac{PE_i}{PE_{RB}} \tag{24}$$

Where *PE* is the primary energy calculated by means of equation (25), considering the total energy consumed $E_i$ and the related primary energy conversion factor $\eta_i$.

$$PE = \frac{E_i}{\eta_i} \tag{25}$$

Finally, the environmental performance is assessed by the $\Delta M_{CO_2}$ index that represents the total equivalent $CO_2$ emitted. The indicator is calculated by:

$$\Delta M_{CO_2} = E_i \cdot F_i \tag{26}$$

Equation (26) involves the energy consumption provided $E_i$ and the related emission factor $F_i$.

It should be underlined that all the energy-saving strategies analysed are assessed only on the basis of an energy balance calculation. Therefore, the indirect $CO_2$ emissions due to exergy destruction are not considered in this analysis, although such index can be an important tool to assess the goodness of renewable energy systems or other nearly-zero carbon applications [147].

## 4.3 Results

This section provides the simulation results of the energy-saving measures investigated to improve the efficiency of the selected building. Energy results are discussed with the aim to assess the performance of a wide range of energy energy-saving strategies and provides guidelines to facility operators within airport industry. To this aim, the building-plant system, as described in section 4.2.2, has been taken as a baseline for comparison purposes. The thermal behaviour of the terminal is summarised in Figure 38 which shows the daily trend of the heating and cooling demand, as well as the average daily temperatures throughout the year. The figure clearly highlights that the total cooling energy demand (about 5 GWh/year) is much higher than the heating requirement (about 0.6 GWh/year), given the high internal heat generated from internal sources such as lighting and equipment, as well as the high crowding of indoor spaces.

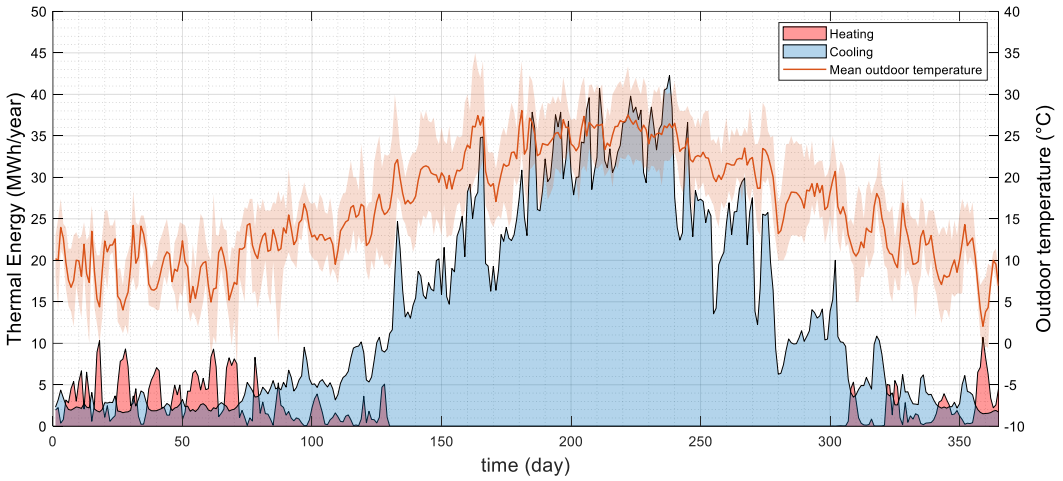


**Figure 38.** Heating and cooling demand of the Reference Building and daily average outdoor temperature of Naples, Italy.

The airport thermal need of the reference building is also reported in Figure 39 both for cooling (Figure 39a) and heating (Figure 39b). The chart also shows the sensible energy shares that the HVAC has to provide to balance lights, equipment and people heat gains, and envelope, infiltration and ventilation heat exchanges for all the investigated strategies. As depicted in the figure, internal heat gains are the most impactful contribution to the heat balance of the building, followed by ventilation/infiltration, and envelope heat loss/gain.

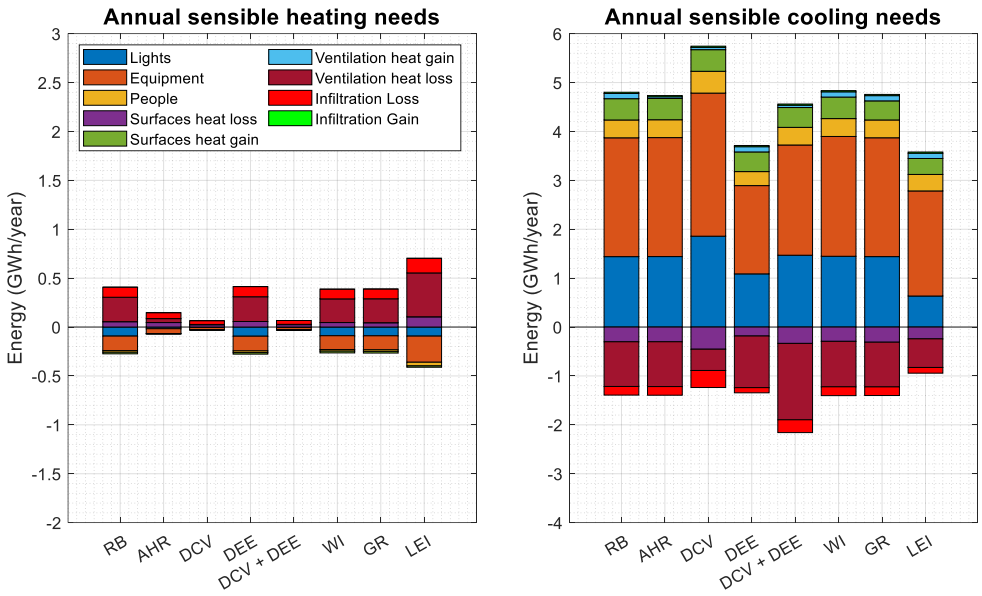


**Figure 39.** Thermal needs balanced by the HVAC system.

Among the investigated strategies, the ones that provided the higher deviation from the baseline are the measures involving the air distribution system (AHR, DEE, DCV+DEE, VAV) and the implementation of more efficient lighting systems (LEI). Building insulation (WI) and high-performance glazing (GR) has a minor impact on the energy demand of the airport terminal because of the high internal loads.

AHR is a convenient strategy to be adopted during the heating season. In the case of the analysed terminal building, the demand for heating is reduced by 60%, while that for cooling only by 1.4%. However, retrofitting the air distribution system with high performance air-to-air heat exchanger led to higher duct pressure drops that entail higher electricity consumption for fans. Specifically, accounting for higher pressure drops, the total electricity consumption of the building increases by 0.5 % which also represents an expenditure in terms of primary energy (PES = -0.5%). DCV is even more convenient than AHR with respect to the reduction of heating demand. With low outdoor temperature, such strategy allows for reduced heat loss by exhausting less air volume. By controlling the amount of air in winter, 76% less energy can be consumed. For the same principle, a

reduced outdoor airflow means a lower ventilation loss whenever outdoor temperature is higher than airport setpoint. On the other hand, the sole DCV lead to a cooling demand higher than the RB, up to 9%, which entails a negative value of PES (PES = -1.2%). In the cooler seasons, when cooling is required and the outside temperature is favourable, higher external air flow rates would bring benefits in terms of cooling energy needs. DCV strategies are more effective if coupled with DEE, which consists in free cooling by means of higher outdoor air volumes. DEE provides a significant reduction in cooling demand, specifically, the annual cooling demand of the terminal decreases by 17%, and 28% if coupled with DCV. In terms of primary energy, such strategies allow PES with values of 3.3% and 5.9% respectively if the entire airport energy consumption is taken into account. The impact of DEE strategy on cooling thermal loads is depicted in Figure 40 where the reference system cooling load (red line) is compared with the proposed one (black line). The chart also reports indoor and outdoor temperatures to understand the behaviour of the free cooling control implemented for the HVAC system. As shown in the figure, the favourable lower outdoor temperature registered during mid-season (March-April) allow important savings mostly in the early and late hours of the day.

As depicted in Figure 39a and Figure 39b, it is estimated that the energy efficiency measures affecting the building envelope, namely WI and GR, allow to save respectively 7% and 8% of heating demand. Nevertheless, WI is even an harmful solution in terms of cooling energy with a 0.5% higher demand, while GR involves a saving of 1%, resulting the energy efficiency measures with lower impact on HVAC consumption. This result was expected, given the lower incidence of envelope thermal loads compared to the other load rates of the thermal balance. Therefore, WI and GR are negligible PES values.

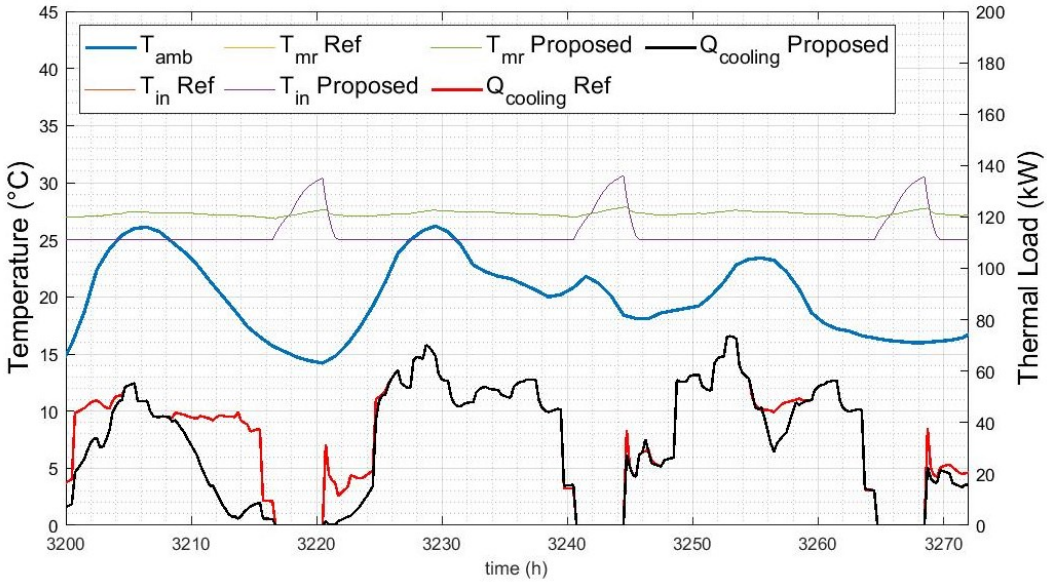


**Figure 40.** Cooling loads in case of free cooling control for air-conditioning system: reference system vs proposed system.

Implementation of high-efficient lamps such as LED lamps to reduce the electricity consumption due to lighting is an interesting solution, which is becoming a standard for new building construction or major renovations. In addition to the important savings that can be obtained from the low electrical absorption, the use of LED lamps also leads to lower consumption of the HVAC system. Indeed, the cooling demand decreases by 25% if lamps are fully replaced with high-efficient LED lamps. Reversely, the total heating demand almost double since internal loads are beneficial wintertime. Of course, less electric loads due to higher lights efficiency has a significative primary energy reduction as high as 14%. This trend is more evident in Figure 41 where variations in the airport electricity consumption are depicted for the VAV, PVGF, PVF, and LPV strategies. All the proposed solution analysed in Figure 41 compared with the reference building (RB), equipped with a constant air volume system (CAV).

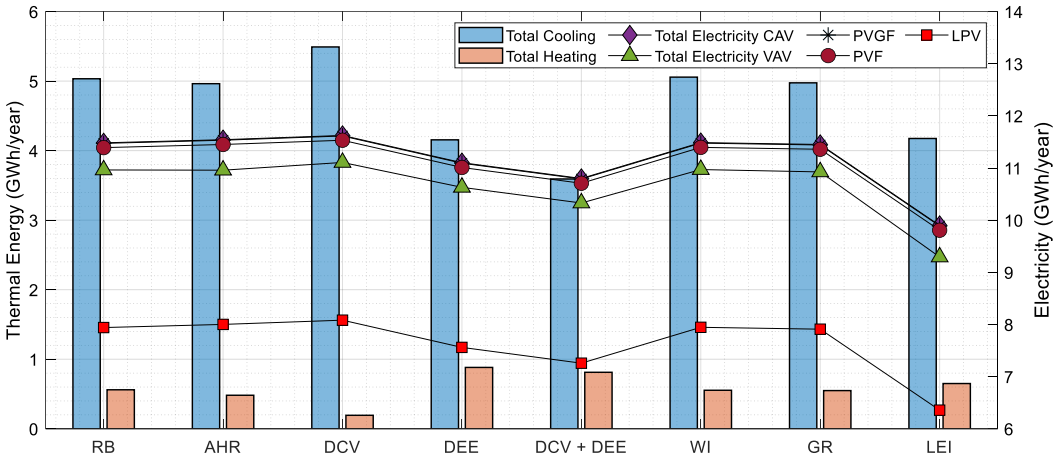


**Figure 41.** Airport electricity demand of proposed strategies.

VAV systems that allow fine control of airflow drop the electricity consumption due to fans. It is demonstrated that by renovating the current air distribution systems and incorporating variable speed motors for fans, pressure sensors, and damper actuators the total airport electricity can be reduced by 4% to 6%.

As regards renewable energy solutions, as expected, both PVGF and PVF have a lower impact on the overall electricity demand. The reduced extension of the surfaces available for the implementation of such solutions implies negligible energy savings. PES values related to PVF, which can convert solar energy more efficiently than PVGF, do not exceed 1%. LPV is very convenient instead, with total annual energy generated of about 3.5 GWh, the large photovoltaic plant allows to reduce the airport electricity demand from the grid up to 30%-36% (square marker in Figure 41).

As airports are very intensive energy consumers, dedicated generation systems are always interesting solutions, which is proved by the results shown in Figure 42 referring to the implementation of a combined cooling heat and power plant (CCHP). The system (described in section 4.2.3.1) covers the electricity demand of the airport due to terminal equipment,

lighting, air handling devices, and part of the electricity needed for heat pumps and chillers integration (green line in Figure 7). The higher energy consumption occurs in August when the total electricity request is balanced both by the co-generators (72%) and the power grid (28%). As observed, heating is almost fully supplied by the recovered thermal energy, while the absorption chiller needs to be integrated by the existing compressor chillers in the April-November period when cooling demand is higher. On annual basis, the primary energy saving (*PES*) of the CCHP is about 90% in case of co-generators supplied by biogas or biodiesel since the primary energy consumption is only due to electricity integration from power grid. The *PES* value in case of adoption of fossil fuels such as natural gas or LPG is about 12% instead.

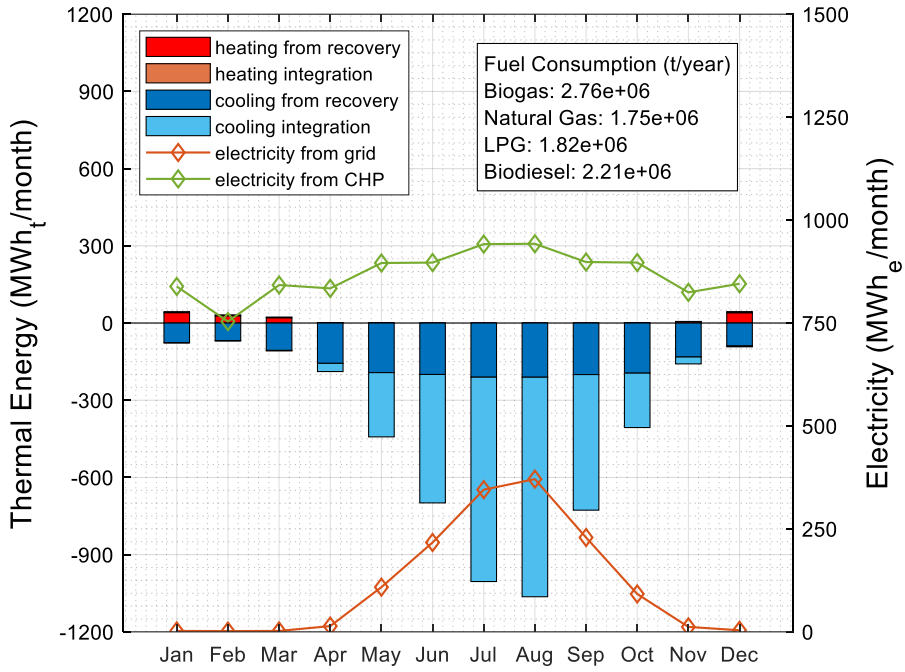


**Figure 42.** Electricity and thermal energy demand with a Combined Cooling Heat and Power plant.

All the investigated strategies are also analyzed from the environmental point of view. Considering an emission factor $F_{el}$ equal to 0.483 t $CO_2$/MWh$_e$, the total carbon dioxide emissions linked to airport activity have been calculated. Results are reported in Table 17 and Table 18. Please note that

the tables also report the percentage of avoided $CO_2$ assessed by comparing all the strategies with the reference building RB (Table 17). Furthermore, energy-saving measures such as VAV, PVGF, PVF, and LPV are compared with the CAV reference system (Table 18). As expected, high penetration of renewable energy and significant reduction of electricity loads are the most convenient solution in terms of operating $CO_2$ emissions. It should be underlined that more the assessment of carbon dioxide emissions does not take into account the entire life cycle of the technologies adopted.

**Table 17.** $CO_2$ emissions of the proposed strategies and percentage of avoided $CO_2$ (comparison with RB).

| | CAV ($ktCO_2$) | CAV (%) | VAV ($ktCO_2$) | VAV (%) | PVGF ($ktCO_2$) | PVGF (%) | PVF ($ktCO_2$) | PVF (%) | LPV ($ktCO_2$) | LPV (%) |
|---|---|---|---|---|---|---|---|---|---|---|
| **RB** | 5.5 | - | 5.3 | - | 5.5 | - | 5.5 | - | 3.8 | - |
| **AHR** | 5.6 | -0.5 | 5.3 | 0.0 | 5.6 | -0.5 | 5.5 | -0.5 | 3.9 | -0.8 |
| **DCV** | 5.6 | -1.2 | 5.4 | -1.3 | 5.6 | -1.2 | 5.6 | -1.2 | 3.9 | -1.8 |
| **DEE** | 5.4 | 3.3 | 5.1 | 3.0 | 5.4 | 3.3 | 5.3 | 3.3 | 3.7 | 4.8 |
| **DCV + DEE** | 5.2 | 5.9 | 5.0 | 5.8 | 5.2 | 6.0 | 5.2 | 6.0 | 3.5 | 8.6 |
| **WI** | 5.5 | 0.0 | 5.3 | -0.1 | 5.5 | 0.0 | 5.5 | 0.0 | 3.8 | -0.1 |
| **GR** | 5.5 | 0.3 | 5.3 | 0.3 | 5.5 | 0.3 | 5.5 | 0.3 | 3.8 | 0.4 |
| **LEI** | 4.8 | 13.8 | 4.5 | 15.2 | 4.8 | 13.8 | 4.7 | 13.9 | 3.1 | 19.9 |

The carbon dioxide emissions for the CCHP plant scenarios are calculated equal to 0.7 $ktCO_2$, 0.7 $ktCO_2$, 4.5 $ktCO_2$, and 4.8 $ktCO_2$ respectively for biogas, biodiesel, natural gas and LPG. It worth noticing that in case of use of *"renewable"* fuels such as biogas and biodiesel, electricity integration is the only contribution to the total $CO_2$ emissions.

**Table 18.** $CO_2$ emissions of the proposed strategies and percentage of avoided $CO_2$ (comparison with CAV).

| | CAV ($ktCO_2$) | VAV ($ktCO_2$) | CAV vs VAV (%) | PVGF ($ktCO_2$) | CAV Vs PVGF (%) | PVF ($ktCO_2$) | CAV Vs PVF (%) | LPV ($ktCO_2$) | CAV Vs LPV (%) |
|---|---|---|---|---|---|---|---|---|---|
| **RB** | 5.5 | 5.3 | 4.5 | 5.5 | 0.1 | 5.5 | 0.8 | 3.8 | 30.8 |
| **AHR** | 5.6 | 5.3 | 5.1 | 5.6 | 0.1 | 5.5 | 0.8 | 3.9 | 30.7 |
| **DCV** | 5.6 | 5.4 | 4.5 | 5.6 | 0.1 | 5.6 | 0.8 | 3.9 | 30.5 |
| **DEE** | 5.4 | 5.1 | 4.3 | 5.4 | 0.1 | 5.3 | 0.8 | 3.7 | 31.9 |
| **DCV + DEE** | 5.2 | 5.0 | 4.4 | 5.2 | 0.1 | 5.2 | 0.9 | 3.5 | 32.8 |
| **WI** | 5.5 | 5.3 | 4.5 | 5.5 | 0.1 | 5.5 | 0.8 | 3.8 | 30.8 |
| **GR** | 5.5 | 5.3 | 4.6 | 5.5 | 0.1 | 5.5 | 0.8 | 3.8 | 30.9 |
| **LEI** | 4.8 | 4.5 | 6.1 | 4.8 | 0.1 | 4.7 | 0.9 | 3.1 | 35.8 |

Both energy and environmental indices calculated are comparable with sustainability indicators estimated for other airports in literature. Specifically, energy consumed per passenger (GWh/PAX) and equivalent carbon dioxide per passenger (t $CO_2$/PAX) have been respectively calculated as high as $4.5 \cdot 10^{-7}$ GWh/PAX and $9.6 \cdot 10^{-4}$ t $CO_2$/PAX, which are lower compared to the *Energy consumption and generation ($D_2$)* and *$CO_2$ emissions and mitigation planning ($D_3$)* indicators of the SRA index [126]. Average values of $D_2$ and $D_3$ for the airports considered in [126] are equal to $1.0 \cdot 10^{-5}$ GWh/PAX and $2.5 \cdot 10^{-3}$, respectively. However, it is worth noticing that such indices are estimated for very energy-intensive structures with higher passenger and cargo volumes, also taking into account non-terminal-related energy consumptions (i.e. energy-intense data centres in the control tower to coordinate inbound and outbound air traffic, transports passengers, baggage and cargo from terminals to the aircraft and back, etc.).

## 4.4 Conclusions

This chapter presented a study on energy saving potential of airport terminals in the Mediterranean areas. In order to provide guidelines to reach the goal of *net zero energy* or *net zero emissions* airports, a wide range of energy-saving strategies have been investigated on the Naples International Airport. A comprehensive study of a wide range of energy-saving actions was carried out by means of a detailed building energy simulation model of a two-story terminal building comprising 91 thermal zones. An innovative approach based on the coupling of Building Information Modelling (BIM) and Building Energy Modelling (BEM) was adopted to model and simulate the building energy performance. The explored solutions were chosen according to their capacity to reduce airport energy demand, HVAC system efficiency, and increase renewable energy production.

The obtained results provide important insights that airport operators may export in the context of airports with similar operating conditions:

- envelope insulation or window renovation solutions do not provide significant energy savings in terms of PES which can lead to unprofitable investments;
- the improvement of the air distribution systems with strategies such as AHR, DCV, DEE, and VAV are valuable solutions to reduce the annual energy consumption of terminal buildings. The time of return of investments can be very short;
- airport facilities should certainly refurbish the lighting system to achieve substantial savings, up to 13%;
- architecturally integrated photovoltaics are convenient solutions only if wide surfaces are available for implementations;
- large photovoltaic plants are fundamental elements to reduce the electricity demand from the power grid;
- dedicated generation systems such as combined cooling heat and power plants (CCHP) are always interesting solutions, as airports are very intensive energy consumers. If “renewable” fuels are adopted *PES* values up to 90% can be achieved.

The study presented in this chapter highlights that the *net zero* goal can be reached only if holistic approaches are adopted, by combining different solutions to both cut energy needs and increase the exploitation of renewable energy sources.

# Chapter 5
# Improving the efficiency of rail network service buildings: free cooling strategies for signaling equipment rooms

## Summary

This chapter aims at proving the validity of free cooling strategies to reduce the energy consumption of technical buildings for signaling equipment located along railway lines.

A typical building used for this purpose was analysed from an energy point of view. Specifically, the air-conditioning system was modelled and dynamically simulated with two different control logics to exploit favourable outdoor air conditions and assess their behaviour in different working conditions, i.e. weather zone, airflow rate, and indoor set-point temperatures. The study demonstrates that railway operators moving toward a high degree of digitalization and electrification may learn from the experience of the telecommunication and IT industries to substantially reduce the energy consumption of high-consuming processes such as the cooling of signaling devices. Standard design can be adopted within railway infrastructures on technical buildings that have similar architectural and mechanical characteristics.

## 5.1 Introduction

The rapid development of railway traffic registered in the last years led to increased interest in the carbon footprint of the whole rail infrastructure. An important slice of the energy consumed by the entire sector is provided by all non-traction aspects such as the operation of station buildings, depots, sub-stations as well as technical buildings intended for traffic control and signaling. This segment of the entire rail industry accounts for 10% [63], which is even higher within metropolitan areas [64].

The serious energy crisis and the rise in the cost of energy in many European countries are pushing railway operator and facilities managers as well as contractors to make the entire infrastructure more efficient and enable significant cost savings [20].

To ensure rail network operation and traffic safety, given the fallible nature of human supervision, attempts are being made to move from traditional light signaling mechanisms, which must be interpreted by train drivers, to modern computer-based control systems based on signals that can be interpreted independently by the on-board control system [148]. These new technologies contributed to foster the spread of High-Speed Railway (HSR) that requires specially built trains with increased power to weight ratio and must have in-cab signaling system. The traditional signaling systems are incapable for high-speed trains [149].

The control and signalling devices need to be dislocated along the rail lines. The management equipment for these signals are placed within dedicated technical buildings installed in different points of the network, which allow to carry out the operation of mechanical devices, check their status and detect faults [150].

Those fundamental technologies along with other auxiliary equipment that guarantee their continuous operations (i.e. transformers, MV / LV cabins, uninterruptible power supply systems, etc.) typically have higher heat loss, so that critical temperatures can be reached within the zone. For this reason, air-conditioning results to be a paramount strategy to guarantee the operation security of all equipment. The space cooling of those technical

rooms may require significant amount of energy which can be reduced by means of natural ventilation or free cooling. While natural ventilation is limited due to security risks, the free cooling can be used in place of air-conditioning. It is recognised as a valuable solution to drop the energy consumption. Free cooling uses the cold outdoor environment or other cold sources as a heat sink when those are in favourable conditions with respect to cooling needs [151]. It is particularly adopted in IT industry to cool down data centers, server rooms or other telecommunication equipment [152] by means of both the air- and fluid-based free cooling [153]. ASHRAE provides specific recommendations to implement effective free cooling strategies and ensure safe environment for this space typology [154]. Given the enormous development of the communication infrastructure worldwide and the massive computerization of companies, their reliability and the management of related energy consumption have become crucial [155]. Zhang et al. [152] highlighted that the cooling energy consumption takes up around 30–50% of the total consumption of data centers due to the inefficient cooling system. The higher share is due to chillers, followed by fans, pumps, and, if available, the cooling tower. A metric, specifically developed for data centers, to assess the effectiveness of free cooling as well as other energy efficiency measures is the Power Usage Effectiveness (PUE). The index is calculated as a fraction of the total power consumed to that used by the IT equipment; ideally, the value of PUE should be equal to 1 [156]. As for data centers, the PUE index may be an useful tool to evaluate communication and signalling systems from an energy point of view.

However, while free cooling is a common measure to cool down the intense energy-consuming IT equipment, there are no studies that specifically address such strategies to improve the efficiency of the cooling system serving the signaling apparatus of railways. It is convenient for infrastructure managers that the equipment have a high degree of standardization given the high number of intermediate stations required along the line. In fact, those plants, as well as the buildings they are in, have similar architectural and mechanical features, although they are built in

different places with different climate conditions. Therefore, it also important for companies to identify standard energy efficiency measures that can be systematically applied to the whole infrastructure. In this context, the study presented in this chapter aims to analyse and optimize several solution to reduce the energy consumption related to the air-conditioning of the wayside rail technical buildings. Specifically, a comprehensive analysis of two different free-cooling strategies was carried out. Also, the influencing parameters were optimized in order to define easy to implement measures on existing plants or design criteria for new constructions. A numerical model of the building thermal zones and a the air loop system has been developed to simulate the actual and proposed systems with a high degree of detail. The BIM2BEM approach (described in Chapter 1) was used to speed up the building modelling. Furthermore, in order to evaluate the energy saving potential od the different strategies, simulations were performed for the case study of a multi-station peripheral base (Posto periferico multistazione, PPM) which contains important equipment for the traffic management and signalling.

## 5.2 Material and Methods

The methodology adopted to carry out the study, is described in the following sections. The selected technical building is presented in section 5.2.1 along with the assumption related to the air-conditioning system. Section 5.2.2 describes the modelling of the building-plant system instead, as well as the energy-saving measures investigated.

### 5.2.1 Description of the case study

A Multi-station peripheral base (Posto periferico multistazione, PPM) is a building typology located on the longest railway lines, housing the equipment that controls the sensors distributed along the tracks to ensure safety and optimally manage the line. These buildings (shown in Figure 43) are generally placed each 20-25 km along the line of the high-speed railway.

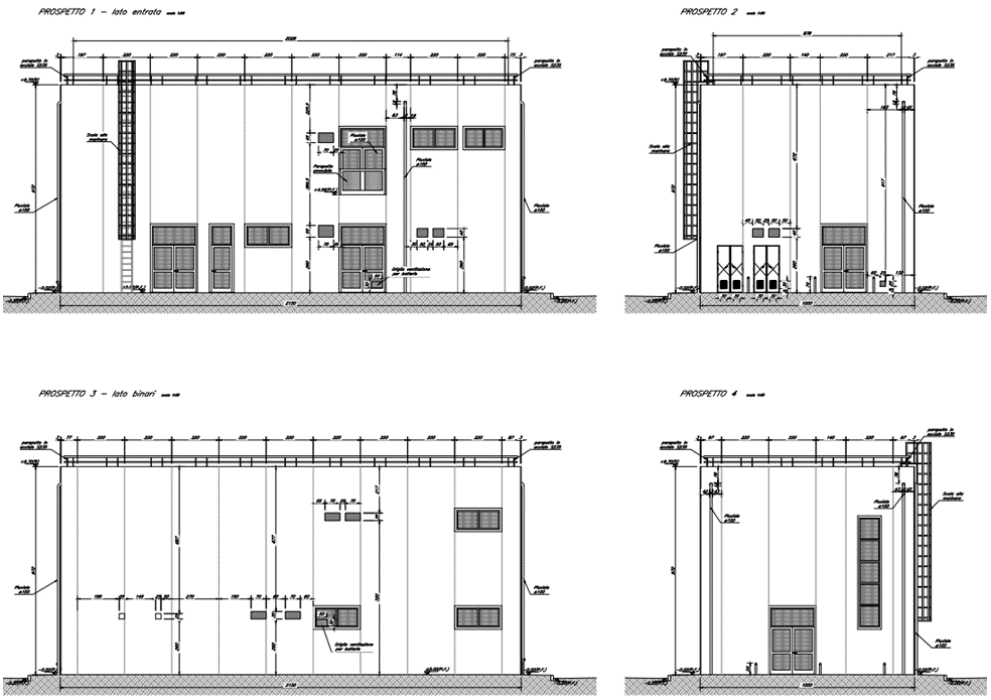


**Figure 43.** Views of the multi-station peripheral station.

The building consists of two floors: the equipment room is located on the upper floor, while on the lower floor are the control units room, the movement office, the toilet, two transformer rooms, and the MV / LV substation room.

The external walls of the building are assembled using prefabricated interlocking panels. These consist of two layers of reinforced concrete which enclose a layer of polystyrene. The roof consists of a hollow core slab insulated and waterproofed. In the control unit and equipment rooms, a floating floor is placed to convey the cooling air for the equipment.

As said, in the building there are rooms with different intended uses and different thermo-hygrometric needs. Currently, several cabinet air conditioners are envisaged for the cooling of the control unit room and the equipment room; only mechanical ventilation is provided for the transformer and cabin rooms, while a split system is installed in the movement office able to provide both hot and cold air. Table 19 summarizes the design indoor conditions of the technical building spaces.

**Table 19.** Indoor thermo-hygrometric design conditions.

| Room | Heating | Cooling |
|---|---|---|
| **Control units and equipment** | T = 24°C<br>UR = n.c. | T = 24°C<br>UR = n.c. |
| **Transformers and MV / LV cabin** | T = 40°C<br>UR = n.c. | T = 40°C<br>UR = n.c. |
| **Movement office** | T = 20°C<br>UR = n.c. | T = 26°C<br>UR = n.c. |
| **W.C.** | T = 20°C<br>UR = n.c. | T = n.c.<br>UR = n.c. |

The uninterruptible power supplies (UPS) equipment and low voltage power supply panels are located in the control unit room, while in the equipment room there are the devices that manage railway traffic. The

equipment located in the control unit room is used to make those in the equipment room work.

Despite having the same thermo-hygrometric needs, the two rooms are equipped with independent air conditioning systems operating with the same logic. The thermal load due to equipment room machineries is estimated as high as 18 kW, while the one due to the control units is calculated as equal to 24 kW. Since the two rooms have a considerable internal thermal load, they need to be constantly conditioned, even in wintertime.

The air conditioning system installed in the two rooms includes a direct expansion cabinet-type air conditioning unit operating with R-410A refrigerant. The main technical characteristics are reported in Table 20. The system attempts to maintain the 24 °C set-point value within the thermal zone and is combined with an economizer to provide free cooling when the outdoor temperature is favourable. The outdoor, indoor, and supply air temperatures are monitored by three sensors placed outside the building, in the air plenum close to recirculating dampers, and in the duct after the cooling coil respectively. The cooling air is supplied through the floating floor.

**Table 20.** Characteristics of the chillers.

| Chiller parameters | Control unit room | Equipment room |
|---|---|---|
| **Total cooling power** [kW] | 24.0 | 18.1 |
| **Absorbed power** [kW] | 6.9 | 4.8 |
| **Fan absorbed power** [kW] | 1.4 | 0.7 |
| **EER** | 3.4 | 3.8 |
| **Flow rate** [$m^3/h$] | 5750 | 4930 |
| **Outdoor fan absorbed power** [kW] | 1.1 | 0.55 |

### 5.2.2 Building and system modelling

The energy model of the reference building was generated by means of the automated BIM-to-gbxml-to-OpenStudio import routine of Autodesk Revit, *Revit Systems Analysis* (refer to Chapter 1 for the workflow description). The building geometry was created according to the actual size of the case study building which is reported in Figure 44.

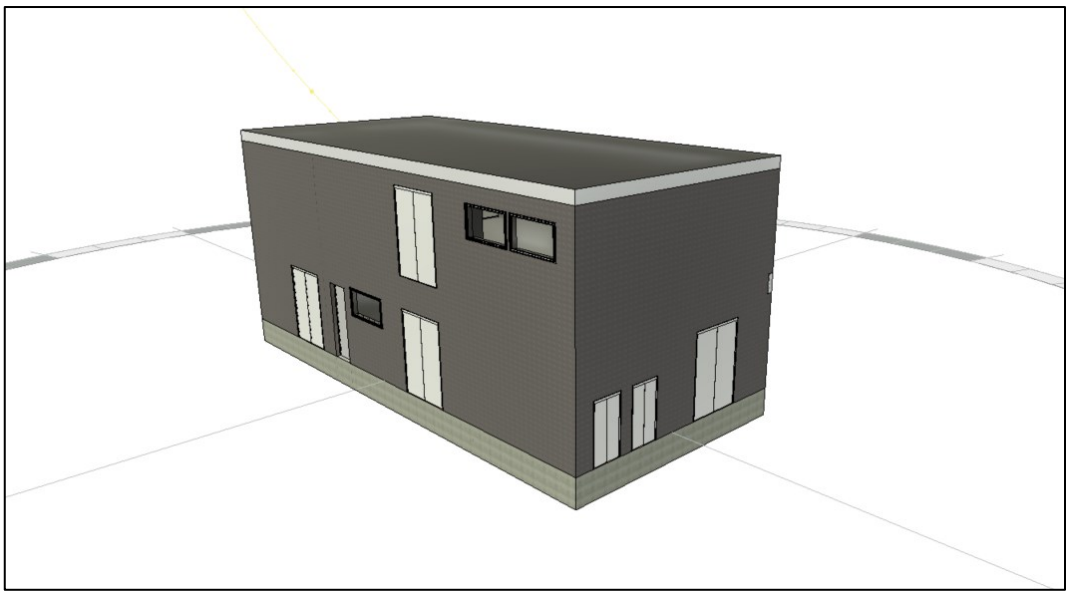

**Figure 44.** External view of the building case study.

The plant was modelled as described in Table 20 while a schematic diagram of the described system is reported in Figure 45. This will be referred as *reference system* hereinafter.

The chiller units are coupled with a plenum that supplies recirculated or fresh air depending on the activated motorized damper. Whenever the outdoor temperature is lower than the indoor one ($T_{out}<T_{in}$) or outdoor temperature is higher than 10 °C ($T_{out} > 10°C$), a constant outdoor flow rate is supplied to the zone; in contrast, whenever outdoor air does not ensure free cooling, indoor air is recirculated and chiller activated. The on-off

constant volume fan is always activated to supply air to the zone both in the case of free cooling and recirculating mode.

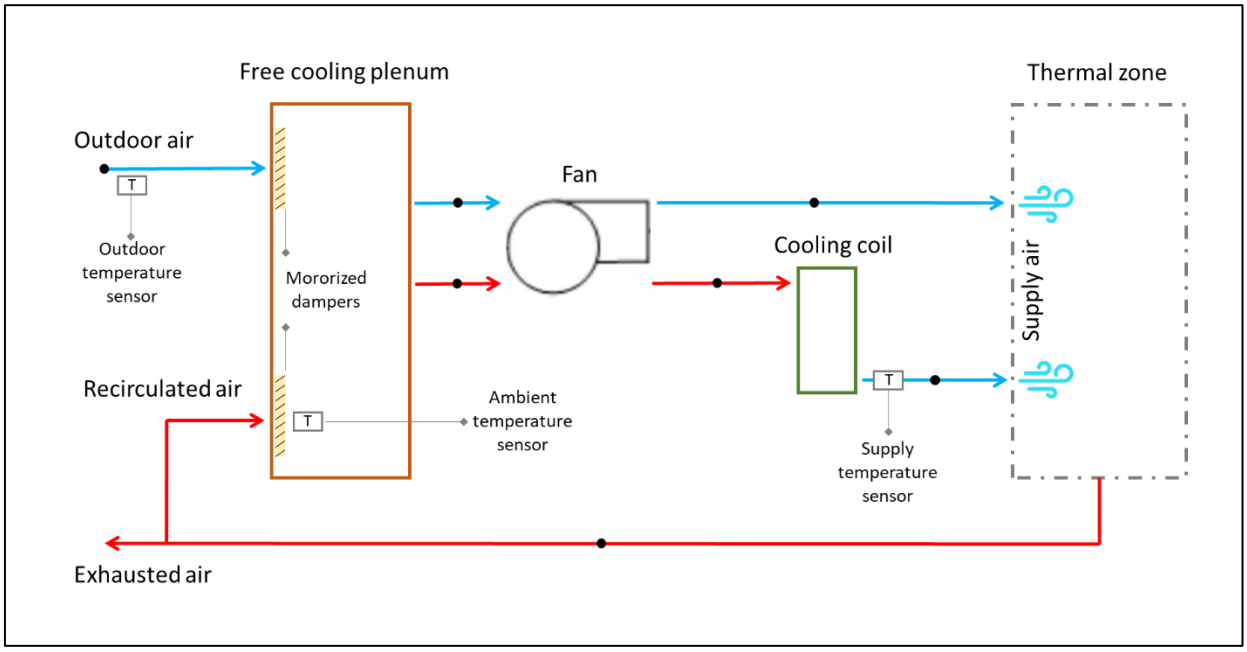


**Figure 45.** Schematic diagram of the considered cooling system.

This system is modelled in OpenStudio environment as an HVAC air loop and the control logic set accordingly to the actual behaviour of the case study system. In addition, a new plant control management strategy is also implemented in order to analyse its performance in terms of the overall energy consumption.

Unlike the reference system control logic, the proposed one allows to:

- cool outdoor air (not only recirculated air) if colder than indoor air temperature;
- mix the recirculated and outdoor air proportionally to control indoor air temperature to set-point value;
- regulate the zone supply airflow rate.

Set-point and airflow values are changed over multiple simulation for optimization purpose.

## 5.3 Results and discussion

This section provides the simulation results of the energy-saving measures investigated to improve the efficiency of the case study system. The analysis focuses on two specific zones of the building which are equipped with the air conditioning system described in sections 5.2.1 and 5.2.2: the i) control unit room and ii) equipment room.

### 5.3.1 Reference system

The behaviour of the system for the control unit room is shown in Figure 46a. Here, the indoor air temperature $T_{in}$ (black curve) and the outdoor air temperature $T_{out}$ (yellow curve) are reported along with the thermal power provided by the refrigeration unit (blue curve) and the cooling rate supplied by the system in free cooling mode (red curve). The chart refers to the first hours of the year, showing the plant operation in the winter period. It is possible to notice that the chiller and free cooling never work simultaneously. For free cooling a minimum external air temperature of 10 °C has been set in order to avoid excessive cooling of the premises (green dashed line); below this value, free cooling switches off and chillers are activated. Furthermore, the plant control does not allow free cooling when outdoor temperature is too high to meet the thermal load, this is evident at hour 15 and 60. The indoor air temperature is kept constant at 24 °C when chillers are on; on the other hand, whenever the economizer is on the indoor air temperature fluctuates as the airflow is not modulated to control a fixed temperature.

As shown in Figure 46b, the chillers mostly work at nominal cooling rate during the summer period; the free cooling is not activated instead. The outside air temperature is too high and, therefore, it would not be able to

guarantee the set point temperature in the room. In the hottest months of the year, the chillers manage to maintain the set point temperature only during night, when the outdoor temperature drops.

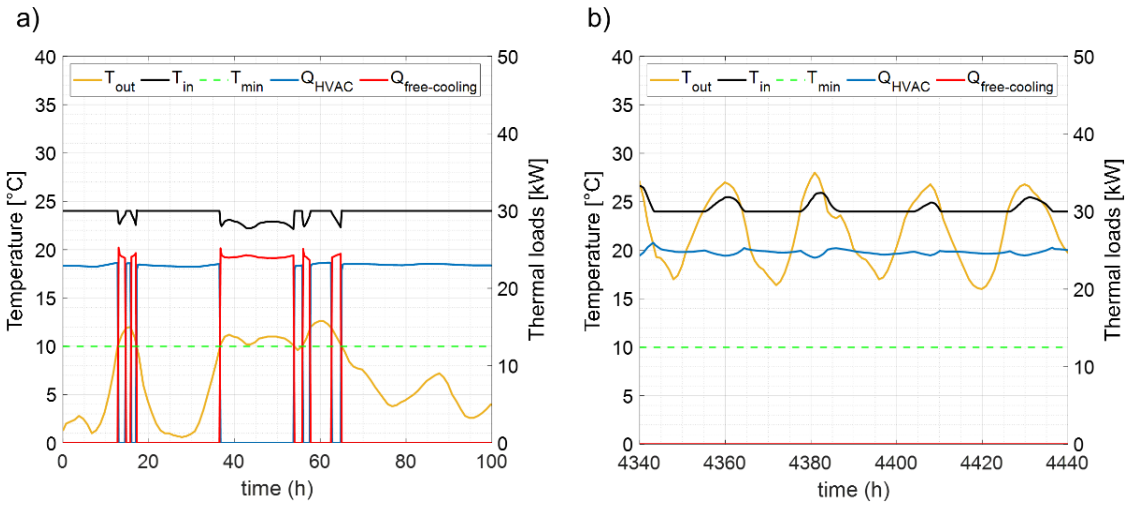


**Figure 46.** Plant behaviour during winter a) and summer season b).

This result is due to the standard size of the chillers, in order to cope with the internal thermal loads and heat gain from the building envelope, a greater size of the chiller is required. However, as said, the fluctuation of temperature is acceptable within certain range; the same size of the chillers is adopted for such application in the rail network due to economic reasons.

Table 21 summarize the thermal energy balanced through the free cooling operation and chillers, both for the control unit and equipment room. In addition, the electricity required, and the hours of operation are also reported. It should be noted that the electricity consumption of free cooling is due to fan operation.

**Table 21.** Summary of the energy consumption of air-conditioning systems.

| Metrics | Control unit room | | Equipment room | |
|---|---|---|---|---|
| | Free cooling | Chiller | Free cooling | Chiller |
| **Cooling energy** [MWh/year] | 23 | 188 | 34 | 118 |
| **Electricity** [MWh/year] | 0.38 | 46 | 0.67 | 28 |
| **Electricity** [kWh/year m3] | 1.18 | 143 | 1 | 42 |
| **Operating hours** | 947 | 7813 | 1920 | 6840 |

### 5.3.2 Increased air flow rates

The reference system ensures the airflows of 1.6 $m^3/s$ and 1.4 $m^3/s$ for the control unit and equipment rooms respectively. In this case, the airflow is not modulated to keep the set-point according to actual thermal loads of the zone. Furthermore, the economizer does not allows that mixed air is supplied to the zones.

To reduce the electricity consumption, a new operating condition based on the same control logic of the *reference system* is proposed. Specifically, the value of the airflow rates were increased in order to reduce the time in which chilled air is required.

The results obtained by increasing the airflow rate of the rooms are shown in Figure 47 (control unit room) and Figure 48 (equipment room). As can be seen, as the supply air increases the free cooling operating hours (blue stack bars) rise since higher ventilation rates allow to lower the internal loads due to equipment heat loss more effectively. This leads the economizer control to admit higher outdoor air temperatures in free cooling operation. However, this effect is less evident for high values of the airflow rates for which the operating time in free cooling mode stabilizes.

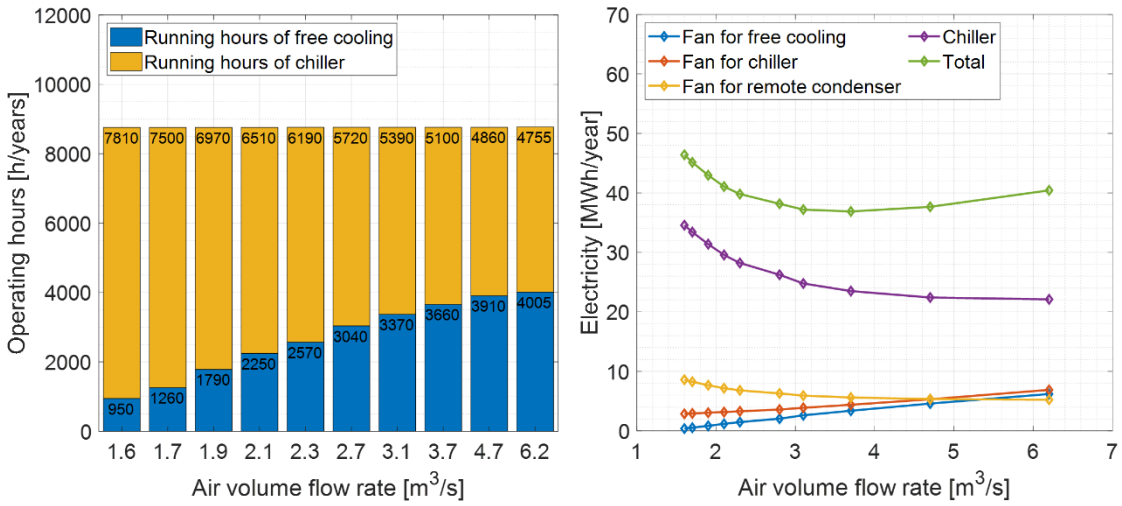


**Figure 47.** Control unit room.

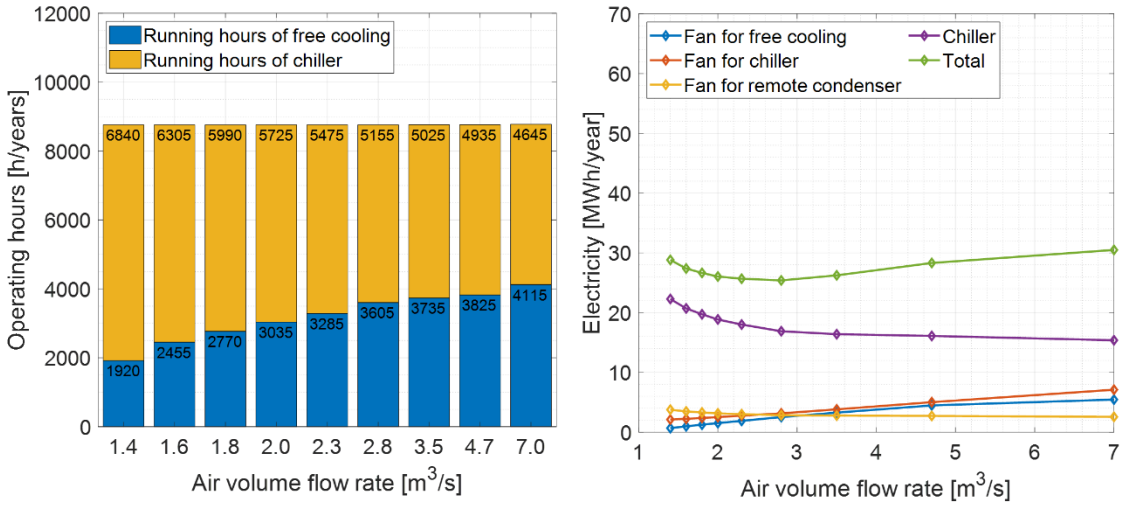


**Figure 48.** Equipment room.

On the contrary, the total amount of electricity required (green line) to operate the cooling system of both the control unit and equipment rooms has a minimum value for flow rates of around 2 - 4 $m^3/s$. Then, it increases as the airflow increases since the electricity consumption of chillers (purple

lines) decreases accordingly to their operating hours. The electricity absorbed by the constant volume fans and other auxiliaries (blue, orange, and yellow lines) changes proportionally to the handled air volumes. The electricity savings are reported in Table 22 an Table 23.

**Table 22.** Summary of the energy consumption of the air-conditioning system in the control unit room as airflow increases.

| | Reference system | Proposed system | | | | | | | | |
|---|---|---|---|---|---|---|---|---|---|---|
| **Set point temperature** [°C] | 24 | 24 | 24 | 24 | 24 | 24 | 24 | 24 | 24 | 24 |
| **Air volume flow rate** [$m^3/s$] | 1.6 | 1.7 | 1.9 | 2.1 | 2.3 | 2.8 | 3.1 | 3.7 | 4.7 | 6.2 |
| **Electricity** [MWh/year] | 46.4 | 45.1 | 43.0 | 41.1 | 39.8 | 38.2 | 37.2 | 36.9 | 37.7 | 40.4 |
| **Electricity saved compared to the current system** [%] | - | 3 | 7 | 12 | 14 | 18 | 20 | 21 | 19 | 13 |

**Table 23**. Summary of the energy consumption of the air-conditioning system in the equipment unit room as airflow increases.

| | Reference system | Proposed system | | | | | | | |
|---|---|---|---|---|---|---|---|---|---|
| **Set point temperature** [°C] | 24 | 24 | 24 | 24 | 24 | 24 | 24 | 24 | 24 |
| **Air volume flow rate** [$m^3/s$] | 1.4 | 1.6 | 1.8 | 2.0 | 2.3 | 2.8 | 3.5 | 4.7 | 7 |
| **Electricity** [MWh/year] | 28.8 | 27.4 | 26.6 | 26.0 | 25.7 | 25.4 | 26.2 | 28.3 | 30.5 |
| **Electricity saved compared to the current system** [%] | - | 5 | 8 | 10 | 11 | 12 | 9 | 2 | -6 |

## 5.3.3 Higher set-point values

Simulations were carried out to analyse the impact of higher set-point temperatures on the energy consumption of the air-conditioning systems. Specifically, the temperature set-points of 24, 25, 26, 27, and 28 °C were taken into consideration. Please note that the control logic and size of chillers are the same as the reference building.

As expected, the free cooling operating hours in the control unit rooms increased significantly from 950 in case of 24°C up to 2810 hours in case of

28 °C. The equipment room which is characterised by lower internal gains behaves similarly, passing from 1920 hours for 24 °C to 3605 hours for a set-point of 28 °C. This is due to the increase of outdoor air temperature range in which free cooling mode can operates to meet the zone thermal loads. Therefore, the optimal solution results to be the highest set-point. These results refer to the reference building airflow rates of 1.6 $m^3/s$ and 1.4 $m^3/s$ for control unit and equipment room respectively.

Table 24 and Table 25 show the values calculated of the total electricity absorbed by the system as the set point temperature and the air flow rate vary. The total electricity is given by the sum of the electricity required by the system fan (both in free cooling and chiller modes), by the fan of the external condenser unit and by the cooling coil. As the set point temperature increases, the electricity required by the system decreases because the hours of free cooling increase.

**Table 24.** Total electricity consumed by the system in the control unit room as the set point temperature and the air flow rate vary

| Air volume flow rate [$m^3/s$] | Set point temperature [°C] | | | | |
|---|---|---|---|---|---|
| | 24 | 25 | 26 | 27 | 28 |
| | Electricity [MWh/year] | | | | |
| 1.6 | 46.4 | 43.4 | 40.9 | 38.3 | 36 |
| 1.7 | 45.1 | 42.2 | 39.4 | 37.3 | 34.8 |
| 1.9 | 43 | 39.9 | 37.8 | 35.3 | 33.1 |
| 2 | 41.1 | 38.7 | 36.2 | 33.6 | 31 |
| 2.3 | 39.8 | 37.4 | 35 | 32.1 | 29.4 |
| 2.7 | 38.2 | 35.6 | 33.1 | 30.3 | 27.2 |
| 3.1 | 37.2 | 34.4 | 31.8 | 29 | 26 |
| 3.7 | 36.9 | 33.6 | 30.5 | 27.9 | 25.4 |
| 4.7 | 38 | 35 | 32.2 | 29.6 | 25.7 |
| 6.2 | 40.4 | 37.9 | 34.9 | 31.9 | 29.5 |

**Table 25.** Total electricity consumed by the system in the equipment room as the set point temperature and the air flow rate vary

| Air volume flow rate [$m^3/s$] | Set point temperature [°C] | | | | |
|---|---|---|---|---|---|
| | 24 | 25 | 26 | 27 | 28 |
| | Electricity [MWh/year] | | | | |
| 1.4 | 28.8 | 26.7 | 25.1 | 23.5 | 21.5 |
| 1.6 | 27.4 | 25.7 | 23.9 | 22 | 20 |
| 1.8 | 26.6 | 24.9 | 23 | 21 | 18.9 |
| 2.0 | 26 | 24.2 | 22.3 | 20.2 | 17.9 |
| 2.3 | 25.7 | 23.4 | 21.2 | 19.3 | 17.1 |
| 2.8 | 25.4 | 22.6 | 20.5 | 18.5 | 16.6 |
| 3.5 | 26.2 | 22.8 | 20.7 | 18.9 | 17.1 |
| 4.7 | 28.3 | 24.6 | 22.2 | 20.2 | 18.7 |
| 7.0 | 30.9 | 28.4 | 25.7 | 23 | 21.1 |

Similarly to the behaviour depicted in Figure 47 and Figure 48 the electricity usage first decrease due to higher free cooling operation. Afterwards, the energy consumption rise since fan expenses become significant compared to savings from chillers. The tables show that the optimal air flow (in the red boxes) is the same for each set point temperature value and corresponds to 3.7 $m^3/s$ for the control unit room and 2.8 $m^3/s$ for the equipment room.

The airflow rates identified by means of the optimization procedures presented ensure much higher free cooling operating hours: from 3660 in case of 24°C up to 5420 hours in case of 28 °C in the control unit room; from 3610 hours for 24 °C to 5450 hours for a set-point of 28 °C in the equipment room.

As discussed in the section 5.3.2, such system configuration does not always ensure a constant temperature in the technical spaces since fan air volume cannot be modulated and cooling coil size may not be adequate to balance summer loads. However, indoor space conditions are kept in a narrow range of humidity and temperature since outdoor temperature limit for free cooling operation is set to 10°C. Figure 49 shows the air thermo-hygrometric conditions in the control unit room (a) and in the equipment room (b) as the set point temperature varies during the year, supplying 1.6

$m^3/s$ and 1.4 $m^3/s$ respectively. As the set point temperature increases, the number of hours in which the internal temperature exceeds the set point decreases because of lower thermal loads. When the outside air is not cold enough to allow free cooling (during the summer) and only indoor air is treated, the air is kept very dry. In contrast, when the economizer works in free cooling mode both humidity ratio and relative humidity increase. On the other hand, it is worth noticing the zones do not require humidity control.

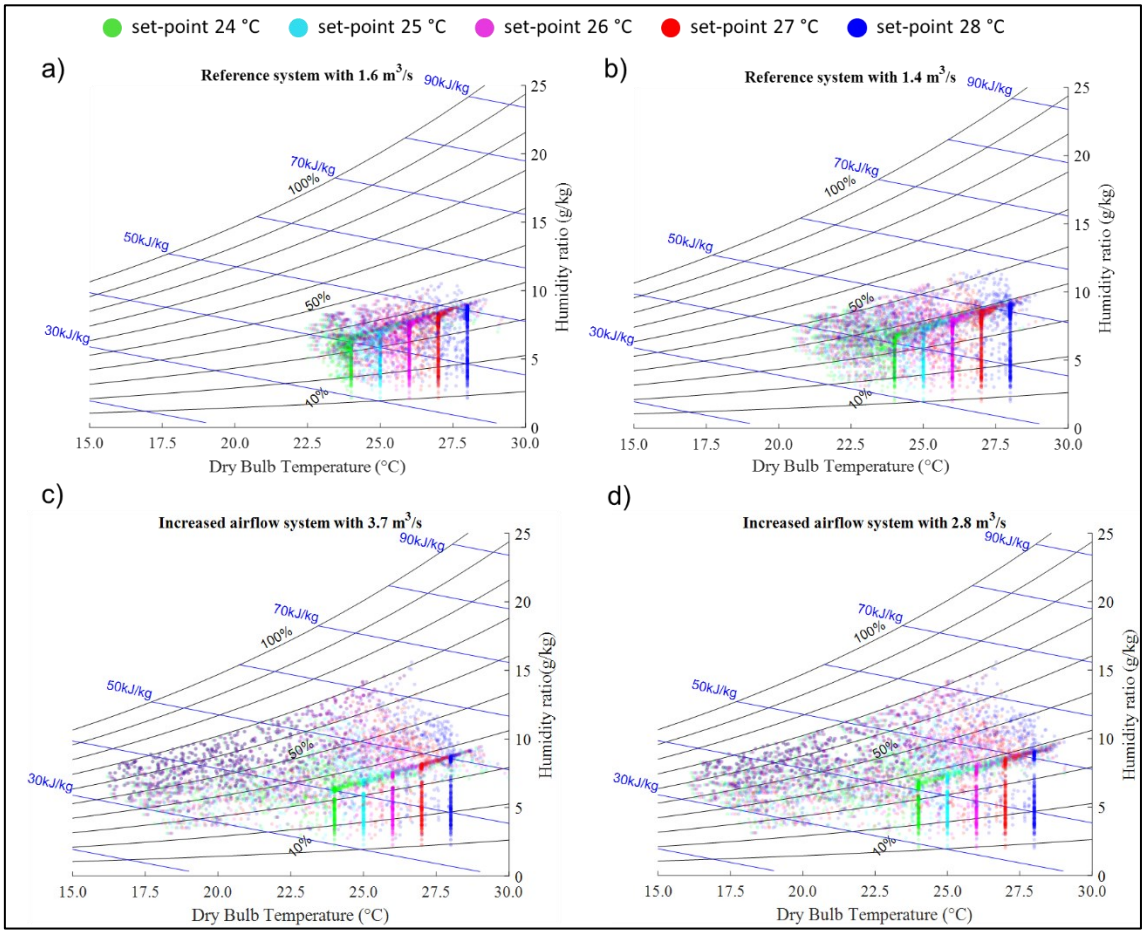


**Figure 49. Thermo-hygrometric**

The results of the numerical simulations are compared with the same system configuration with optimal airflow rates, namely 3.7 $m^3/s$ (c) and 2.8 $m^3/s$ (d). It is clear that increased free cooling potential due to higher air change rates lead to greater humidity fluctuations. Furthermore, they also reduce the minimum air temperature recorded in the zones. Nevertheless, the humidity ratio does not exceed 15 g/kg and relative humidity is always lower (except for rare circumstances) than 70% which may be considered acceptable. Keeping the size and operating logic of the system unchanged, the optimal airflow values ensure energy savings of 21% and 12% for the control unit and the equipment rooms, respectively. By also increasing the set point temperature, the savings can exceed 40% for both rooms as reported in Table 26 and Table 27.

**Table 26.** Summary of the energy consumption of the air-conditioning system in the control unit room as airflow increases.

| | Reference system | Proposed system | | | | |
|---|---|---|---|---|---|---|
| **Set point temperature** [°C] | 24 | 24 | 25 | 26 | 27 | 28 |
| **Air volume flow rate** [$m^3/s$] | 1.6 | 3.7 | 3.7 | 3.7 | 3.7 | 3.7 |
| **Electricity** [MWh/year] | 46.4 | 36.9 | 33.6 | 30.5 | 27.9 | 25.4 |
| **Electricity saved compared to the reference system** [%] | - | **20** | **28** | **34** | **40** | **45** |

**Table 27.** Summary of the energy consumption of the air-conditioning system in the equipment room as airflow increases.

| | Reference system | Proposed system | | | | |
|---|---|---|---|---|---|---|
| **Set point temperature** [°C] | 24 | 24 | 25 | 26 | 27 | 28 |
| **Air volume flow rate** [$m^3/s$] | 1.4 | 2.8 | 2.8 | 2.8 | 2.8 | 2.8 |
| **Electricity** [MWh/year] | 28.8 | 25.4 | 22.6 | 20.5 | 18.5 | 16.6 |
| **Electricity saved compared to the reference system** [%] | - | **12** | **22** | **29** | **36** | **42** |

### 5.3.4 Variable volume fan and air mixing control

In order to maximize the cooling potential due to outdoor air exploitation for air conditioning of the control unit and equipment rooms, the plant control logic has been adapted, keeping the same size and maximum supply airflow of the reference building. Specifically, a system exploiting the advantages of mixing the outdoor air with the indoor air has been simulated. With the new plant configuration, the motorized dampers are now proportionally controlled to reach a favourable temperature in the plenum (see Figure 45) and lower the cooling coil rate. Furthermore, the variable volume fan modulates the amount of supply air to ensure the set point temperatures.

In order to show the new control logic proposed for the air conditioning of the rail technical compartments, the results are shown in Figure 50 and Figure 51 referring to the control unit room. The dynamic temperature and load profiles referring to the equipment room are omitted for sake of brevity, as the systems behave similarly.

When outdoor temperature is low (wintertime, Figure 50a), the system is able to meet the needs of the room maintaining the indoor air temperature (orange line) at the set-point value. In order to guarantee the set point temperature, the zone supply airflow should have a temperature (yellow line) of about 12 °C (15 °C for the equipment room). It can be outdoor, recirculated, or mixed air depending on temperature conditions. When the outdoor air temperature (green curve) is close or higher to 12 °C, the airflow is completely taken from outside and there is the need for chiller activations (Figure 50b) to cool down the air stream. Reversely, mixed air is supplied to the zone whenever outdoor temperature is such as to meet the zone thermal load.

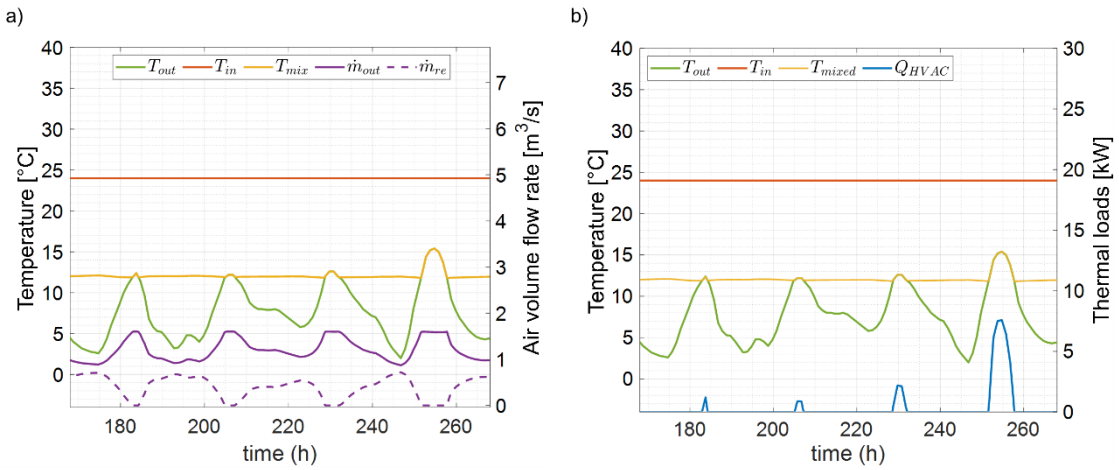


**Figure 50.** Air conditioning system behaviour for four winter days (control unit room). Temperature and airflow profiles (a); Temperature and cooling load profiles (b).

As shown in Figure 51, which depicts what happens in a week in August, the fan only treats recirculated air when the outdoor air temperature (green line) is higher than the indoor temperature (orange line). In this case the internal temperature $T_{in}$ and the mixed air temperature $T_{mix}$ (yellow line) overlap. Similarly, Figure 51b demonstrates that cooling is constantly required both with outdoor and recirculated airflow. Furthermore, it is noticed that neither the free cooling or chillers are able to maintain the set-point, as occurs with the reference system too.

The results obtained from the simulation of the proposed system are compared with those obtained from the simulation of the plant as it stands. The latter can introduce a constant air volume to the spaces, which can be outdoor (free cooling) or recirculated air with chiller activation. The two scenarios differ in the operating control logic, while the size of the system and the supply airflow are the same (1.6 $m^3/s$ for the control unit room and 1.4 $m^3/s$ for the equipment room). The latter are maximum values in the proposed system since the fans can modulate the flow according to request. The new system, on the other hand, has more operating modes: it can work in free cooling (outdoor air only or mixed air), or by supplying outdoor, recirculated, or mixed air coupled with the cooling coil.

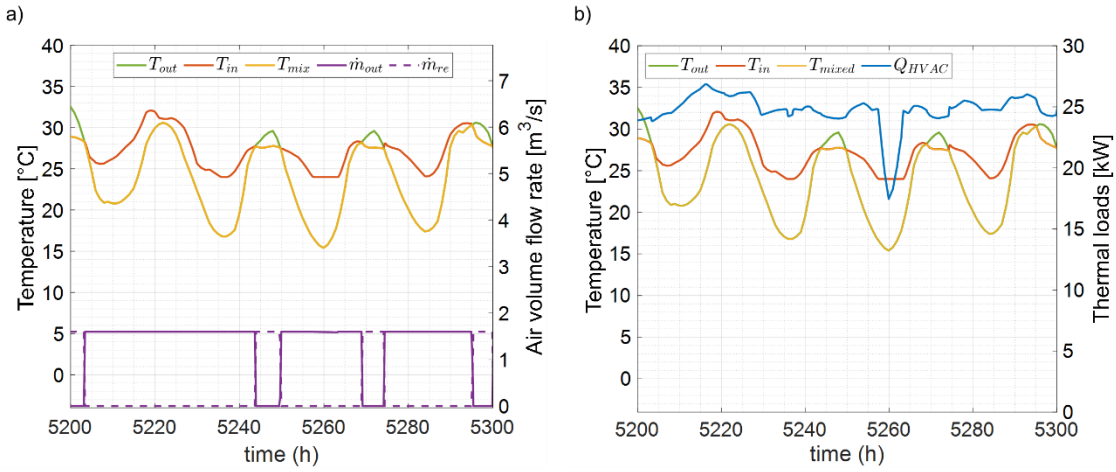


**Figure 51.** Air conditioning system behaviour for four summer days (control unit room). Temperature and airflow profiles (a); Temperature and cooling load profiles (b).

In the current state, the chiller operates for most of the year, the free cooling affects only 11% of the hours for the control unit room (22% in the equipment room). See Figure 52. With the proposed system the slice relating to the free cooling mode increases considerably, reaching 32% of the hours (45% in the equipment room). The increase in free cooling hours is due to the possibility of mixing the outdoor and indoor air which allows the system to exploit the outdoor air stream in the coldest hours of the year with no risk of lowering the temperature too much. In fact, in the current state, the minimum outdoor temperature allowed to operate free cooling is 10 °C. Most of the time, the proposed system works with the cooling coil that chills the outdoor air. This happens since the outdoor air temperature, although it is not low enough to cool down the zone to the set-point temperature, is lower than the indoor one. Therefore, it is not convenient to adopt the operating mode of the system as it stands (the cooling mode with recirculated air and chiller works only 2% of the time).

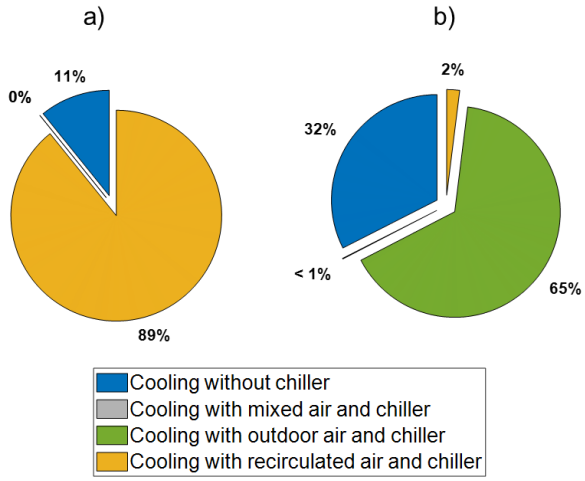


**Figure 52.** Percentage of activation time of the system operating modes for the control unit room. Reference system a); Proposed system b).

The pie charts in Figure 53 show the shares of the energy required by the systems in the various operating modes. It should be noted that the total electricity required differs from the current state and the proposed system. Specifically, the proposed system allows an electricity saving of about 31% (29% for equipment room) compared to the reference system. Moreover, as free cooling is greatly exploited in the proposed system, its share of electricity consumption is higher. It goes from 1% to 4% in the control unit room (and from 2% to 7% in the equipment room). The rest of the energy is used to run chillers and auxiliaries. It is worth pointing out that the energy used in free cooling mode only refers to electricity consumption due to fan operation. This is why the share is very low compared to operating modes with chiller activation.

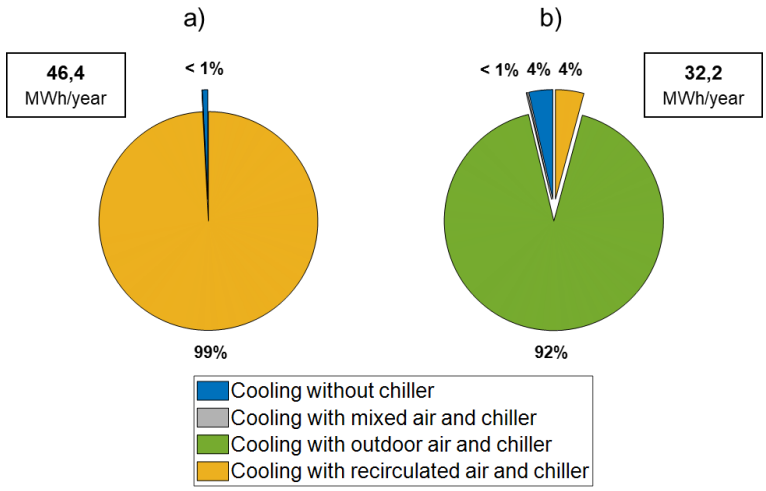


**Figure 53.** Percentage of energy required for the system operating modes in the control unit room. Reference system a); Proposed system b).

The behaviour of the system described so far is also depicted in Figure 54, where the monthly trends in electricity consumption are reported. Each bar consists of three rates: the electricity required by the fans (blue stack), the electricity required for sensible cooling (purple stack), and that required for latent cooling (gray stack).

As mentioned, it increases as outdoor temperature rises. In winter, the proposed system requires less energy than the reference system as it is able to use more free cooling. In summer, however, the energy required in the two cases is comparable despite the fact that the air is treated at a lower temperature. This happens because the quantity of supplied air is the same, as the proposed system stabilizes on the maximum flow rate value. It should also be noted that the proposed system entails a significant amount of electricity usage due to latent thermal energy compared to the reference system. The latent rate is very high in summer because mostly outdoor air is supplied to the zone which is characterized by a higher humidity ratio than indoor air.

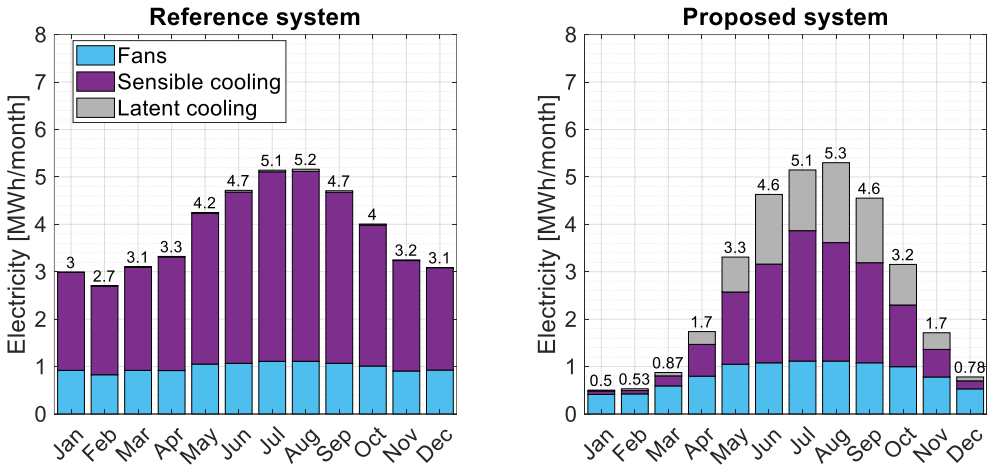


**Figure 54.** Monthly electricity consumption for the reference and proposed system.

By combining the new control logic with higher airflow rates, it was possible to further minimize the energy consumption of the system. An optimization procedure similar to that reported in section 5.3.2 has been carried out.

Figure 55 shows the variability of the electricity demand for the two cases analysed (reference system and proposed system) as the maximum air flow rate varies. The electricity required by the reference system is initially decreasing and then has an increasing trend, while it is always decreasing with regard to the proposed system. For the lowest values of the flow rate there is an increase in the electricity consumption related to free cooling (blue stack). The flow rate of 4.7 $m^3/s$ results in a lower electricity consumption equal to 24.7 MWh/year which is a saving of 23% if compared with the initial flow rate value of the proposed system (1.6 $m^3/s$), of 35% compared with the same flow rate value of the reference system (4.7 $m^3/s$), 33% compared with the optimal flow rate of the reference system (3.7 $m^3/s$) and 47% when compared with the initial flow rate of the current state ( 1.6 $m^3/s$).

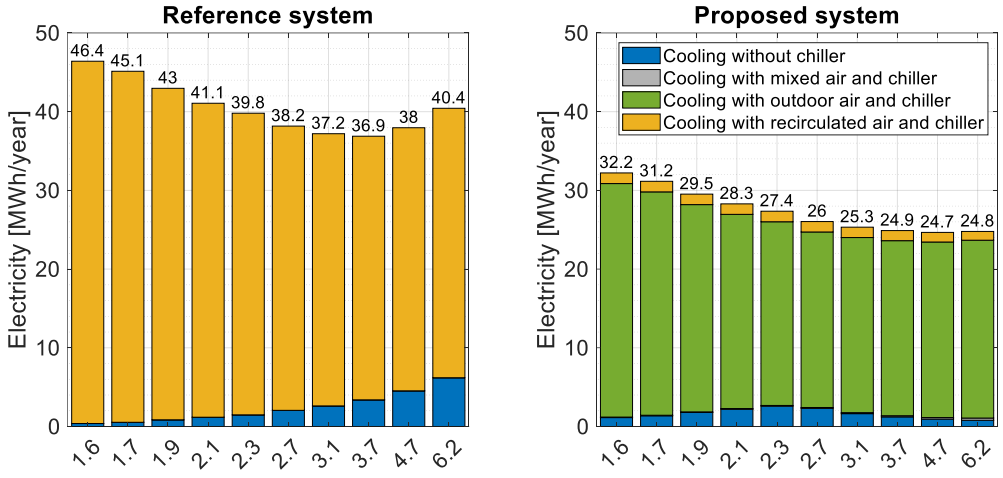


**Figure 55.** Variability of the system electricity required for different airflow rates.

Finally, as proven for the control logic of the reference system, higher set-point values also lead to lower electricity consumptions. Figure 56 reports the results referring to the different strategies analysed. As expected, the most effective one is the one with the 28 °C set-point which entails an energy saving of 17% and 44% if compared to the 24 °C set-point in the case of the reference and proposed system respectively.

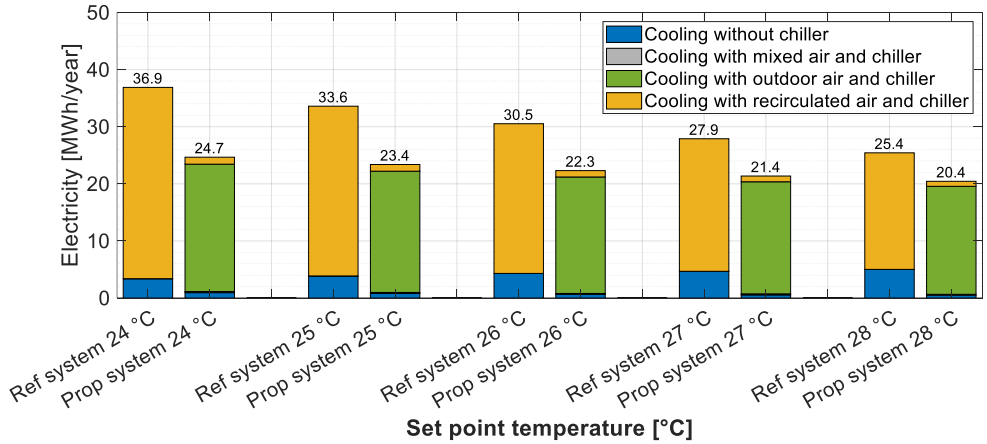


**Figure 56.** Electricity consumption varying with set-point values for optimal airflow configuration (3.7 $m^3$/s for the reference system vs 4.7 m3/s for the proposed system).

### 5.3.5 Impact of outdoor condition

With the aim to identify the optimal plant configuration to be adopted as the standard layout for all the similar technical buildings of the railway network, the system has been simulated in different climate conditions. In fact, this type of buildings must be placed every 20-25 km of high-speed track, located throughout the Italian territory. Specifically, the weather data of Palermo, Napoli, Roma, Torino and Tarvisio were used representing the Italian weather zones B, C, D, E and F, respectively. The weather zone A was excluded as it affects only the islands of Lampedusa and Linosa while the other ones are defined according to the Italian regulation (Annex A of DPR 412/93) [109] that categorise them according to the Heating Degree Days (HDDs). A summary of the main climatic data of the considered location are reported in Figure 57.

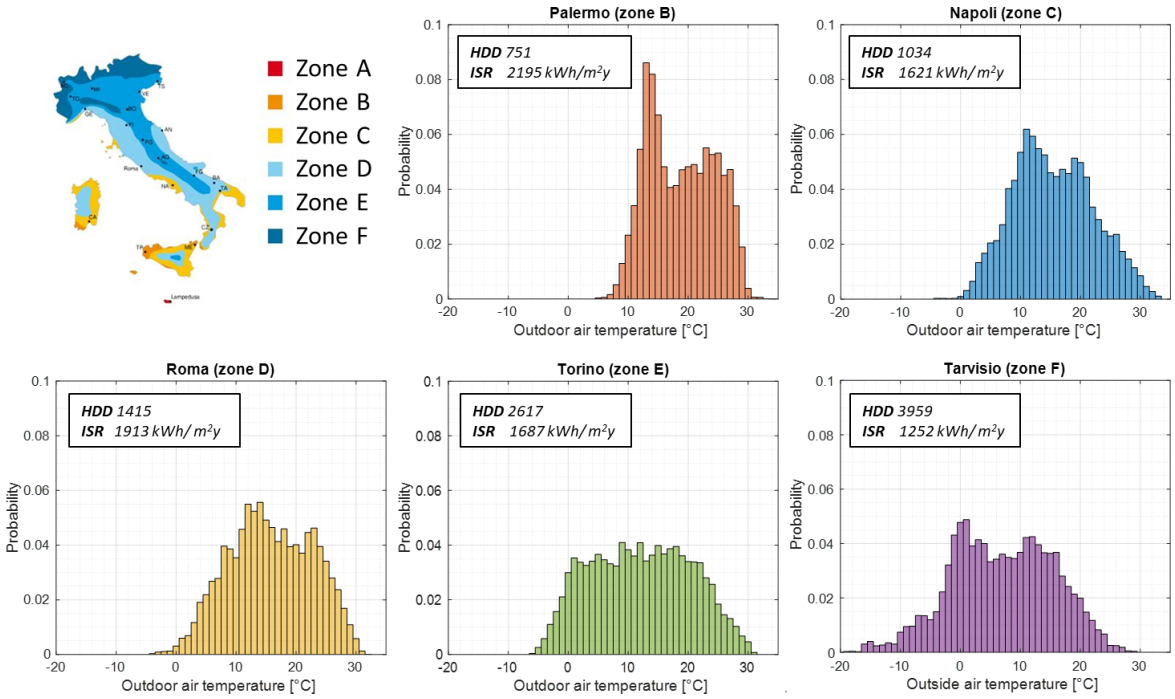


**Figure 57.** Summary of main weather conditions for the considered locations.

The simulations were performed to calculate the electricity consumption, the number of hours in which the system works in free cooling mode and with the chiller activation. The results are respectively reported for the control unit room in Figure 58 and Figure 59. The simulation data relating to the reference system were compared with those of the proposed system as supply airflow changes, with the set point temperature equal to 24 ° C and keeping unchanged the size of the chiller.

As shown in Figure 58, the electricity required by the reference system does not vary considerably as the climatic location varies. As expected, the greatest differences are recorded between climatic zones B and F, however, the differences are reduced as the supply air flow increases. Since free cooling cannot be used when the outdoor air temperature is below 10 °C, the buildings located in colder zones do not necessarily benefit from this control logic.

The described behavior is particularly evident in Figure 59, which shows the number of hours in the two operating modes. Despite the lower energy consumption, the hours of operation in free cooling mode for the reference system decrease when passing from climate zone B to F, as mentioned, due to the rather small range of outdoor temperatures in which the free cooling can operate. In this case, the airflow rate for which the lowest energy consumption is recorded in the control unit room is 3.7 $m^3/s$ (2.3 $m^3/s$ for the equipment room), the same for all locations.

With regard to the proposed system, energy consumption is significantly lower than that of the reference system. The chillers have the possibility to cool the outdoor air or mixed air whose temperature can be controlled and maintained in a temperature range between 10 °C and the indoor set-point temperature. This entails a considerable increase in the hours in which free cooling is used (see Figure 59 relating to the proposed system). The colder locations benefit most from this new operating logic, in fact, the percentage savings in terms of electricity consumption goes from 8-15% to 64-79% for the weather zone B to F, respectively. The optimal maximum airflow for the

proposed system ranges from 3.7 $m^3/s$ to 6.2 $m^3/s$. However, lower airflows can be adopted as the relative percentage changes in electricity consumption are low for airflows above 3.7 $m^3/s$.

| Air volume flow rate [$m^3/s$] | Reference system | | | | |
|---|---|---|---|---|---|
| | Location end climate zone | | | | |
| | PALERMO (B) | NAPOLI (C) | ROMA (D) | TORINO (E) | TARVISIO (F) |
| | Electricity [MWh/year] | | | | |
| 1.6 | 51.5 | 46.4 | 47.6 | 46.2 | 43.9 |
| 1.7 | 50.2 | 45.1 | 46.6 | 45.4 | 42.6 |
| 1.9 | 46.6 | 43.0 | 44.4 | 43.9 | 40.9 |
| 2 | 43.5 | 41.1 | 42.6 | 43.0 | 39.8 |
| 2.3 | 41.7 | 39.8 | 41.2 | 41.9 | 40.2 |
| 2.7 | 40.0 | 38.2 | 39.5 | 40.7 | 37.4 |
| 3.1 | 39.1 | 37.2 | 38.8 | 40.1 | 36.4 |
| 3.7 | 38.9 | 36.9 | 38.5 | 40.1 | 36.1 |
| 4.7 | 40.3 | 38.0 | 39.4 | 41.1 | 38.0 |
| 6.2 | 42.6 | 40.4 | 42.4 | 44.0 | 39.7 |
| Air volume flow rate [$m^3/s$] | Proposed system | | | | |
| | Location end climate zone | | | | |
| | PALERMO (B) | NAPOLI (C) | ROMA (D) | TORINO (E) | TARVISIO (F) |
| | Electricity [MWh/year] | | | | |
| 1.6 | 43.9 | 32.2 | 34.2 | 26.3 | 15.7 |
| 1.7 | 42.6 | 31.2 | 33.2 | 25.6 | 14.8 |
| 1.9 | 39.9 | 29.5 | 31.6 | 24.4 | 13.5 |
| 2 | 38.2 | 28.3 | 30.4 | 23.5 | 12.6 |
| 2.3 | 37.1 | 27.4 | 29.5 | 22.8 | 12.0 |
| 2.7 | 36.2 | 26.0 | 28.4 | 21.5 | 10.8 |
| 3.1 | 35.9 | 25.3 | 28.0 | 20.6 | 9.3 |
| 3.7 | 35.7 | 24.9 | 27.6 | 20.1 | 8.5 |
| 4.7 | 35.9 | 24.7 | 27.6 | 19.9 | 7.9 |
| 6.2 | 36.6 | 24.8 | 27.9 | 19.9 | 7.5 |

**Figure 58.** Electricity consumption of the reference and proposed systems.

| Air volume flow rate [$m^3/s$] | Reference system | | | | | | | | | |
|---|---|---|---|---|---|---|---|---|---|---|
| | Location end climate zone | | | | | | | | | |
| | PALERMO (B) | | NAPOLI (C) | | ROMA (D) | | TORINO (E) | | TARVISIO (F) | |
| | Operating hours | | | | | | | | | |
| | Free cooling | Chiller | Free cooling | Chiller | Free cooling | Chiller | Free cooling | Chiller | Free cooling | Chiller |
| 1.6 | 625 | 8135 | 950 | 7810 | 811 | 7949 | 520 | 8240 | 249 | 8511 |
| 1.7 | 944 | 7816 | 1260 | 7500 | 1050 | 7710 | 741 | 8019 | 566 | 8194 |
| 1.9 | 1765 | 6995 | 1790 | 6970 | 1597 | 7163 | 1126 | 7634 | 1005 | 7755 |
| 2 | 2453 | 6307 | 2250 | 6510 | 2044 | 6716 | 1407 | 7354 | 1309 | 7450 |
| 2.3 | 2890 | 5870 | 2570 | 6190 | 2389 | 6371 | 1689 | 7071 | 1309 | 7450 |
| 2.7 | 3385 | 5375 | 3040 | 5720 | 2870 | 5890 | 2083 | 6677 | 2008 | 6752 |
| 3.1 | 3709 | 5051 | 3370 | 5390 | 3157 | 5603 | 2355 | 6405 | 2332 | 6428 |
| 3.7 | 4005 | 4754 | 3660 | 5100 | 3438 | 5321 | 2587 | 6173 | 2609 | 6151 |
| 4.7 | 4152 | 4608 | 3905 | 4855 | 3665 | 5095 | 2792 | 5968 | 2666 | 6093 |
| 6.2 | 4363 | 4397 | 4005 | 4755 | 3724 | 5036 | 2870 | 5890 | 2941 | 5819 |
| Air volume flow rate [$m^3/s$] | Proposed system | | | | | | | | | |
| | Location end climate zone | | | | | | | | | |
| | PALERMO (B) | | NAPOLI (C) | | ROMA (D) | | TORINO (E) | | TARVISIO (F) | |
| | Operating hours | | | | | | | | | |
| | Free cooling | Chiller | Free cooling | Chiller | Free cooling | Chiller | Free cooling | Chiller | Free cooling | Chiller |
| 1.6 | 762 | 7998 | 2846 | 5914 | 2667 | 6093 | 4136 | 4624 | 5506 | 3254 |
| 1.7 | 1096 | 7664 | 3210 | 5550 | 3002 | 5758 | 4388 | 4372 | 5800 | 2960 |
| 1.9 | 2022 | 6738 | 3760 | 5000 | 3546 | 5214 | 4764 | 3996 | 6272 | 2488 |
| 2 | 2692 | 6068 | 4190 | 4570 | 4009 | 4751 | 5066 | 3694 | 6627 | 2133 |
| 2.3 | 3172 | 5588 | 4510 | 4250 | 4337 | 4423 | 5353 | 3407 | 6904 | 1856 |
| 2.7 | 3397 | 5363 | 4730 | 4030 | 4513 | 4247 | 5608 | 3152 | 7294 | 1466 |
| 3.1 | 3408 | 5352 | 4710 | 4050 | 4482 | 4278 | 5562 | 3198 | 7287 | 1473 |
| 3.7 | 3405 | 5355 | 4700 | 4060 | 4472 | 4288 | 5557 | 3203 | 7283 | 1477 |
| 4.7 | 3433 | 5327 | 4720 | 4040 | 4521 | 4239 | 5573 | 3187 | 7280 | 1480 |
| 6.2 | 3438 | 5322 | 4730 | 4030 | 4529 | 4231 | 5571 | 3189 | 7285 | 1475 |

**Figure 59.** Operating hours of the reference and proposed systems.

### 5.3.6 Environmental and economic analysis

With the aim of exhaustively evaluating the enterprise of implementing the proposed system configurations, an economic analysis has been carried out for each considered airflow rate. Only the results related to the revamping of the control unit room systems are shown for sake of brevity. The costs of each component used to enhance the system such as fans, economizer with motorized dumpers, and temperature sensors were considered in order to calculate the investment costs. In the case of the proposed system, a VAV box was considered too. The purchase price of electricity was considered equal to 250 € / MWh. The capital costs are estimated in the range 13.5 – 17.8 k€ depending on airflows and fan size. As depicted in Figure 60, very low pay back periods are obtained in case of higher airflows. The investment costs are contained, and the savings are substantial as the air flow varies. However, for very high flow rates the SPB values sudden increase, given the higher energy consumption linked to air handling.

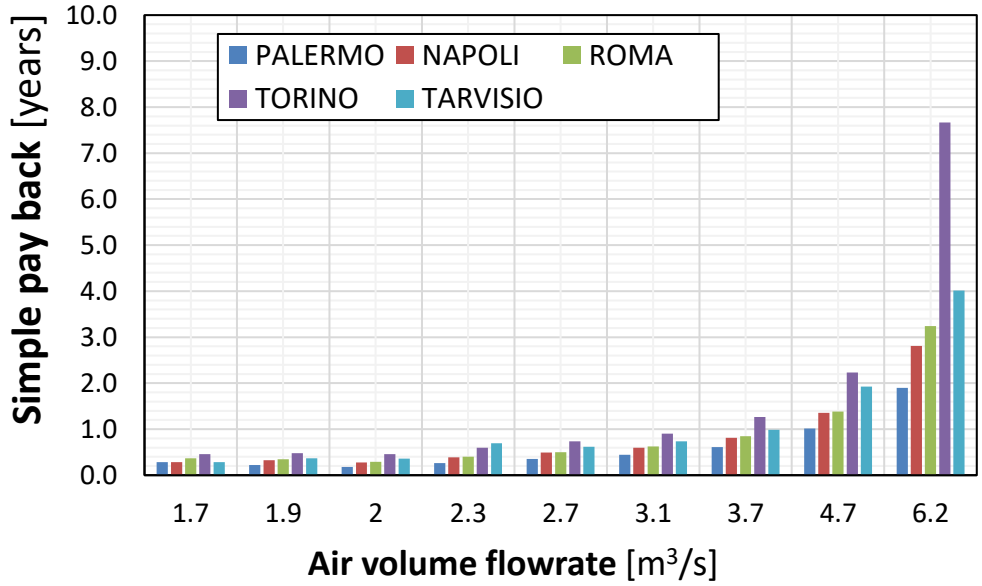


**Figure 60.** Simple pay back values for increased airflows in the reference system.

At contrast, as regards the system proposed with optimized control logic, the SPB is on average higher. However, the latter does not exceed 6 years (see Figure 61). The proposed system in fact involves higher investment costs (in the range 17.4 - 35 k €) and, at the same time, higher operating savings. It should be noted that the locations with more severe winters are penalized also in economic terms with the current control logic of the reference system, given the impossibility of using outdoor air at temperatures lower than 10 ° C.

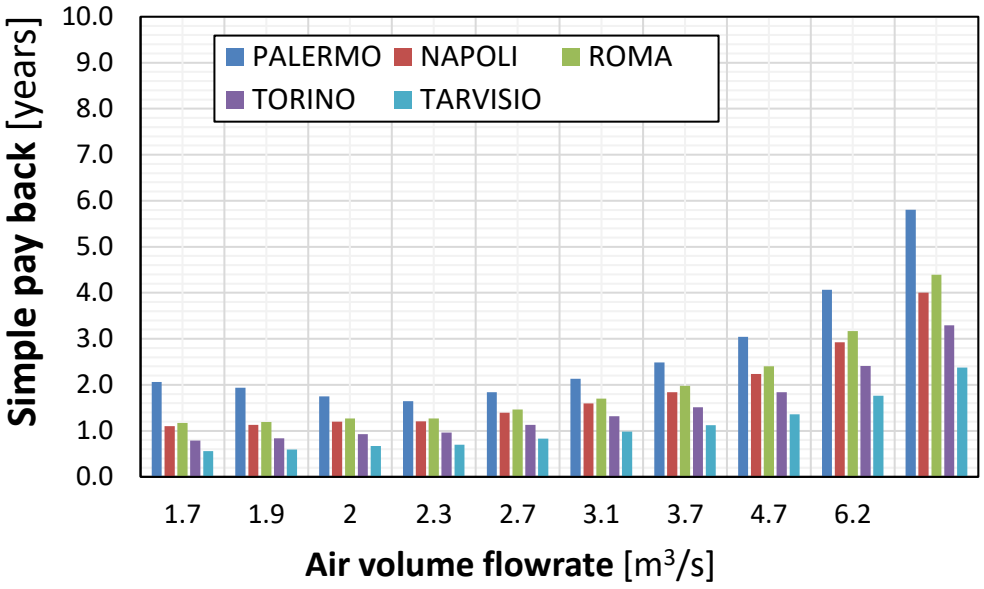


**Figure 61.** Simple pay back values for increased airflows in the proposed system.

The energy results previously shown imply the environmental ones presented, for all the investigated ventilation strategies, Table 28 and Table 29. Note that these results have been obtained by considering an emission factor equal to 0.483 tCO2/MWh$_{el}$. It is possible to notice, in accordance with the energy results shown in the previous sections, that both increased airflow rates and the proposed system control logic return remarkable $CO_2$ emission reduction

**Table 28.** $CO_2$ emissions for increased airflows in the reference system.

| **$CO_2$ emissions** [$tCO_2$/anno] | | | | | |
|---|---|---|---|---|---|
| Airflow rates [$m^3/s$] | Palermo | Napoli | Roma | Torino | Tarvisio |
| 1.6 | 24.7 | 22.3 | 22.8 | 22.2 | 21.1 |
| 1.7 | 24.1 | 21.6 | 22.4 | 21.8 | 20.4 |
| 1.9 | 22.4 | 20.6 | 21.3 | 21.1 | 19.6 |
| 2 | 20.9 | 19.7 | 20.4 | 20.6 | 19.1 |
| 2.3 | 20.0 | 19.1 | 19.8 | 20.1 | 19.3 |
| 2.7 | 19.2 | 18.3 | 19.0 | 19.5 | 18.0 |
| 3.1 | 18.8 | 17.9 | 18.6 | 19.2 | 17.5 |
| 3.7 | 18.7 | 17.7 | 18.5 | 19.2 | 17.3 |
| 4.7 | 19.3 | 18.2 | 18.9 | 19.7 | 18.2 |
| 6.2 | 20.4 | 19.4 | 20.4 | 21.1 | 19.1 |

**Table 29.** $CO_2$ emissions for increased airflows in the proposed system.

| **$CO_2$ emissions** [$tCO_2$/anno] | | | | | |
|---|---|---|---|---|---|
| Airflow rates [$m^3/s$] | Palermo | Napoli | Roma | Torino | Tarvisio |
| 1.6 | 24.7 | 22.3 | 22.8 | 22.2 | 21.1 |
| 1.7 | 21.1 | 15.5 | 16.4 | 12.6 | 7.5 |
| 1.9 | 20.4 | 15.0 | 15.9 | 12.3 | 7.1 |
| 2 | 19.2 | 14.2 | 15.2 | 11.7 | 6.5 |
| 2.3 | 18.3 | 13.6 | 14.6 | 11.3 | 6.0 |
| 2.7 | 17.8 | 13.2 | 14.2 | 10.9 | 5.8 |
| 3.1 | 17.4 | 12.5 | 13.6 | 10.3 | 5.2 |
| 3.7 | 17.2 | 12.1 | 13.4 | 9.9 | 4.5 |
| | 17.1 | 12.0 | 13.2 | 9.6 | 4.1 |
| | 17.2 | 11.9 | 13.2 | 9.6 | 3.8 |
| | 17.6 | 11.9 | 13.4 | 9.6 | 3.6 |

## 5.4 Conclusions

This chapter presented a study on the energy saving potential of different free cooling strategies for the space cooling of communication and signaling device rooms which serve the railway infrastructures. In order to identify the most convenient solutions to reduce the energy impact and define standard design criteria for the air conditioning systems, two different control logics to exploit favourable outdoor air conditions were investigated for a technical building located along the railway. A detailed building energy model was developed to simulate the air conditioning system coupled with different air economizers.

The obtained results provided important insights that both infrastructure designers and operators should take into account:

- free cooling potential can be enhanced in existing buildings by means of higher airflow rates. As demonstrated, up to 21% of electricity can be saved by increasing the airflow up to 3.7 $m^3/s$;
- higher set-point value is an easy to implement solution that leads to significant energy savings with no costs. For instance, about 40% of electricity is consumed by maintaining the set-point to 28 °C;
- innovative free cooling strategies that allow modulating and mixing the outdoor and indoor airflows have an energy saving potential of around 50%. Such systems have less capacity to keep humidity ratio in a narrow range, however, it is demonstrated that both temperature and humidity are kept in an acceptable working range;
- both traditional and innovative economizer control logics have advantages with colder weather. Nevertheless, the proposed system allows exploiting the outdoor temperatures more. The percentage savings of electricity in weather zone E is 80%.

The analysis carried out in this study points out the high impact that some easy-to-implement solutions to handle the supply air of railway technical buildings have.

# Main findings and design criteria

Traffic infrastructures such as railway/metro and maritime stations, airports, etc. have a key role as they are important nodes of the transportation systems; they represent the interface between the passengers and the infrastructures. The number and high quality of services provided to customers led to increasing attention to energy efficiency.

In this context, this thesis has pursued the following research objectives:

- analyse the **state of the art** of the current energy-saving solutions adopted in the design and the management of transport infrastructures, i.e. railway and maritime stations, airports, etc.;
- identify **new technologies, innovative methodologies and good practices** to be adopted in the design workflow of these buildings in order to minimize their environmental and economic impact;
- provide **recommendations** for assessing and designing highly-efficient transportation infrastructures moving toward the concept of zero-energy infrastructures.

The study was carried out by analysing energy-saving opportunities for port areas (Chapter 2), railways stations (Chapter 3), airport facilities (Chapter 4), and railway technical buildings (Chapter 5) with the aim of extrapolating design criteria for new constructions and refurbishment projects. First, the appropriate technologies for such applications were identified, then, the analysis of suitable case studies, found to analyse the several traffic buildings typologies that are the subject of this study, were performed by means of detailed building energy models. The latter were developed on purpose by means of advanced whole-building energy performance simulation tools proposing novel workflows based on Building Information Modeling to Building Energy Modeling (BIM2BEM) methodologies.

As discussed in Chapter 1, the high degree of complexity of traffic infrastructures makes **design and analysis tools** crucial for managing the project and improving its sustainability. Both the BIM and BEM are attractive approaches to be adopted to improve the efficiency of buildings, bringing significant advantages from the point of view of project management and the decision-making process. The ***simulation-aided design*** turns out to be very convenient at an early stage of the project when energy analyses can guide concept design toward the most sustainable choices. The BIM2BEM facilitates the work of energy modellers and helps in the enhancement of the integrative design, enhancing project schedule by avoiding the creation of redundant and time-consuming models. Therefore, the adoption of advanced modelling and simulation tools for building envelope and HVAC systems (BEM), as well as project management information tools (BIM) that allow for reduced costs, should be considered as the most effective energy efficiency measure to be adopted in the design of transport infrastructures, encouraging and supporting *value engineering* in the design process (Figure 62).

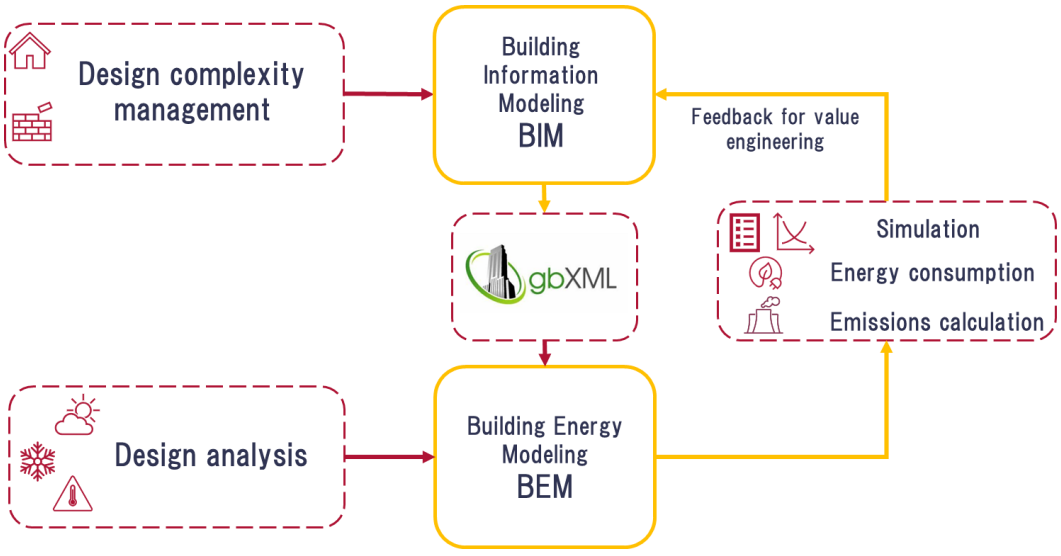


**Figure 62.** Schematic diagram of simulation-aided design using BIM2BEM.

On the other hand, the methodology is also suitable as a tool in facility management and **continuous improvement processes**. The energy model may follow the actual building during its life. In this way, the digital model accompanies the improvement process, facilitating the facility management and supporting decisions aimed at reducing air pollution and increasing energy efficiency. However, BIM2BEM is not a mature methodology and needs to be further investigated. Information may be lost during the export and import process. Therefore, greater integration between the two techniques and the development of increasingly reliable workflows capable of extending modelling capabilities starting from information models are required.

In light of the study carried out in this thesis, a set of promising energy efficiency measures to reduce energy consumption in this context have been identified and summarized in this section. A graphical overview of the selected strategies is shown in Figure 63.

It is clear that the greatest energy saving potential for **port buildings** is offered by the use of renewable energy sources. This is demonstrated by the case study analysis of the *Molo Beverello* maritime station which is a new construction project in Naples, Italy. Specifically, the implementation of building integrated photovoltaics (PV glass) allows about 25% of primary energy savings, whereas traditional photovoltaic installations may push the PES up to 40%. Of course, greater plant sizes compared to that analysed in Chapter 2 may lead to much higher energy saving. The use of highly efficient heat pumps / chillers is the second strategy as regards primary energy saving. Given the availability of sea water source in the close proximity of the considered buildings, the water-source heat pumps / chillers have a great impact on consumption.

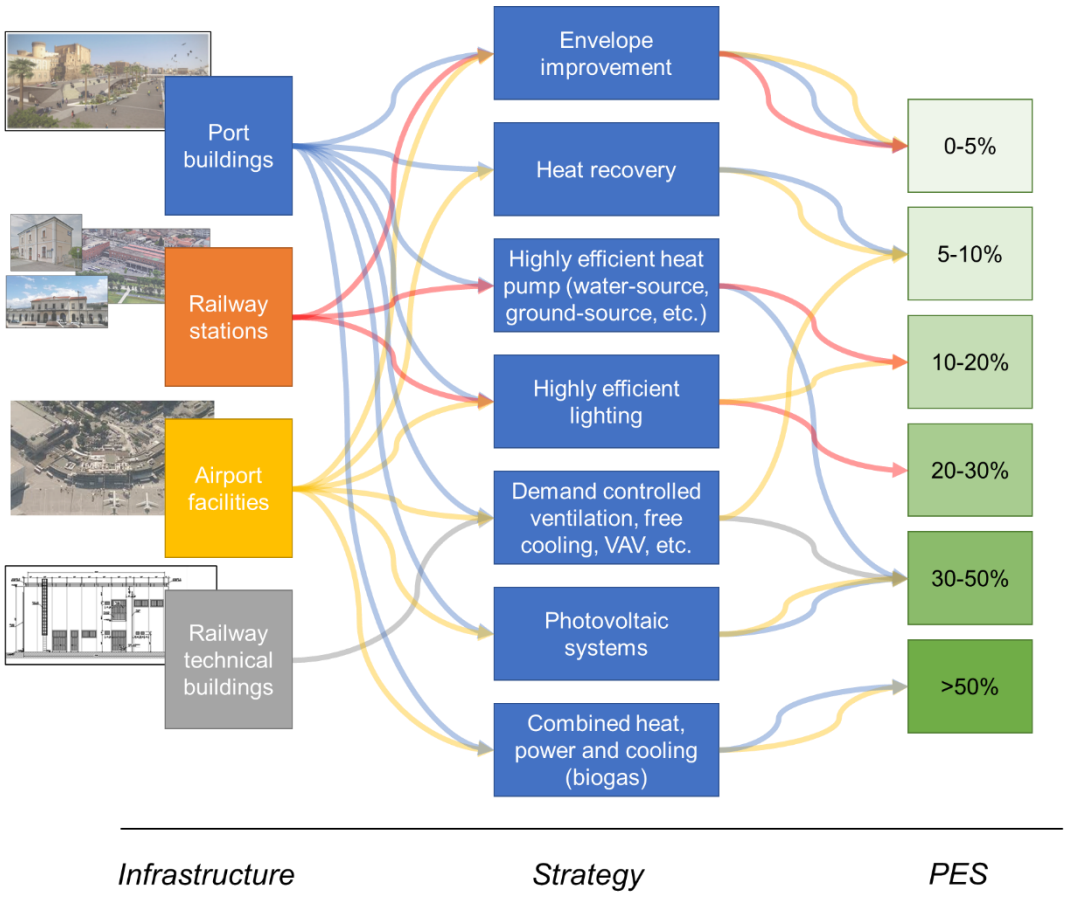


**Figure 63.** Summary of the energy saving strategies analysed and approximate primary energy saving potential.

As proven, this application for Mediterranean weather and seawater temperature conditions implies a PES value of 42%. Moreover, if chillers are equipped with heat recovery systems they can save about 10% of electricity. As concern **railway stations**, the major energy and economic benefits can be obtained by the reduction of electric load intensities that are the most impacting energy consumptions. Systematic efficiency actions on lighting and appliances are highly encouraged. As demonstrated in Chapter 3, an overall primary energy saving of 26% can be reached by means of highly-efficient lighting systems (e.g. LED lamps). The pay back periods of the investment may be very low. Energy measures such as envelope improvement and replacement of HVAC with more efficient systems have a

lower impact on the station heritage instead. Only a limited number of stations are equipped with air conditioning systems. So, the primary energy savings are estimated as high as 1.2% for envelope improvement and 14.3% for HVAC system renovations. Nevertheless, it should be highlighted that those strategies systematically applied to the station building stock may lead to negative net present values over 25 years. Those findings were obtained by means of the bottom-up modelling of the Italian railway station building stock. A data-driven model, derived by the detailed physics-based models of the station *archetypes*, resulted a valuable tool for railway infrastructure managers to plan building renovation on large scale.

**Airport terminals** are probably the most energy-intensive facilities among those covered by this dissertation. Their energy consumption is comparable with small cities. Dedicated generation systems such as combined cooling heat and power plants (CCHP) are always interesting solutions for airports. If *renewable* fuels such as biogas are adopted, PES values up to 90% can be achieved. It worth noticing that cogeneration, or trigeneration, well fits the need of harbour areas as they are intensive energy consumers too. For the same reason, large photovoltaic plants are profitable solutions for airports since a very high rate of self-consumption can be reached. The photovoltaic power plant analysed in Chapter 4 for the *International Airport of Naples* leads to a saving in energy consumption up to 35%, however, very high peak power are required to reach this value. In contrast, architecturally integrated photovoltaics are convenient solutions only if wide surfaces are available for implementations.

Similarly, to other building infrastructures, airport operators should certainly refurbish the lighting system of the facility since substantial savings, up to 13%, can be achieved. Furthermore, since airports have large consumption due to HVAC systems, and the one analysed in Chapter 4 is no exception, strategies on ventilation have to be taken into consideration. The combination of air heat recovery, demand-controlled ventilation, free cooling or variable air volume strategies low the energy consumption up to 6% on the total electricity consumed in the terminal. It is observed that the

implementation of air economizers for free cooling strategies in airports located in mild climate zones can be a beneficial solution since the cooling period is extended due to higher internal gains (crowding spaces, high equipment heat loss, etc.). For the same reason, envelope insulation or window façade replacement do not have advantage of significant energy savings.

Modern transportation systems are strongly dependent on advanced digital infrastructures that require high energy-consuming processes, i.e. data centers in the control tower to coordinate inbound and outbound air traffic, **communication and signaling equipment** for rail network operation and traffic safety, etc. The control and signaling devices need to be dislocated along the rail lines within dedicated technical buildings throughout the railway network which also require significant energy consumption for auxiliaries and air-conditioning systems. It is found that the standard systems adopted to cool down signaling equipment rooms are inadequate to make the most of low winter or mid-season temperatures to perform direct free cooling. The optimization of outdoor airflow may lead to electricity savings of up to 21-40% if acceptable indoor conditions range are relaxed (upper temperature and humidity limits of 28°C and 70%). However, the best performance from an energy point of view is achieved by controlling the air distribution system that allows the mixing of indoor and outdoor air. As proven in Chapter 5, economizers that implement advanced controls can reduce electricity consumption by 50%, up to 80% for extreme weather conditions, underling the high impact that some easy-to-implement energy-saving measures can have on high energy-consuming processes.

Finally, the main contributions of this thesis can be summarized as follows:

**Development of a design methodology based on the BIM2BEM approach:** a customized methodology is proposed to model the infrastructure buildings considered for each modelled case study.

**Analysis of case studies focused on different infrastructures building typologies** (maritime stations, railway stations, airports, and

railway technical buildings) to learn and make use of advanced technologies in building energy management.

**Modelling of the Italian railway building stock via physics-based and data-driven building models**: a large-scale analysis of the entire building heritage of railway stations is carried out.

**Identification of suitable design criteria** for designers, constructors, infrastructure managers and stakeholders to improve sustainability and reduce overall infrastructure costs.

While many studies on net-zero energy buildings have been carried out in the literature, few focused on the goal of *net-zero* for large facilities such as the ones investigated. And none of them have been investigated through whole-building performance simulation approaches, customized for the aims of this thesis. For this reason, this work represents the first original research covering the topic of infrastructure sustainability by investigating a wide range of building typologies.

# Final remarks

Although an attempt has been made to identify general guidelines for the implementation of highly efficient systems at the service of transport infrastructures, there are no *one-size-fits-all* solutions or approaches. The design of these facilities has different needs and constraints that must be assessed on a case-by-case basis. Therefore, the content of this thesis can be used to support the implementation of innovative technologies in the various areas analysed but the planning and design of these important infrastructures cannot be separated from a careful study of the specific case. Designers should engage in developing accurate analytical models to reach the highest degree of energy and economic savings. Their application

needs to be extended to concept design as the early phases of the project are crucial to reach the *net-zero* goal.

# References


1. Blau, J.R. *The Paris Agreement*. 2017.
2. Allen, A., et al., *Evaluation of low-exergy heating and cooling systems and topology optimization for deep energy savings at the urban district level.* Energy Conversion and Management, 2020. **222**: p. 113106.
3. Commision, E. *Renovation Wave: doubling the renovation rate to cut emissions, boost recovery and reduce energy poverty*. 2020 [cited 2022; Available from: https://ec.europa.eu/commission/presscorner/detail/en/ip_20_1835.
4. Ortega Alba, S. and M. Manana, *Energy Research in Airports: A Review.* 2016. **9**(5): p. 349.
5. Bank, A.D., *Improving Energy Efficiency and Reducing Emissions Through Intelligent Railway Station Buildings*, A.D. Bank, Editor. 2015.
6. Fantozzi, F., et al., *Monitoring CO2 concentration to control the infection probability due to airborne transmission in naturally ventilated university classrooms.* Architectural Science Review, 2022. **65**(4): p. 306-318.
7. Zhou, Y., *Low-carbon transition in smart city with sustainable airport energy ecosystems and hydrogen-based renewable-grid-storage-flexibility.* Energy Reviews, 2022. **1**(1): p. 100001.
8. Asdrubali, F., et al., *A Round Robin Test on the dynamic simulation and the LEED protocol evaluation of a green building.* Sustainable Cities and Society, 2022. **78**: p. 103654.
9. Sreenath, S., K. Sudhakar, and A.F. Yusop, *Sustainability at airports: Technologies and best practices from ASEAN countries.* Journal of Environmental Management, 2021. **299**: p. 113639.
10. E. DURSUN, S.V.N.a.B.K., *Green Building Certification of Urban Public Railway Transport Systems for Sustainable Cities.* BALKAN JOURNAL OF ELECTRICAL & COMPUTER ENGINEERING, 2020.
11. Ramakrishnan, J., et al., *Towards greener airports: Development of an assessment framework by leveraging sustainability reports and rating tools.* Environmental Impact Assessment Review, 2022. **93**: p. 106740.
12. Simoiu, M.S., et al., *Optimising the self-consumption and self-sufficiency: A novel approach for adequately sizing a photovoltaic plant with application to a metropolitan station.* Journal of Cleaner Production, 2021. **327**: p. 129399.
13. Elnabawi, M.H., *Building Information Modeling-Based Building Energy Modeling: Investigation of Interoperability and Simulation Results.* 2020. **6**(193).
14. Barone, G., et al., *Passive and active performance assessment of building integrated hybrid solar photovoltaic/thermal collector prototypes: Energy, comfort, and economic analyses.* Energy, 2020. **209**: p. 118435.
15. Buonomano, A. and A. Palombo, *Building energy performance analysis by an in-house developed dynamic simulation code: An investigation for different case studies.* Applied Energy, 2014. **113**: p. 788-807.

16. Barone, G., et al., *Building Energy Performance Analysis: An Experimental Validation of an In-House Dynamic Simulation Tool through a Real Test Room.* 2019. **12**(21): p. 4107.
17. Mazzarella, L. and M. Pasini. *OpenBPS: A new building performance simulation tool*. in *Building Simulation Applications*. 2017.
18. Shamsi, M.H., et al., *Feature assessment frameworks to evaluate reduced-order grey-box building energy models.* Applied Energy, 2021. **298**: p. 117174.
19. Piccinini, A., M. Hajdukiewicz, and M.M. Keane, *A novel reduced order model technology framework to support the estimation of the energy savings in building retrofits.* Energy and Buildings, 2021. **244**: p. 110896.
20. Barone, G., et al., *Enhancing trains envelope – heating, ventilation, and air conditioning systems: A new dynamic simulation approach for energy, economic, environmental impact and thermal comfort analyses.* Energy, 2020. **204**: p. 117833.
21. Gao, H., C. Koch, and Y. Wu, *Building information modelling based building energy modelling: A review.* Applied Energy, 2019. **238**: p. 320-343.
22. Larsson, N.J.R.t., International Initiative for a Sustainable Built Environment, *The integrated design process; history and analysis.* 2009.
23. Andreas Athienitis, W.O.B., *Modeling, Design, and Optimization of Net-Zero Energy Buildings*. 2015.
24. Wen, Q.-J., et al., *The progress and trend of BIM research: A bibliometrics-based visualization analysis.* Automation in Construction, 2021. **124**: p. 103558.
25. Zhuang, D., et al., *A performance data integrated BIM framework for building life-cycle energy efficiency and environmental optimization design.* Automation in Construction, 2021. **127**: p. 103712.
26. Bastos Porsani, G., et al., *Interoperability between Building Information Modelling (BIM) and Building Energy Model (BEM).* 2021. **11**(5): p. 2167.
27. International, b. *Industy Foundation Classes (IFC)*. [cited 2021; Available from: https://www.buildingsmart.org/standards/bsi-standards/industry-foundation-classes/.
28. Studio, G.B. *Green Building XML (gbXML)*. [cited 2021; Available from: https://www.gbxml.org/About_GreenBuildingXML_gbXML.
29. Pezeshki, Z., A. Soleimani, and A. Darabi, *Application of BEM and using BIM database for BEM: A review.* Journal of Building Engineering, 2019. **23**: p. 1-17.
30. Kamel, E. and A.M. Memari, *Review of BIM's application in energy simulation: Tools, issues, and solutions.* Automation in Construction, 2019. **97**: p. 164-180.
31. Gourlis, G. and I. Kovacic, *Building Information Modelling for analysis of energy efficient industrial buildings – A case study.* Renewable and Sustainable Energy Reviews, 2017. **68**: p. 953-963.
32. Carriço de Lima Montenegro Duarte, J.G., et al., *Building Information Modeling approach to optimize energy efficiency in educational buildings.* Journal of Building Engineering, 2021. **43**: p. 102587.
33. O Donnell, J., et al., *Transforming BIM to BEM: Generation of Building Geometry for the NASA Ames Sustainability Base BIM*. 2013.
34. El Sayary, S. and O. Omar, *Designing a BIM energy-consumption template to calculate and achieve a net-zero-energy house.* Solar Energy, 2021. **216**: p. 315-320.
35. Schlueter, A. and F. Thesseling, *Building information model based energy/exergy performance assessment in early design stages.* Automation in Construction, 2009. **18**(2): p. 153-163.

36. Tushar, Q., et al., *An integrated approach of BIM-enabled LCA and energy simulation: The optimized solution towards sustainable development.* Journal of Cleaner Production, 2021. **289**: p. 125622.
37. Bonomolo, M., S. Di Lisi, and G. Leone, *Building Information Modelling and Energy Simulation for Architecture Design.* 2021. **11**(5): p. 2252.
38. Bracht, M.K., A.P. Melo, and R. Lamberts, *A metamodel for building information modeling-building energy modeling integration in early design stage.* Automation in Construction, 2021. **121**: p. 103422.
39. Sušnik, M., L.C. Tagliabue, and M. Cairoli, *BIM-based energy and acoustic analysis through CVE tools.* Energy Reports, 2021.
40. Abbasi, S. and E. Noorzai, *The BIM-Based multi-optimization approach in order to determine the trade-off between embodied and operation energy focused on renewable energy use.* Journal of Cleaner Production, 2021. **281**: p. 125359.
41. Utkucu, D. and H. Sözer, *Interoperability and data exchange within BIM platform to evaluate building energy performance and indoor comfort.* Automation in Construction, 2020. **116**: p. 103225.
42. Rocha, A., et al., *A case study to improve the winter thermal comfort of an existing bus station.* Journal of Building Engineering, 2020. **29**: p. 101123.
43. Kota, S., et al., *Building Information Modeling (BIM)-based daylighting simulation and analysis.* Energy and Buildings, 2014. **81**: p. 391-403.
44. 50001, I., *Energy Management System*. 2018.
45. Architects, A.I.o. *AIA*. [cited 2021; Available from: https://www.aia.org/.
46. Andriamamonjy, A., D. Saelens, and R. Klein, *A combined scientometric and conventional literature review to grasp the entire BIM knowledge and its integration with energy simulation.* Journal of Building Engineering, 2019. **22**: p. 513-527.
47. Revit, A. *Help*. Available from: https://help.autodesk.com/view/RVT/2022/ENU/.
48. Darbra Roman, R.M., C. Wooldridge, and M. Puig Duran, *ESPO Environmental report 2020-EcoPortsinsights 2020.* 2020.
49. 16001, U.C.E., *Sistemi di gestione dell'energia - Requisiti e linee guida per l'uso*. 2011.
50. Sdoukopoulos, E., et al., *Energy Efficiency in European Ports: State-Of-Practice and Insights on the Way Forward.* 2019. **11**(18): p. 4952.
51. Hippinen, I. and J.J.S.o.t.B.S.R.E.C.H. Federley, Finland, *Fact-finding study on opportunities to enhance the energy efficiency and environmental impacts of ports in the Baltic Sea Region.* 2014.
52. Yu, S., *Introduction of Water Source Heat Pump System*, in *Handbook of Energy Systems in Green Buildings*, R. Wang and X. Zhai, Editors. 2018, Springer Berlin Heidelberg: Berlin, Heidelberg. p. 473-519.
53. Pitaccolo, M., *Action Plan for a Sustainable and Low Carbon Port of Venice*. 2019.
54. Carou, F., *Port Lands Energy Plan - Guidelines for a Net Zero District*. 2017.
55. Kevin Vaher, M.M., Peter Haab, *Sustainable Energetic Solutions for Cruise Terminal Buildings*. 2017.
56. EQUA. *IDA Indoor Climate and Energy*. [cited 2021; Available from: https://www.equa.se/en/ida-ice.
57. Sfakianakis, D. and D. Vassalos, *Dynamic modelling of thermal energy flows in ships*. 2013.
58. Michel, B. *EBSG Architectes*. 2021.

59. Rospi, G., et al., *Analysis of Energy Consumption of Different Typologies of School Buildings in the City of Matera (Southern Italy).* Energy Procedia, 2015. **82**: p. 512-518.
60. Ghiassi, N. and A. Mahdavi, *Reductive bottom-up urban energy computing supported by multivariate cluster analysis.* Energy and Buildings, 2017. **144**: p. 372-386.
61. Athienitis, A.K., et al., *Assessing active and passive effects of façade building integrated photovoltaics/thermal systems: Dynamic modelling and simulation.* Applied Energy, 2018. **209**: p. 355-382.
62. *Energy Consumption and CO2 Emissions, Focus on Passenger Rail Services* in *Railway Handbook 2017*. 2017.
63. *Guidance on Non-traction Energy Efficiency* 2017, Rail Safety and Standards Board.
64. Galaï-Dol, L., et al., *On the Use of Train Braking Energy Regarding the Electrical Consumption Optimization in Railway Station.* Transportation Research Procedia, 2016. **14**: p. 655-664.
65. Brons, M., M. Givoni, and P. Rietveld, *Access to railway stations and its potential in increasing rail use.* Transportation Research Part A: Policy and Practice, 2009. **43**(2): p. 136-149.
66. Jia, X., et al., *Field studies on thermal comfort of passengers in airport terminals and high-speed railway stations in summer.* Building and Environment, 2021. **206**: p. 108319.
67. Lv, R., et al., *Model Predictive Control with Adaptive Building Model for Heating Using the Hybrid Air-Conditioning System in a Railway Station.* 2021. **14**(7): p. 1996.
68. Barone, G., et al., *Improving the Efficiency of Maritime Infrastructures through a BIM-Based Building Energy Modelling Approach: A Case Study in Naples, Italy.* 2021. **14**(16): p. 4854.
69. Zhao, K., J. Weng, and J. Ge, *On-site measured indoor thermal environment in large spaces of airports during winter.* Building and Environment, 2020. **167**: p. 106463.
70. Yang, L. and J. Xia, *Case Study of Space Cooling and Heating Energy Demand of a High-speed Railway Station in China.* Procedia Engineering, 2015. **121**: p. 1887-1893.
71. Ma, W.-w., et al., *Research on the waiting time of passengers and escalator energy consumption at the railway station.* Energy and Buildings, 2009. **41**(12): p. 1313-1318.
72. RFI, *Piano Commerciale edizione speciale PNRR*. 2021.
73. Mata, É., A. Sasic Kalagasidis, and F. Johnsson, *Building-stock aggregation through archetype buildings: France, Germany, Spain and the UK.* Building and Environment, 2014. **81**: p. 270-282.
74. Martínez Fernández, P., et al., *A review of modelling and optimisation methods applied to railways energy consumption.* Journal of Cleaner Production, 2019. **222**: p. 153-162.
75. Tuchschmid, M., et al., *Carbon Footprint and environmental impact of Railway Infrastructure.* 2011. **2**.
76. Lin, L., et al., *Energy consumption index and evaluation method of public traffic buildings in China.* Sustainable Cities and Society, 2020. **57**: p. 102132.

77. Su, Z. and X. Li, *Multiple regression analysis on the HVAC energy consumption of railway passenger stations.* IOP Conference Series: Materials Science and Engineering, 2019. **609**: p. 052014.
78. Ahn, J., *A benchmark methodology to assess the energy performance of train station complexes.* 2019. **19**: p. 5-12.
79. Wang, Y.-Z., S. Zhou, and X.-M. Ou, *Development and application of a life cycle energy consumption and CO2 emissions analysis model for high-speed railway transport in China.* Advances in Climate Change Research, 2021. **12**(2): p. 270-280.
80. Liu, Y., et al., *Enhancing building energy efficiency using a random forest model: A hybrid prediction approach.* Energy Reports, 2021. **7**: p. 5003-5012.
81. Grillone, B., et al., *A review of deterministic and data-driven methods to quantify energy efficiency savings and to predict retrofitting scenarios in buildings.* Renewable and Sustainable Energy Reviews, 2020. **131**: p. 110027.
82. Zhao, F., S.H. Lee, and G. Augenbroe, *Reconstructing building stock to replicate energy consumption data.* Energy and Buildings, 2016. **117**: p. 301-312.
83. Luddeni, G., et al., *An analysis methodology for large-scale deep energy retrofits of existing building stocks: Case study of the Italian office building.* Sustainable Cities and Society, 2018. **41**: p. 296-311.
84. Barone, G., et al., *A novel dynamic simulation model for the thermo-economic analysis and optimisation of district heating systems.* Energy Conversion and Management, 2020. **220**: p. 113052.
85. Goy, S., V. Coors, and D. Finn, *Grouping techniques for building stock analysis: A comparative case study.* Energy and Buildings, 2021. **236**: p. 110754.
86. Swan, L.G. and V.I. Ugursal, *Modeling of end-use energy consumption in the residential sector: A review of modeling techniques.* Renewable and Sustainable Energy Reviews, 2009. **13**(8): p. 1819-1835.
87. Li, Y., et al., *A Comparison of Various Bottom-Up Urban Energy Simulation Methods Using a Case Study in Hangzhou, China.* 2020. **13**(18): p. 4781.
88. Barone, G., et al., *Sustainable energy design of cruise ships through dynamic simulations: Multi-objective optimization for waste heat recovery.* Energy Conversion and Management, 2020. **221**.
89. Ferrando, M., et al., *Urban building energy modeling (UBEM) tools: A state-of-the-art review of bottom-up physics-based approaches.* Sustainable Cities and Society, 2020. **62**: p. 102408.
90. Prataviera, E., et al., *EUReCA: An open-source urban building energy modelling tool for the efficient evaluation of cities energy demand.* Renewable Energy, 2021. **173**: p. 544-560.
91. Bellia, L., P. Mazzei, and A. Palombo, *Weather data for building energy cost-benefit analysis.* 1998. **22**(14): p. 1205-1215.
92. Consortium, O.G. *CityGML*. [cited 2022 07/01/2022]; Available from: https://www.ogc.org/standards/citygml.
93. *GeoJSON*. [cited 2022 07/01/2022]; Available from: https://geojson.org/.
94. Abolhassani, S.S., et al., *A new workflow for detailed urban scale building energy modeling using spatial joining of attributes for archetype selection.* Journal of Building Engineering, 2021: p. 103661.

95. Dabirian, S., K. Panchabikesan, and U. Eicker, *Occupant-centric urban building energy modeling: Approaches, inputs, and data sources - A review.* Energy and Buildings, 2022. **257**: p. 111809.
96. Loga, T., B. Stein, and N. Diefenbach, *TABULA building typologies in 20 European countries—Making energy-related features of residential building stocks comparable.* Energy and Buildings, 2016. **132**: p. 4-12.
97. Ballarini, I., S.P. Corgnati, and V. Corrado, *Use of reference buildings to assess the energy saving potentials of the residential building stock: The experience of TABULA project.* Energy Policy, 2014. **68**: p. 273-284.
98. Carnieletto, L., et al., *Italian prototype building models for urban scale building performance simulation.* Building and Environment, 2021. **192**: p. 107590.
99. Johari, F., et al., *Urban building energy modeling: State of the art and future prospects.* Renewable and Sustainable Energy Reviews, 2020. **128**: p. 109902.
100. Frazzica, A., et al., *Experimental Validation and Numerical Simulation of a Hybrid Sensible-Latent Thermal Energy Storage for Hot Water Provision on Ships.* 2022. **15**(7): p. 2596.
101. *RFI Rete Ferroviaria Italiana*. 2020 [cited 2020; Available from: https://www.rfi.it/it/rete/la-rete-oggi.html.
102. ISTAT. *Codici statistici delle unità amministrative territoriali: Comuni, Città metropolitane, Province e Regioni*. 2022; Available from: https://www.istat.it/it/archivio/6789#Elencodeicodiciedelledenominazionidelleunitterritoriali-0.
103. Italiana, R.-R.F., *Network Statement*. 2021.
104. Runge, J. and R. Zmeureanu, *Forecasting energy use in buildings using artificial neural networks: A review.* Energies, 2019. **12**(17): p. 3254.
105. Fumo, N., M.J. Torres, and K. Broomfield, *A multiple regression approach for calibration of residential building energy models.* Journal of Building Engineering, 2021. **43**: p. 102874.
106. Deb, C. and A. Schlueter, *Review of data-driven energy modelling techniques for building retrofit.* Renewable and Sustainable Energy Reviews, 2021. **144**: p. 110990.
107. Ciulla, G. and A. D'Amico, *Building energy performance forecasting: A multiple linear regression approach.* Applied Energy, 2019. **253**: p. 113500.
108. Barone, G., et al., *Increasing renewable energy penetration and energy independence of island communities: A novel dynamic simulation approach for energy, economic, and environmental analysis, and optimization.* Journal of Cleaner Production, 2021. **311**: p. 127558.
109. *Allegato A - Dpr 412/93*.
110. 10339:1995, U., *Impianti aeraulici al fini di benessere. Generalità, classificazione e requisiti. Regole per la richiesta d'offerta, l'offerta, l'ordine e la fornitura.* 1995.
111. Vassiliades, C., et al., *Assessment of an innovative plug and play PV/T system integrated in a prefabricated house unit: Active and passive behaviour and life cycle cost analysis.* Renewable Energy, 2022. **186**: p. 845-863.
112. Barone, G., et al., *Implementing the dynamic simulation approach for the design and optimization of ships energy systems: Methodology and applicability to modern cruise ships.* Renewable and Sustainable Energy Reviews, 2021. **150**: p. 111488.
113. Maturo, A., et al., *Design and environmental sustainability assessment of energy-independent communities: The case study of a livestock farm in the North of Italy.* Energy Reports, 2021. **7**: p. 8091-8107.
114. IEA, *Aviation*. 2021: Paris.

115. Greer, F., J. Rakas, and A. Horvath, *Airports and environmental sustainability: a comprehensive review.* Environmental Research Letters, 2020. **15**(10): p. 103007.
116. Ortega Alba, S. and M. Manana, *Energy Research in Airports: A Review.* Energies, 2016. **9**(5).
117. Costa, A.B., L. M.; Donnelly, C.; Keane, M. M., *Review of EU airport energy interests and priorities with respect to ICT, energy efficiency and enhanced building operation.* Energy Systems Laborator, 2012.
118. Yildiz, O.F., M. Yilmaz, and A. Celik, *Reduction of energy consumption and CO2 emissions of HVAC system in airport terminal buildings.* Building and Environment, 2022. **208**: p. 108632.
119. Akyüz, M.K., Ö. Altuntaş, and M.Z. Söğüt, *Economic and Environmental Optimization of an Airport Terminal Building's Wall and Roof Insulation.* Sustainability, 2017. **9**(10).
120. Ortega Alba, S. and M. Manana, *Characterization and Analysis of Energy Demand Patterns in Airports.* Energies, 2017. **10**(1).
121. Gu, X., et al., *Prediction of the spatiotemporal passenger distribution of a large airport terminal and its impact on energy simulation.* Sustainable Cities and Society, 2022. **78**: p. 103619.
122. *Airport Carbon Accreditation*. 2022; Available from: https://www.airportcarbonaccreditation.org/.
123. *Leadership in Energy and Environmental Design*. 2022; Available from: https://www.usgbc.org/leed.
124. Kim, S.-C., H.-I. Shin, and J. Ahn, *Energy performance analysis of airport terminal buildings by use of architectural, operational information and benchmark metrics.* Journal of Air Transport Management, 2020. **83**: p. 101762.
125. Xianliang, G., et al., *Analysis to energy consumption characteristics and influencing factors of terminal building based on airport operating data.* Sustainable Energy Technologies and Assessments, 2021. **44**: p. 101034.
126. Kılkış, Ş. and Ş. Kılkış, *Benchmarking airports based on a sustainability ranking index.* Journal of Cleaner Production, 2016. **130**: p. 248-259.
127. Kılkış, B., *Energy consumption and CO2 emission responsibilities of terminal buildings: A case study for the future Istanbul International Airport.* Energy and Buildings, 2014. **76**: p. 109-118.
128. Baxter, G., et al., *Sustainable airport energy management: The case of kansai international airport.* 2018. **8**(3).
129. Baxter, G., P. Srisaeng, and G. Wild, *An Assessment of Airport Sustainability, Part 1—Waste Management at Copenhagen Airport.* 2018. **7**(1): p. 21.
130. Baxter, G., P. Srisaeng, and G. Wild, *An Assessment of Airport Sustainability, Part 2—Energy Management at Copenhagen Airport.* 2018. **7**(2): p. 32.
131. Sigler, D., et al., *Route optimization for energy efficient airport shuttle operations – A case study from Dallas Fort worth International Airport.* Journal of Air Transport Management, 2021. **94**: p. 102077.
132. Cardona, E., A. Piacentino, and F. Cardona, *Energy saving in airports by trigeneration. Part I: Assessing economic and technical potential.* Applied Thermal Engineering, 2006. **26**(14): p. 1427-1436.
133. de Rubeis, T., et al., *Multi-year consumption analysis and innovative energy perspectives: The case study of Leonardo da Vinci International Airport of Rome.* Energy Conversion and Management, 2016. **128**: p. 261-272.

134. Qiong, L., M. Qinglin, and Z. Lihua. *Energy efficiency design of an airport terminal building*. in *2010 International Conference on Advances in Energy Engineering*. 2010.
135. Abdallah, A.S.H., A. Makram, and M. Abdel-Azim Nayel, *Energy audit and evaluation of indoor environment condition inside Assiut International Airport terminal building, Egypt.* Ain Shams Engineering Journal, 2021. **12**(3): p. 3241-3253.
136. Liu, X., et al., *Energy saving potential for space heating in Chinese airport terminals: The impact of air infiltration.* Energy, 2021. **215**: p. 119175.
137. Liu, X., et al., *Outdoor air supply in winter for large-space airport terminals: Air infiltration vs. mechanical ventilation.* Building and Environment, 2021. **190**: p. 107545.
138. Pichatwatana, K., et al., *An integrative approach for indoor environment quality assessment of large glazed air-conditioned airport terminal in the tropics.* Energy and Buildings, 2017. **148**: p. 37-55.
139. Sher, F., et al., *Fully solar powered Doncaster Sheffield Airport: Energy evaluation, glare analysis and CO2 mitigation.* Sustainable Energy Technologies and Assessments, 2021. **45**: p. 101122.
140. Teofilo, A., et al., *Investigating potential rooftop solar energy generated by Leased Federal Airports in Australia: Framework and implications.* Journal of Building Engineering, 2021. **41**: p. 102390.
141. Sreenath, S., K. Sudhakar, and A.F. Yusop, *Energy-exergy-economic-environmental-energo-exergo-enviroecono (7E) analysis of solar photovoltaic power plant: A case study of 7 airport sites in India.* Sustainable Energy Technologies and Assessments, 2021. **47**: p. 101352.
142. Jiang, M., et al., *National level assessment of using existing airport infrastructures for photovoltaic deployment.* Applied Energy, 2021. **298**: p. 117195.
143. Sreenath, S., et al., *Solar PV energy system in Malaysian airport: Glare analysis, general design and performance assessment.* Energy Reports, 2020. **6**: p. 698-712.
144. Jia, Q., H.-q. Hu, and J.-l. Yu, *The model construction in airport renewable energy system scale planning based in Multi-Criteria Decision Making.* Energy Reports, 2021. **7**: p. 92-98.
145. Xiang, Y., et al., *Techno-economic design of energy systems for airport electrification: A hydrogen-solar-storage integrated microgrid solution.* Applied Energy, 2021. **283**: p. 116374.
146. Hoelzen, J., et al., *H2-powered aviation at airports – Design and economics of LH2 refueling systems.* Energy Conversion and Management: X, 2022. **14**: p. 100206.
147. Kilkis, B., *Net-zero buildings, what are they and what they should be?* Energy, 2022. **256**: p. 124442.
148. Chang, Y., et al., *The energy use and environmental emissions of high-speed rail transportation in China: A bottom-up modeling.* Energy, 2019. **182**: p. 1193-1201.
149. Watson, I., *High-Speed Railway.* 2021. **1**(3): p. 665-688.
150. Ogunsola, A. and A. Mariscotti, *Signalling and Communication Systems*, in *Electromagnetic Compatibility in Railways: Analysis and Management*, A. Ogunsola and A. Mariscotti, Editors. 2013, Springer Berlin Heidelberg: Berlin, Heidelberg. p. 95-177.
151. Güğül, G.N., F. Gökçül, and U. Eicker, *Sustainability analysis of zero energy consumption data centers with free cooling, waste heat reuse and renewable energy systems: A feasibility study.* Energy, 2022: p. 125495.

152. Zhang, H., et al., *Free cooling of data centers: A review.* Renewable and Sustainable Energy Reviews, 2014. **35**: p. 171-182.
153. Li, J. and Z. Li, *Model-based optimization of free cooling switchover temperature and cooling tower approach temperature for data center cooling system with water-side economizer.* Energy and Buildings, 2020. **227**: p. 110407.
154. Amado, E.A., P.S. Schneider, and C.S. Bresolin, *Free cooling potential for Brazilian data centers based on approach point methodology.* International Journal of Refrigeration, 2021. **122**: p. 171-180.
155. Dai, J., D. Das, and M. Pecht, *Prognostics-based risk mitigation for telecom equipment under free air cooling conditions.* Applied Energy, 2012. **99**: p. 423-429.
156. Nadjahi, C., H. Louahlia, and S. Lemasson, *A review of thermal management and innovative cooling strategies for data center.* Sustainable Computing: Informatics and Systems, 2018. **19**: p. 14-28.